POST-SURGICAL NATURAL KILLER T CELL ACTIVATION AS A POTENTIAL THERAPY FOR METASTATIC BREAST CANCER

by

Daniel R. Clattenburg

Submitted in partial fulfillment of the requirements
for the degree of Master of Science

at

Dalhousie University
Halifax, Nova Scotia
December 2012

DALHOUSIE UNIVERSITY

DEPARTMENT OF MICROBIOLOGY AND IMMUNOLOGY

The undersigned hereby certify that they have read and recommended to the Faculty of Graduate Studies for acceptance of this thesis entitled "POST-SURGICAL NATURAL KILLER T CELL ACTIVATION AS A POTENTIAL THERAPY FOR METASTATIC BREAST CANCER" by Daniel R. Clattenburg in partial fulfillment of the requirements for the degree of Master of Science.

Dated: December 14, 2012

Supervisor: _____

Readers: _____

_____

_____

DALHOUSIE UNIVERSITY

DATE: December 14, 2012

AUTHOR: Daniel R. Clattenburg

TITLE: POST-SURGICAL NATURAL KILLER T CELL ACTIVATION AS A POTENTIAL THERAPY FOR METASTATIC BREAST CANCER

DEPARTMENT OR SCHOOL: Department of Microbiology and Immunology

DEGREE: MSc CONVOCATION: May YEAR: 2013

_____

Signature of Author

TABLE OF CONTENTS

LIST OF TABLES

LIST OF FIGURES

ABSTRACT

Natural Killer T (NKT) cells are a specialized group of immune-regulatory T lymphocytes. NKT cells have been shown to limit primary tumor growth and target distant metastatic disease in murine cancer models and in human clinical trials. The focus of this work was to utilize NKT cell activation as a post-surgical immunotherapy in models of metastatic breast cancer. In our model, mammary carcinoma cells were injected into the mammary fat pad of syngeneic mice and primary tumors were resected twelve days later. The following day, mice were treated with NKT cell-activating glycolipids or glycolipid-loaded dendritic cells (DCs) to examine the effect on metastatic disease. Treatment with free glycolipids transiently reduced metastatic disease but did not enhance survival. In contrast, treatment with glycolipid-loaded DCs was effective in limiting metastasis, prolonging survival, and decreasing tumor-associated immune suppression. Our data suggest that NKT cell activation via transfer of glycolipid-loaded self-DCs holds promise as an immunotherapy for metastatic breast cancer.

LIST OF ABBREVIAIONS USED

4T1	murine breast cancer cell line syngeneic to BALB/c mice
5-FU	5-Fluorouracil
6-TG	6-Thioguanine
α-GC	α-galactosylceramide
α-C-GC	α-C-galactosylceramide
Ab	Antibody
Ag	Antigen
ANOVA	one-way analysis of variance
APC(s)	antigen presenting cell(s)
ATRA	all-trans retinoic acid
Breg	B-regulatory cell
CFU	colony forming units
CTC(s)	circulating tumor cells
CTL(s)	cytotoxic T lymphocytes
DC(s)	dendritic cells(s)
DCIS	ductal carcinoma in situ
DMEM	Dulbecco's Modified Eagle's Medium
DMSO	dimethyl sulphoxide
E0771	murine breast cancer cell line syngeneic to C57BL/6 mice
EMT	epithelial-to-mesenchymal transition
ER	estrogen receptor
FACS	fluorescence activated cell sorting
FBS	fetal bovine calf serum
GM-CSF	granulocyte monocyte-colony stimulating factor
gMDSC(s)	granulocytic myeloid derived suppressor cells
HER2/neu	human endothelial growth factor receptor 2
HSP(s)	heat shock proteins
IAV	influenza A virus
IDO	Indoleamine 2,3 dioxygenase

IFN	interferon
IL	interleukin
ImC	immature cells
IMDM	Iscove's Modified Dulbecco's Medium
NK	natural killer cell
iNKT	invariant natural killer T cell
is.	intrasplenic
iv.	intravenous
LCIS	lobular carcinoma in situ
MMP(s)	matrix metalloproteaseas
MDSC(s)	myeloid-derived suppressor cells
NK(s)	natural killer cell(s)
PBS	phosphate buffered saline
PCR	polymerase chain reaction
PFA	paraformaldehyde
PGE2	prostaglandin E2
PSA	prostate-specific antigen
RNS	reactive nitrogen species
ROS	reactive oxygen species
RPMI	Roswell Park Memorial Institute medium
sc.	subcutaneous
SEM	standard error of the mean
TAA	tumor associated antigen
TAM(s)	tumor associated macrophage(s)
TCR	T cell receptor
TGF-β	transforming growth factor β
TNF-α	tumor necrosis factor α
Treg	regulatory T cell
TRAIL	TNF-related apoptosis-inducing ligand
TSA	tumor specific antigen
VEGF	vascular endothelial growth factor

ACKNOWLEDGEMENTS

I would like to thank Dr. Brent Johnston for his knowledge and guidance over the past two years. Thank you to Simon Gebremeskel for your motivation towards the end of my stay with the lab and for helping me to complete my final experiments. Simon provided substantial contributions to the myeloid derived suppressor cell experiments including cytospin analysis, long-term blood cell monitoring and functional immunosuppression assays. I would also like to thank Linnea Veinotte and Robyn Cullen for filling in the loose ends and helping with experiments involving FACS analysis, intravenous adoptive cell transfers and cytokine analysis. Thank you to Drew Slaunwhite, Erin Chamberlain, Olga Bogacheva and Natasa Zatazola for your viewpoints and support during my stay with the Johnston lab. Thank you to the Dr. Jean Marshall lab for supplying 4T1 and E0771 cell lines and the Dr. Craig McCormick lab for supplying GFP-expressing retrovirus and reagents. Finally, thank you to the Canadian Breast Cancer Foundation Atlantic Region and the BHCRI Cancer Research Training Program for training and financial support.

Chapter 1: Introduction

1.1 Cancer and Metastasis

The term cancer refers to a disease state in which abnormal body cells grow out of control and gain the ability to invade other tissues [1]. A benign lesion such as a thyroid adenoma is non-invasive and exhibits a non-aggressive growth pattern. Malignant lesions such as stage IV metastatic breast cancers have an aggressive and invasive pattern of growth. There are over 100 different types of cancer which can arise in any given organ or tissue in both somatic and germ line cell types [2]. Cancer arises from a single or multiple cells of origin which accumulate cancer-promoting mutations until the point at which they replicate in a dysregulated manner to form a primary tumor [3]. Genetic aberrations may already exist at the time of birth, leading to an increased risk of childhood onset cancers. An example of a cancer arising from such a mutation is retinoblastoma, where a mutation exists in the tumor suppressor gene RB1, leading to the development of ocular cancers in young children [4]. Inherited mutations may also predispose one to develop cancers later in life as is seen with BRCA1 and BRCA2 mutations in breast and ovarian cancer [5]. Five to ten percent of all breast cancer cases are hereditary, but for those with BRCA1 or BRCA2 mutations, the risk of developing breast cancer is 57% and 49% respectively [6]. As we age and cells continue to undergo repeated cycles of replication, genetic mutations will naturally arise and accumulate in cells. Environmental factors also play an important role in promoting DNA damage. Cancer-causing agents known as carcinogens increase the rate of DNA damage directly and indirectly. Common carcinogens include such compounds as benzene and environmental toxins like the fungi-derived aflatoxins [7, 8]. Cigarette smoke contains over 40 known carcinogens and nearly 90% of lung cancer incidence and lung cancer-related deaths can be attributed to smoking [9]. Smoking alone accounts for ~25% of all cancer related deaths, with ~35% related to dietary factors and ~20% related to infections [10]. Other cancer-promoting factors include UV exposure, obesity, excessive alcohol consumption, radiation and exposure to certain viruses such as the cervical cancer causing human papilloma virus [10].

1.1.1 *Cancer*

A tumor can be compared to an early stage embryo. Both share a number of features including an increase in retrotransposon activity, genetic deprogramming, genome-wide demethylation and conversion into a replicative undifferentiated cell state [11]. Both seek a means

of growth by provision of nutrients and oxygen, while evading attacks by the immune system. The difference between a growing embryo and a tumor is the lack of regulatory signals and unresponsiveness to differentiation signals in the cancerous growth.

Cancer types fall under the general classifications of carcinoma, sarcoma, leukemia, lymphoma, or cancer of the central nervous system [12]. Carcinomas arise from epithelial tissue with a common subtype of carcinomas known as adenocarcinomas arising from glandular epithelial tissue. Sarcomas arise from connective tissues, leukemias from leukocyte populations and lymphomas from lymphocyte populations. Leukemias present as a disease involving cancerous cells circulating in the blood and bone marrow while lymphomas present as a combination of solid masses and circulating cancer cells. Carcinomas, sarcomas and cancer of the central nervous system present as solid masses.

Ten hallmarks have been described to characterize cancers. Six of these hallmarks described in 2000 are self-sufficiency in growth signals, insensitivity to antigrowth signals, tissue invasion and metastasis, limitless replicative potential, sustained angiogenesis, and evasion of apoptosis [2]. Added to this list in 2011 were abnormal metabolic pathways, immune system evasion, DNA instability and chromosome abnormalities, and tumor-promoting inflammation [13]. Carcinogenesis, also known as oncogenesis or tumorigenesis, refers to the transition of a normal somatic or germ line cell into a cancerous cell state. As cells accumulate mutations in genes that regulate the cell cycle, DNA repair mechanisms, apoptosis, and metabolism, the cells become more self-sustaining and resistant to stresses that would signal for elimination of a normal cell. A major component of this oncogenic transition is a process known as epithelial-mesenchymal transition (EMT) [14]. There are three types of EMT; type 1 EMT is involved in embryogenesis, type 2 EMT functions in wound healing and inflammation, and type 3 EMT involves the transition of epithelial cancer cells into migratory mesenchymal cancer cells [14]. Characteristics of EMT include down-regulation of surface E-cadherin and tight junction molecules, loss of adhesion, loss of cellular polarity, and increased expression of molecules such as fibronectin and S100 proteins [15]. In wound healing, EMT is important for migration of epithelial cells into sites of tissue damage where adhesion proteins are re-expressed, allowing for wound closure [15]. The combined effect of a loss of E-cadherin expression and increased expression of matrix metalloproteases (MMPs) has been used as a negative prognostic indicator for various forms of metastatic disease [15]. Certain molecular markers are common to various cancer types and have

been used to both diagnose and further understand carcinogenesis; an example of this being p53. p53 is a tumor suppressor protein that responds to DNA damage by inducing cell growth arrest or apoptosis [16]. Mutations of p53 are found in 50% of cancers, leading to the accumulation of cells with DNA damage [17]. The net effect of multiple mutations in many cells is the initiation of cancerous cell growth.

A growing tumor mass will eventually require a blood supply in order to survive. As the rapidly dividing cells continue to outstrip the surrounding blood supply and available nutrients, they will require increased levels of micronutrients and other factors supplied by tumor-induced neoangiogenic vessels. The key factor involved in this tumor-induced neoangiogenesis is vascular endothelial growth factor (VEGF) [18]. By providing itself with vasculature, a tumor can proceed to grow further, generate a pre-metastatic niche in distant organ sites and metastasize to these distant sites. VEGF in addition to promoting neoangiogenesis, also functions as an immunosuppressive molecule, suppressing T cell activity and negatively influencing the development of DCs and other cell types [19, 20, 21]. Anti-VEGF antibody-based treatments such as Bevacizumab (Avastin) have been used in both in mouse models and human clinical trials for the treatment of various cancer types with some success. However, issues have arisen with these treatments related to the selection for more aggressive cancer cells capable of surviving both hypoxic and low nutrient conditions. Despite this, work continues to be done targeting VEGF as a means of inhibiting tumor neoangiogenesis and VEGF-associated immunosuppression. An example of this is CIGB-247, a novel vaccine combining bacteria-based adjuvants and a recombinant antigen representative of VEGF-A. CIGB-247 reduced the incidence of lung metastasis in mouse models of lung, breast and colon cancer [22].

1.1.2 *Metastasis*

Cancer metastasis accounts for greater than 90% of cancer-related deaths [23]. Metastasis is defined as the spread of malignant cancer cells from the primary tumor mass to a local or distant secondary tissue site via the lymphatic system or circulatory system [24]. As reviewed in Chiang (2008) [25], metastasis is a multistep process that begins with local invasion of malignant cells into nearby tissues. This is followed by intravasation of cancer cells into lymphatic or blood vessels. Cancer cells then traffic via lymphatic and/or hematogenous routes to various sites in the body. Less than 0.01% of these circulating cancer cells have the ability to survive and form metastases

in distant tissues [26]. Upon reaching capillary beds in tissue sites such as the lungs and liver, the cancer cells will arrest and extravasate across the vessel walls into the surrounding tissue. These cancer cells may then begin to proliferate and form small tumors known as micrometastases. Micrometastases will continue to grow by acquiring vasculature and obtaining circulating oxygen and nutrients. Once these metastatic lesions have grown large enough in size, cancerous cells will also start to seed from these tumor masses into circulation to form new micrometastases in local and distant tissue sites.

As reviewed in Fidler (2002) [27], the process of metastasis is understood through multiple overlapping models. The seed and soil hypothesis explains that metastasis occurs to distinct sites as a result of factors present in the target tissue naturally or as a result of the tumor generating a pre-metastatic niche through release of conditioning factors such as epiregulin, COX2, MMP1, MMP2 and PTGS2 [28]. In contrast, the anatomical-mechanical hypothesis suggests that metastasis occurs in the tissues which circulating tumor cells are most likely to encounter first or where there is the highest degree of vessel narrowing (such as the lung and liver), thus causing cells to slow down and accumulate faster, allowing for a higher chance of invading through the endothelium. It is likely that both of these processes play a role to varying degrees in the numerous forms of metastatic cancer. Regardless of cancer type, the lungs and liver are the two most common sites for cancer metastasis [25]. One reason for this is the high density of capillary beds that can trap tumor cells. Molecular factors also play a role in promoting site-specific metastasis. For example, up-regulation of the metadherin protein in breast cancer cells is involved in site-specific adhesion in pulmonary vasculature [29]. Up-regulation of the tyrosine phosphatase PRL-3 in metastatic colorectal carcinomas is linked to both pulmonary and hepatic metastasis [29].

Barriers to achieving distal spreading for CTCs include local tissue architecture, endothelial walls, and trafficking routes in body fluids. Metastatic cells must lose local cellular adhesion, increase invasiveness and intravasation, and survival in the vascular system, in order to extravasate, survive and proliferate in a new site [24]. A cell having undergone epidermal mesenchymal transition (EMT) will secrete factors to influence the local environment; one crucial factor being VEGF [30]. By providing itself with a blood supply, the growing tumor establishes both a means of supplying oxygen and nutrients for sustained growth, but also a means of trafficking throughout the body. EMT is also associated with a change in cell

morphology, including up-regulation of motility characteristics, tissue remodeling enzymes such as matrix metalloproteases and adhesion molecules [31].

Metastatic disease can be treated with systemic therapies including chemotherapy, biological therapy, targeted therapy, and hormonal therapy or with local therapies, including surgery and radiation therapy [32]. Although metastasectomy can become extensive and often morbid in nature, it can also be beneficial for select patients, for example to remove lung and liver metastases in select breast cancer patients [33]. When surgery cannot be performed, minimally invasive radiofrequency ablation is often an alternative [33].

1.1.3 *Breast Cancer*

In developed countries including Canada, four key cancers account for the majority of cancer incidence and cancer-related deaths – lung, colorectal, prostate, and breast [34]. Breast cancer is the second leading cause of cancer-related death among Canadian women, behind lung cancer, with 5,100 deaths and 23,400 new cases in 2011 [34]. Globally, 425,000 breast-cancer related deaths occurred in 2010 [35]. Breast cancer incidence has increased from 641,000 new cases in 1980 to 1,643,000 new cases in 2010 [35], although part of this increase can be attributed to advancements in detection and increases in public breast cancer screening and awareness.

Based on microarray-based molecular profiling and histopathological features such as estrogen receptor status, breast cancers are now grouped into five major subtypes, Luminal-A, Luminal-B, Basal-like, HER2-enriched and Normal-like [36, 37] (Table 1). While Normal-like breast cancer has a similar gene expression profile to normal adipose breast tissue, the other four major subtypes have distinct molecular expression profiles which contribute to variation in growth, invasiveness and treatment responses [38] (Table 1). Luminal A breast cancers have the best prognosis owing to their less aggressive growth profile and high percentage expressing the ER [38]. Basal-like breast cancers have the worst prognosis owing to an increased tendency for an aggressive growth profile and low receptor expression level, decreasing their responsiveness to hormone receptor and HER2-targeted therapies [38] (Table 1). Breast cancer can be broadly classified into four distinct TNM (Tumor, Node, Metastasis) stages – Stage I includes ductal carcinoma in situ (DCIS) and lobular carcinoma in situ (LCIS), Stage II includes local spreading and involvement of local lymph nodes, Stage III involves invasive spreading with lymph node

involvement, and Stage IV includes all metastatic forms of breast cancer [39]. The average survival time for women with advanced stage IV breast cancer is 2 years [40].

As metastatic disease accounts for 90% of cancer related deaths, it is of great importance to generate anti-cancer therapies that target metastatic disease. Breast cancer most commonly metastasizes to the lungs, bone, and liver [40]. Metastasis to the bone results in an average 5-year survival rate of 33% and a median survival of 48 months, while visceral metastasis reduces the 5-year survival rate to 13% and median survival to 17 months [41, 42].

At this time there are many different treatment options for breast cancer and treatment protocols vary somewhat in a case-dependent manner. The standard treatment for breast cancer involves one or more of the following: surgical resection, radiation therapy, chemotherapy, receptor-directed therapy, targeted therapy or experimental therapies such as cell-based immunotherapies [40]. Various patient factors influence which combinations to utilize; these include such factors as disease type, staging, number of disease sites, prior hormone treatment and age [40].

Approximately 80% of breast cancers are ER^+, making them susceptible to endocrine therapies [43]. For ER^+ tumors, a 50-60% response rate is observed using first-line hormonal agents [40]. Patients with estrogen and progesterone-positive tumors have a 65-75% response rate to hormone therapy [44].

HER2-neu is an oncogene that encodes the epidermal growth factor receptor ErbB2 and is overexpressed in the breast cancer cells of 25-30% of patients [45, 46]. Trastuzumab, an anti-HER2-neu monoclonal antibody, targets the extracellular domain of HER2 and inhibits tumor cell growth via antibody-dependent cellular toxicity, inhibition of intracellular signaling, and decreased angiogenesis and DNA repair [47, 48]. As an addition to standard chemotherapy regimens for breast cancer, trastuzumab has reduced the risk of relapse and death by 50% and 30% respectively [49, 50]. However, as a result of issues with cardiotoxicity, cost and drug-resistance related to treatment with trastuzumab, novel anti-HER2 therapies are being developed such as Lapatinib, a small molecule inhibitor that targets HER2 tyrosine kinase activity [48, 51].

Besides anthracycline (doxorubicine, valrubicin) compounds which prevent cellular replication through DNA/RNA intercalation and topoisomerase inhibition, the taxanes (paclitaxel, docetaxel) which disrupt microtubule function are the most effective treatments for metastatic breast cancer [40]. Response rates of 40-94% have been observed with some combined

anthracycline-taxane first-line treatments, with complete remission observed in 12-41% of patients [52]. Side-effects related to the use of the chemotherapeutic drugs are extensive and include myelosuppression, fatigue, fluid retention, neurosensory toxicity and stomatitis [40]. Disease progression following anthracycline and taxane treatments leads to the administration of second line chemotherapeutic agents such as gemcitabine, vinorelbine and 5-fluorouracil which have response rates of approximately 10-20% [53].

Table 1: Comparison of four major breast cancer subtypes.

Subtype	Luminal A	Luminal B	HER2-Enriched	Basal-Like
$ER^+/HER2^-$ (%)	87	82	20	10
$HER2^+$ (%)	7	15	68	2
$ER^-/PR^-/HER2^-$ (%)	2	1	9	80
DNA Mutations (% mutated)	TP53 (12) PIK3CA (49) GATA3 (14) MAP3K1 (14)	TP53 (32) PIK3CA (32) MAP3K1 (5)	TP53 (75) PIK3CA (42) PIK3R1 (8)	TP53 (84) PIK3CA (7)
TNM Stage (%)				
1	55.3	35.7	28.4	39.0
2	35.1	50.0	55.2	51.0
3	4.6	7.1	10.4	6.2
4	3.7	2.4	6.0	3.3

Adapted from The Cancer Genome Atlas Network, *Nature* 2011 and Haque, *Canc Epid* 2012.

Breast cancer subtypes listed are based on molecular profiling of tumor samples. **Luminal A and Luminal B:** most dominant feature is high expression of the luminal expression signature, which contains ESR1, GATA3, FOXA1, XBP1 and MYB. **HER2-Enriched:** not all tumors in this subtype are clinically $HER2^+$. Tumors within this subtype have elevated levels of mRNAs encoding genes including EGFR, pEGFR, HER2, pHER2 and FGFR4. **Basal-Like:** main feature is the absence of expression of the receptors ER, PR and HER2. Deficiencies in TP53 activity are observed in nearly all tumors. A characteristic gene expression signature containing keratins 5, 6 and 17 and genes associated with cell proliferation is observed in most samples.

1.1.4 *Animal Models of Breast Cancer*

The 4T1 mammary carcinoma model, syngeneic to BALB/c mice, is a commonly used model of spontaneously metastasizing breast cancer that mimics many features of advanced human stage IV metastatic breast cancer and is the primary model used in this body of work. The tumor line was isolated from a spontaneous mammary carcinoma and initially described by Aslakson and Miller in 1992, and later characterized by Pulaski and Ostrand-Rosenberg in 2001. In the 4T1 model, tumor cells are injected orthotopically into the subcutaneous mammary fat pad, establish a primary tumor and metastasize throughout the mouse within two weeks of implantation [54, 55, 56, 57]. The main site of metastasis is to the lungs via the hematogenous route of spread; metastasis via the lymphatic route plays only a minor role in this model [57]. Beyond 2 weeks of implantation, systemic metastasis can be observed to sites including the liver, lymph nodes, kidneys, bone, and brain tissue [57]. Originally derived from a single spontaneously arising mammary tumor in BALB/c mice, 4T1 tumor cells are readily cultured *in vitro* [54]. Multiple cell lines were derived from the heterogeneous mixture of tumor cells; 4T1 cells demonstrated the highest rate of metastasis to the lungs and liver and through selective culturing in 6-thioguanine (6-TG) they are fully resistant to this drug [54]. 6-TG is a guanine analogue that is commonly used in the treatment of leukemias, acting by disrupting DNA synthesis, leading to cell cycle arrest and apoptosis [58]. 6-TG resistance in 4T1 cells allows for tissue metastasis to be directly measured by culturing dissociated tissue suspensions with 6-TG and enumerating the number of colony forming units that are present [54, 55]. A further benefit to using the 4T1 model is the ability to track myeloid derived suppressor cells (MDSCs) in the peripheral blood of tumor-challenged mice [59, 60, 61]. It has been shown that with the progression of malignant disease, peripheral blood MDSC levels also increase (see section 1.2.3) [1, 59, 60].

The other model of metastatic breast cancer used in this body of work is the E0771 model. The E0771 murine breast carcinoma model, syngeneic to C57BL/6 mice, was initially used by Goodson et al. in 1955 to test the ability of various compounds to inhibit primary tumor growth [62]. This model has been characterized to a lesser extent than the 4T1 model. Compared to the 4T1 model, there is reduced lung metastasis in the E0771 model, but similar primary tumor growth kinetics [63]. E0771 tumor cells are ER^+ while 4T1 cells are ER^-, making the E0771 model more representative of a hormone therapy responsive breast carcinoma [63, 64]. Using NKT cell activating treatment in combination with a targeted hormone therapy would therefore be

possible in this particular model. Moreover, the use of two models with unique metastasis patterns and disparate genetic profiles acts to validate the treatment results observed in each of the models. The ER^- status of 4T1 cells makes this a good model to use as ER^- cancers are more difficult to treat and in more need of novel therapies [65].

Although other murine models of breast cancer are available, most lack the selective markers and detailed characterization of the 4T1 model. This is also the case for the E0771 model. Therefore, effort is needed to develop methods to track metastasis in this model.

1.2 Tumor Immunology

The immune response to tumors is highly diverse, encompassing responses associated with both the innate and adaptive arms of immunity. Cancers however are highly evasive with respect to the immune system, evading anti-tumor responses and facilitating pro-tumor immunity [66]. The tumor microenvironment consists of a complex array of cells, blood vessels, lymphatic vessels, extracellular matrix, nutrients and signaling molecules [67]. All cell types in this microenvironment play some role in shaping the tumor growth and metastasis profile. In many solid tumors, cancer-associated fibroblasts are the most prominent cell type [68], and have been shown to play an important role in the initiation and progression of cancers, in addition to facilitating the metastatic process [67].

The main concepts associated with anti-tumor and pro-tumor immunity revolve around immunosurveillance and tumor-associated immune suppression. Tumor immunosurveillance involves the specific targeting of cancerous and pre-cancerous cells based on their expression of distinct tumor-associated antigens (TAAs) and tumor-specific antigens (TSAs) [69]. Tumor immunosurveillance leads to three possible outcomes; recognition of tumor antigens can lead to complete elimination of all cancer cells, an equilibrium state where selective growth of tumor cell sub-populations is matched by host immunity, or tumor escape where select tumor subpopulations evade host detection to grow and spread unimpeded. Tumor immune escape can result from defects in host immunity or in a process known as immunoediting, where tumor cell modification of molecular structures through further mutation allows for immune evasion [70].

Tumor-associated immunosuppression involves the expression of immune-regulatory cytokines and molecules by tumor cells, facilitating the proliferation and accumulation of immunosuppressive cell types such as Tregs, MDSCs and tumor-associated macrophages [71].

These immune-regulatory and suppressive cell types produce further cytokines and other molecules which promote an immunosuppressive network wherein the proliferation and activity of anti-tumor effector cells are suppressed, allowing for sustained tumor growth [71, 72] (Figure 1).

1.2.1 *Anti-Tumor Immune Response*

With heritable immunodeficiencies, it is mainly virus-induced cancers such as Epstein-Barr virus-induced lymphoblastic lymphomas and Kaposi's sarcoma that increase in frequency, rather than common epithelial cancers such as lung, colon and prostate cancers [73]. As patients with heritable immunodeficiencies rarely live beyond their 40's, adult onset cancers have much less opportunity to arise; it is nevertheless apparent that an important component of antitumor immunity is the recognition and targeting of cancer-inducing pathogens [74]. Murine studies investigating immune defects and immune deficiencies have demonstrated that an intact immune response is important for preventing and decreasing tumor growth [75, 76, 77]. In cancer patients, infiltration of anti-tumor effector cells such as $CD8^+$ T cells into tumor tissues has been associated with positive clinical outcomes [78, 79].

Innate effector cells such as natural killer (NK) cells and subsets of T cells including γδ T cells, $CD8^+$ cytotoxic T lymphocytes (CTLs), and natural killer T (NKT) cells, possess inhibitory and stimulatory surface receptors which enable anti-tumor responses [80]. Families of receptors involved in the innate anti-tumor response include NKR-P1, NKG2/CD94 heterodimers, Ly49 molecules found in rodents, and killer cell immunoglobulin (Ig) - like receptors (KIRs) found in humans [80, 81, 82]. Recognition of stress-induced major histocompatibility complex (MHC) class I-like molecules present on tumor cells or down-regulation of class I MHC on tumor cells via members of these receptor families can lead to eradication of transformed cells [80, 83]. Innate effector cells also use cell surface molecules such as Fas ligand (FasL) and TNF-related apoptosis-inducing ligand (TRAIL) to recognize tumor cell surface expressed receptors and induce tumor cell apoptosis [80]. Recognition of tumor cell-surface antigens can also lead to the release of effector molecules such as perforin, granzyme and cytokines to induce tumor cell apoptosis [80, 84, 85]. Activation of NK cells following exposure to cytokines including IL-2, IL-12 and IFNγ can lead to a rapid increase in cytolytic, secretory and proliferative activity [80, 86].

Signals from transformed cells including cytokines such as IFNα, IL-1β and TNF, and other molecules such as heat shock proteins (HSPs) function as indicators of cellular stress or

"danger" signals, and lead to the activation of antigen presenting dendritic cells (DCs) [80, 87]. Capture of TSAs and TAAs such as melanoma-associated antigen (MAGE) and prostate-specific antigen (PSA) by DCs leads to activation of the adaptive anti-tumor immune response [88]. Following antigen capture and activation via "danger" signals, DCs up-regulate and express co-stimulatory molecules such as B7, migrate to the draining lymph node and present tumor antigen-derived peptides to $CD4^+$ and $CD8^+$ T cells via MHC class II and MHC class I molecules, respectively [80]. Following secondary activation via tissue APCs presenting TAAs, TAA-specific $CD8^+$ T cells develop into CTLs and $CD4^+$ T cells into $CD4^+$ helper cells [80]. $CD4^+$ helper cells aid further in stimulating CTLs via cytokine release and CD40-CD40L interactions [80, 89]. CTLs elicit direct tumor cell lysis via the directed release of perforins following the recognition of tumor cell-associated peptides presented by tumor cells in the context of MHC class I [80]. Memory $CD4^+$ and $CD8^+$ T cells maintain protective anti-tumor immunity through the recognition of tumor-derived stress signals such as HSPs and IFNα [72].

Glycolipid-based TAAs may be presented by tumor cells and APCs via MHC molecules or members of the MHC class I-like family of CD1 molecules [90, 91]. NKT cells recognize glycolipid antigen presented in the context of CD1d molecules and are capable of eliciting direct anti-tumor cytotoxicity, in addition to activating downstream anti-tumor effector cells such as NK cells and CTLs following activation via generation of activating cytokines [90, 92, 93].

B cells are commonly found to infiltrate tumors and their presence is associated with improved prognosis of patients with breast cancer [72]. Tumor-infiltrating B cells may undergo antigen-driven proliferation and maturation within the tumor, producing antibodies specific to tumor cell-associated molecules [94, 95]. B cells may also function as local APCs and in provide co-stimulatory signals to T cells at the tumor site [80].

1.2.2 *Tumor-Associated Immune Suppression*

The tumor microenvironment consists of tumor cells, stromal cells, extracellular matrix, cytokines and growth factors, blood vessels, lymphatic vessels and infiltrating immune cells. Tumor-associated factors within this microenvironment such as tumor derived IL-6, and tumor-associated macrophages (TAMs) and MDSCs play important roles in mediating the immune suppression observed in moderate to advanced forms of cancer (Figure 1).

Tumors implement many strategies to both evade and modify host immunity. Similar to viruses undergoing antigenic drift to evade the immune response, tumors are able to down-regulate immunogenic antigens. Tumors can decrease expression of certain antigens as is seen with the melanoma antigen Melan-A/MART-1 where the gene promoter is silenced [96], as well as decrease antigen presentation through changes in antigen processing and presentation machinery [97]. Another important strategy used by cancer cells to survive is evasion of apoptosis. This can be accomplished through the up-regulation of anti-apoptotic proteins like $FLIP_{L,S}$, survivin and Bcl-2 [98, 99, 100] Tumor cells can also evade apoptosis through disrupting the CTL perforin/granzyme B cytotoxic pathway and by expressing soluble decoy death receptors which disrupt FasL-mediated cell death [101, 102]. Tumor cells can over-express IDO (Indoleamine 2,3 dioxygenase) to cause the breakdown of tryptophan and promote apoptosis and cell cycle arrest in effector T cells [103].

Tumor-derived IL-10 inhibits the proliferation and development of Th1 responses by peripheral blood mononuclear cells (PBMCs), skewing the host immune response towards a Th2 pro-tumor profile [104] (Figure 1). Tumors also produce pro-inflammatory molecules including PGE2, IL-6 and S100A8/A9 which induce a local pro-inflammatory environment, recruiting immunosuppressive cell types such as MDSCs [1], and promoting tumor growth and survival [105, 106, 107] (Figure 1).

Defects in DCs represent an important component in tumor evasion of the immune response [71]. Defects include decreased levels of functional antigen-presenting DCs, accumulation of immature DCs and elevated levels of tolerogenic DCs [108]. Importantly, tumors induce the proliferation and accumulation of MDSCs [109]. MDSCs are a heterogeneous mixture of immature myeloid cells in various stages of differentiation which exhibit an immunosuppressive phenotype. In mice, these cells can be identified through their expression of the cell-surface markers Gr-1 and CD11b [110]. There are various subtypes of MDSCs with Ly6C and Ly6G acting as major differentiation markers for monocytic and granulocytic MDSCs respectively. MDSCs accumulate in the blood and tissue in proportion to primary and metastatic tumor growth. MDSCs inactivate $CD4^+$ and $CD8^+$ T cells, inhibit CTL IFNγ production through cell-cell contact and ROS production [111], induce the accumulation of Tregs and drive the immune system towards a pro-tumor Th2 phenotype [111].

Natural killer T (NKT) cells are a subset of T cells possessing characteristics of both T lymphocytes and NK cells, and play an important role in regulating innate and adaptive immunity (discussed later – see section 1.3) [112]. Invariant NKT (iNKT) cells which possess invariant T cell receptors (TCRs) and recognize glycolipid antigen (see section 1.3.1), comprise the majority of the NKT cell population and play an important anti-tumor role [113-115]. Type II NKT cells in contrast have a more diversified TCR repertoire, recognize mainly sulfatide-based antigens and play a pro-tumor role. iNKT cells are suppressed and rendered anergic through the activity of Type II NKT cells [116, 117]. Type II NKT cells are induced through tumor activity, inhibiting NKT cell and CTL function and enhancing the function of TAMs and MDSCs through IL-13 production [116, 118].

Tumor and TAM production of certain chemokines such as CCL17 and CCL22 leads to the recruitment of Tregs into the tumor environment; tumor cells also promote the differentiation and expansion of Tregs [71]. Natural and inducible Tregs function to suppress immunity through mechanisms including the production of cytokines like IL-10 and TGFβ, release of immunosuppressive factors and cell-cell contact-mediated effector T cell inhibition [119, 120]. As reviewed in [121] and [122], Tregs play a significant pro-tumor role in the tumor microenvironment by promoting immunological tolerance towards the tumor and inhibiting anti-tumor immunity. Tregs secrete immunosuppressive molecules including IL-35, IL-10 and TGF-β, negatively influencing the expansion, cytokine production and effector function of effector T cells [121]. Tregs also produce VEGF which promotes tumor angiogenesis, kill tumor-targeting leukocytes through cytolytic activity, and induce up-regulation of IDO in DCs, leading to the depletion of tryptophan and subsequent suppression of effector T cell function [123, 124, 125, 126]. Tregs accumulate in cancer patients and have been correlated with a poor prognosis in breast, gastric and ovarian cancers [120]. In addition, depletion of Tregs facilitates tumor rejection and anti-tumor immunity in mouse models of cancer [127, 128].

TAMs can account for up to 50% of a tumor mass and function to promote tumor growth [129]. Typically, TAMs are M2 or alternatively activated macrophages which are associated with tissue repair, angiogenesis, down-regulation of the adaptive arm of the immune response, Th2-skewed T cell responses, and most importantly pro-tumor responses [130]. Monocytes are recruited to tumor sites early on by tumor-produced chemokines such as CCL2, differentiating pro-tumor M2 type macrophages in the presence of tumor-derived M-CSF and the differentiating cytokines

IL-4 and IL-13 [131, 132]. These M2 differentiated macrophages are desired in wound healing where they function in angiogenesis, tissue repair and scavenging [133]. However, in the case of a tumor, the production of inflammatory cytokines and chemokines like IL-6, CXCL8 and CCL2 enhances tumor angiogenesis and the recruitment of immunosuppressive myeloid cell populations [134].

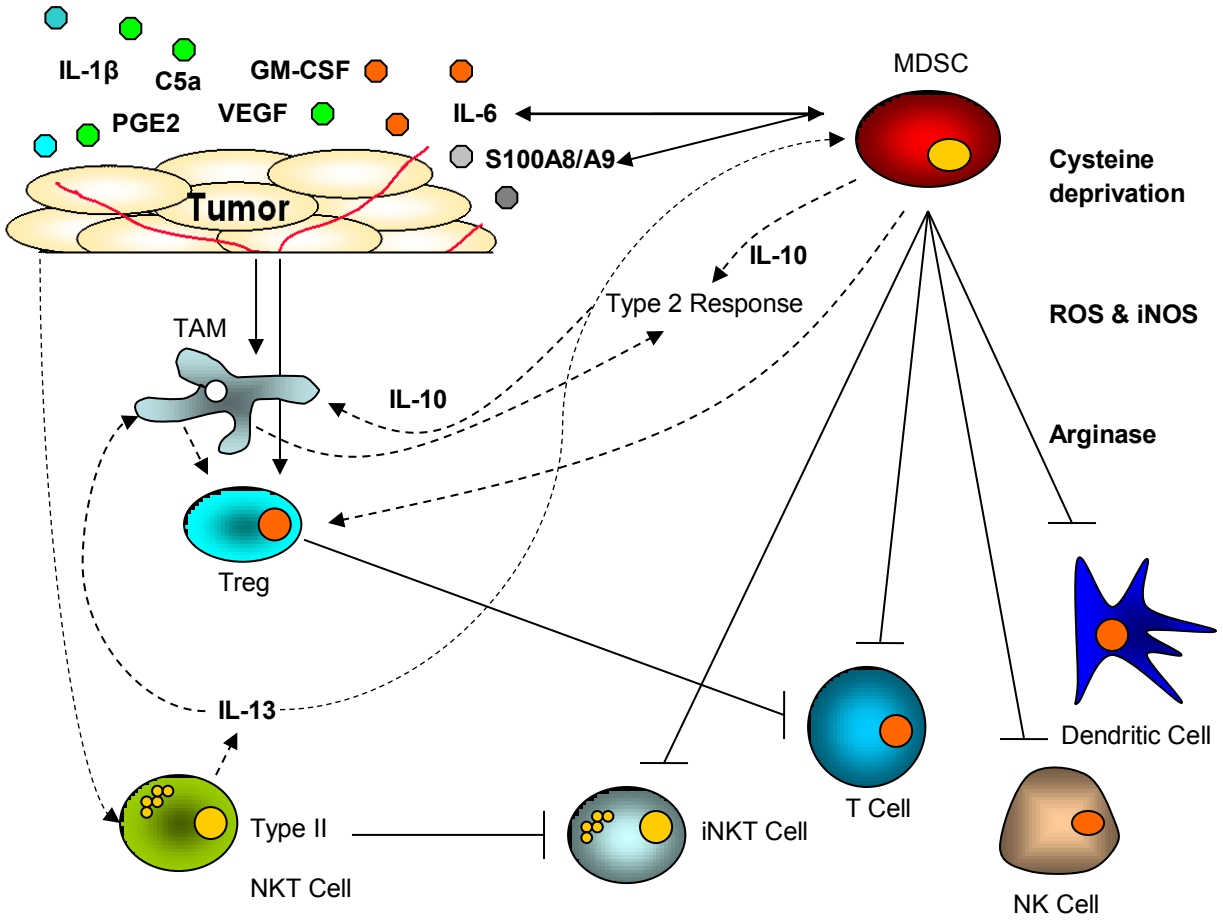

Figure 1: **Overview of immune cell activity induced with tumor-associated immune suppression.** Tumor-derived factors such as PGE2, IL-6 and S100A8/A9 molecules induce the expansion and accumulation of immunosuppressive cell types such as MDSCs, Tregs and TAMs. MDSCs promote a pro-tumor environment through suppressing T cell, NK cell, iNKT cell and DC function via cysteine deprivation, ROS and RNS production, and arginase activity. MDSCs also induce Treg and TAM activity. TAMs and MDSCs inhibit Th1 type T cell responses and produce IL-10, inducing a Th2-skewed pro-tumor T cell response. Tumor-induced Type II NKT cells directly inhibit iNKT cells and produce IL-13, positively reinforcing the activity of TAM and MDSC populations.

1.2.3 *Myeloid-Derived Suppressor Cells*

MDSCs originally known simply as immature cells (ImCs) were shown to accumulate in the peripheral blood of cancer patients [135]. By comparison, dramatic reductions in both number and function of circulating DCs have been observed [135]. One third of the peripheral blood ImC population was identified as immature DCs and macrophages, with the other two thirds representing early stage undifferentiated myeloid cells that could be differentiated into mature DCs in the presence of all-trans retinoic acid (ATRA) [135]. The ImCs were shown to inhibit the T cell stimulatory function of DCs and Ag-specific T cell responses [135].

Described as a highly heterogeneous group of undifferentiated myeloid cells possessing immunosuppressive properties, MDSCs can be found accumulating in the blood and tissues in a wide variety of conditions including chronic inflammatory diseases, viral infections and cancer [136]. MDSCs are not limited to a single cell type, but instead encompass a wide array of cell types and variants. Individual subsets are detected through distinct cell surface markers, variations in secreted factors, and mechanisms of immune suppression. An IL-1β-induced $Ly6C^-$ MDSC population identified in BALB/c mice has been shown to suppress NK cell development and function [137]. With disease progression, and especially in cancer, MDSCs accumulate in a variety of tissues including the spleen, blood, lungs and bone marrow [105]. MDSCs have been described in both mouse models of disease and in humans, with some variation in the immunosuppressive function and cell surface protein marker expression between the two species [138]. In mice, MDSCs can be detected using FACS analysis with selection for $Gr\text{-}1^+CD11b^+$ cells [59]. Monocytic MDSC populations are characterized as being $CD11b^+Ly6C^{high}Ly6G^-$ and capable of differentiating into macrophages and DCs [139]. Granulocytic MDSCs, representing ~75% of the MDSC population in common strains of mice including BALB/c mice, are $CD11b^+Ly6C^{low}Ly6G^+$, cannot be maintained cultured and do not differentiate into macrophages or DCs [139]. In humans, MDSCs are broadly defined as cells expressing the cell surface marker profile $CD11b^+CD33^+CD14^-$HLA-DR- [135, 140, 141, 142]. MDSCs accumulate in the blood, lymphatic tissues and tumor sites of cancer patients, promoting tumor growth, angiogenesis, and metastasis [143, 144]. In this body of work, the term MDSC will be used to refer to immature myeloid cells with immunosuppressive activity, which accumulate proportionally with cancer progression.

Tumor-associated factors such as prostaglandin E2 (PGE2) and pro-inflammatory S100 proteins are able to promote tumor progression by promoting the accumulation of MDSCs in the tumor environment [105, 145] (Figure 2A). MDSCs contribute to immune suppression through a number of mechanisms. Direct cross-talk between MDSCs and macrophages leads to the subversion of tumor immunity towards a type 2 response [146]. Direct MDSC-macrophage cross-talk leads to elevated IL-10 production by MDSCs and decreased IL-12 production by macrophages [146]. Treatment with the chemotherapeutic drug gemcitabine, was shown to partially reverse the skewing of the type 2 response by reducing MDSC levels [146]. Inflammation and more specifically inflammation-associated factors such as IL-6, IL-1, S100 proteins, and prostaglandins are extremely important in promoting the accumulation of MDSCs. Limiting tumor-associated inflammation both delays the accumulation of MDSCs and limits tumor progression [59]

MDSCs use a variety of mechanisms to inhibit the anti-tumor response. Using a C26 murine adenocarcinoma model, it was shown that MDSCs decrease IFNγ responsiveness of splenocytes through the up-regulation of iNOS which generates NO that inhibits phosphorylation of STAT1 in splenocytes [147]. MDSCs produce various reactive oxygen species (ROS) and deplete the local environment of available $_L$-arginine, limiting the viability of T cells by limiting their arginine supply [148]. ROS and NOS such as peroxynitrite ($ONOO^-$) can cause T cell suppression and tolerance via nitration of TCRs and CD8 molecules, decrease anti-tumor responses by CTLs through post-translational modification to peptide-MHC I complexes, and block migration of T cells to the tumor site via nitration of chemokines such as CCL2 [149]. MDSCs inhibit T-cell activation by depleting available cysteine and cystine [150]. MDSCs use the enzymatic properties ADAM17 to down-regulate the expression of L-selectin on $CD4^+$ and $CD8^+$ T cells [60]. This decreases trafficking of naïve T cells to peripheral lymph nodes where they would normally become activated. This property of MDSCs explains a common observation of reduced L-selectin levels on T cells in cancer patients [151]. In addition to acting as immunosuppressive agents, MDSCs also promote tumor angiogenesis through production of factors such as MMPs, VEGF and basic fibroblast growth factor (bFGF) [144, 152, 153]. Sunitinib, an angiogenesis inhibitor which targets receptor tyrosine kinases, has been shown to significantly reduce the accumulation of peripheral MDSCs in both human cancer patients and in various murine tumor models [154, 155]. Sunitinib inhibits the proliferation of monocytic MDSCs and

impairs the survival of granulocytic MDSCs, although these effects are observed in models demonstrating widely varying anti-tumor activity in response to sunitinib treatment [155]. Despite antiangiogenic treatments such as sunitinib, localized availability of growth factors such as GM-CSF can lead to the proliferation of intratumoral MDSCs which can promote antiangiogenic resistance [144, 152, 155, 156]. MDSCs are able to induce the proliferation of $CD4^+CD25^+FoxP3^+$ Tregs in human hepatocellular carcinoma patients [157].

In some gastric cancers, IL-1β has been shown to enhance IL-6 production in MDSCs via activation of the NF-κB pathway [158]. The use of an NF-κB inhibitor in IL-1β transgenic mice inhibited MDSC activity and suppressed the development of gastric cancer [159]. Curcumin, a compound derived from the herb *Curcuma longa Linn* has demonstrated anticancer activities, some of this activity being mediated through suppressing NF-κB activity [160]. In various cancer models including a murine model of gastric cancer, curcumin has been shown to inhibit MDSC activity and proliferation [161].

MDSCs can be therapeutically targeted by a number of means. Vincent et al. (2010) screened a number of common cytotoxic chemotherapeutic drugs including 5-fluorouracil (5FU), cyclophosphamide, gemcitabine, oxaliplatin, and doxorubicin for their ability to kill tumor-associated MDSCs. They demonstrated that a common chemotherapeutic drug, 5FU is capable of selectively killing MDSCs and as a result, enhancing T cell-dependent anti-tumor immunity [162]. In line with these findings, another of these chemotherapeutic drugs, gemcitabine, was shown to selectively eliminate splenic MDSCs in tumor-bearing mice, resulting in enhanced antitumor activity [110]. $CD4^+CD25^+$ T regulatory cells are sensitive to the effects of cyclophosphamide, which has been taken advantage of in mouse models of anti-cancer immunotherapy where treatments were curative for established tumors [163]. Thus, in addition to their direct cytotoxic effects on highly replicative cells, a number of chemotherapeutic agents also demonstrate the ability to selectively target certain immunosuppressive cell populations including MDSCs and Tregs. MDSCs can be targeted therapeutically via cytotoxic and immune cell stimulating agents or through natural mechanisms. All-trans retinoic acid (ATRA) treatment has been used in cancer models to induce differentiation of immature MDSCs into mature cell forms [164, 165]. This strategy was successfully combined with anti-cancer vaccine protocol in murine cancer models to relieve MDSC-immune suppression and enhance the vaccine effectiveness [164].

NKT cell activity has been shown to decrease MDSC number and function in a mouse model of influenza A virus infection via a TCR and CD40L-dependent mechanism [166] (Figure 2C). In this model, mice lacking iNKT cells had a substantial increase in MDSC levels, resulting in decreased anti-influenza immunity, increased virus titer and increased mortality [166]. These findings were comparable to human infection where $CD11b^+$ MDSCs were isolated from the peripheral blood of IAV-infected patients. The suppressive activity of these MDSCs was inhibited by treating them with ARG1 or iNOS inhibitors or by culturing them with α-GC-stimulated human iNKT cells [166]. Based on these findings, we were interested in looking at the effects of iNKT cell activation on MDSC function in mouse models of breast cancer. As MDSCs are an important target for decreasing cancer-related immune suppression, it is important to implement therapy strategies that both target tumor cells and decrease immune suppressive cell types such as MDSCs. The use of cytotoxic chemotherapeutic compounds has been shown to be effective in targeting MDSCs. However, the toxic side-effects of these compounds should be avoided if at all possible. If iNKT activation can be effective in targeting both metastatic tumor cells and decreasing tumor-associated immune suppression, the requirement for substantial levels of toxic chemotherapeutic chemicals could be dramatically reduced. Even if iNKT activation does not have MDSC-targeted effects, it may be effective to target MDSCs and immune suppressive cells in combination therapies involving iNKT cell-based treatments and additional therapy options. This could be accomplished through the use of a compound such as gemcitabine which has been shown to decrease MDSCs while preserving iNKT cell number and function [110, 167]. In a mouse model of mesothelioma, gemcitabine treatment reduced the number of MDSCs while selectively preserving viability of $CD4^+$ and $CD8^+$ T cells [167].

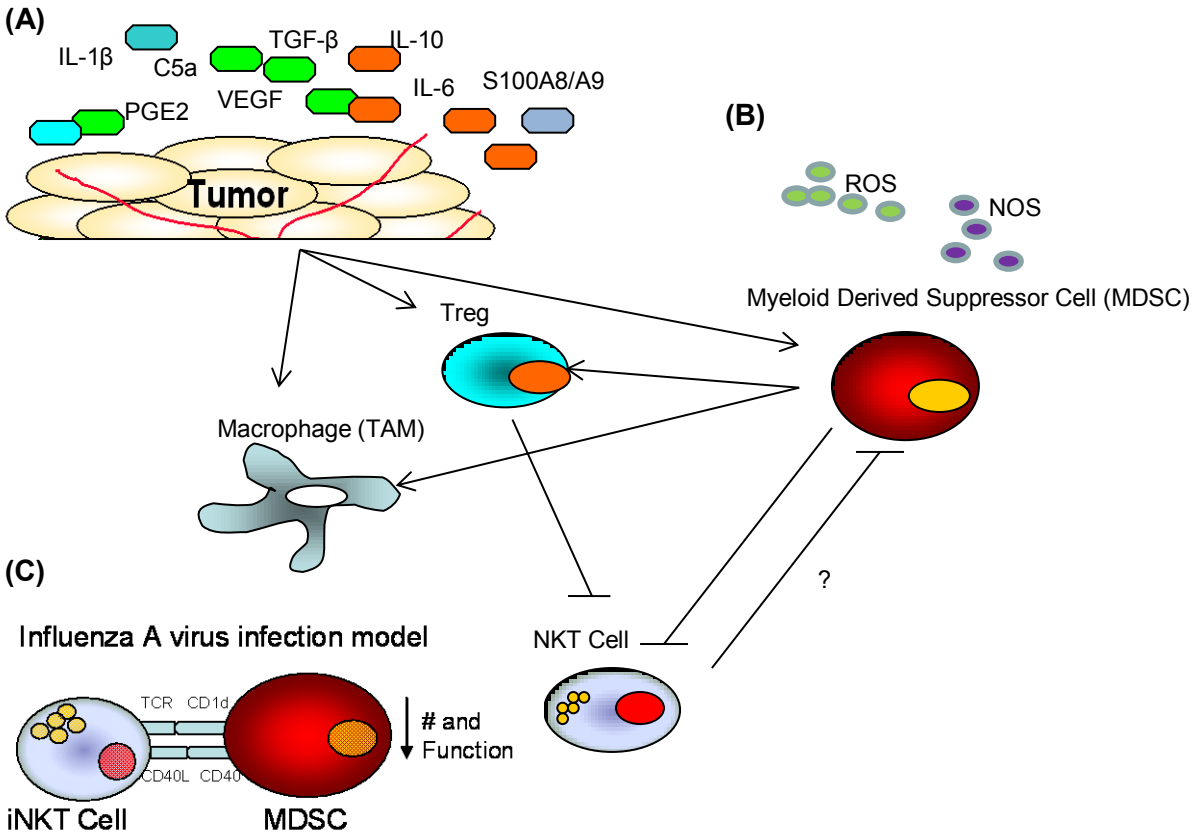

Figure 2: Tumor-associated MDSC proliferation and MDSC activity leads to the suppression of NKT cell function. (A) The tumor microenvironment produces a variety of pro-inflammatory molecules (IL-6, C5a, prostaglandins), immunosuppressive molecules (IL-1β, IL-10), and tumor-related growth and pro-angiogenic factors (TGF- β, VEGF). These molecules induce immune-suppressive leukocyte populations including Tregs, TAMs, and MDSCs to traffic to and accumulate in tumor tissues. **(B)** MDSCs produce immunosuppressive molecules such as ROS and NOS which inhibit T cell and NKT cell function. **(C)** NKT cell activity in viral infection has been shown to decrease both the frequency and immunosuppressive activity of MDSCs in a TCR-CD1d/CD40L-CD40 dependent manner, indicating a possibility for NKT cells to function similarly in cancer models.

1.3 Natural Killer T Cells

NKT cells are a subset of T cells which possess phenotypic and functional properties of both natural killer cells and T lymphocytes [168]. Identified in 1986 [169], and later given the name natural killer T cell in 1994 [170], NKT cells express intermediate levels of αβ T cell receptors (TCRs) in addition to NK cell markers and products, including surface NK1.1 and intracellular perforin and granzyme [168]. $CD4^+$ and $CD8^+$ T cells respond via diverse TCR specificities to peptide antigens presented by antigen presenting cells (APCs) on the major histocompatibility complex (MHC) class II and class I, respectively [171]. In contrast NKT cells respond via invariant TCRs to glycolipid molecules presented by APCs via the MHC class I-like molecule CD1d [171] (Figure 3). Various cell types including dendritic cells, B cells and macrophages express cell surface CD1d and are capable of presenting glycolipid to and activating NKT cells [172].

Invariant NKT (iNKT) cells, expressing a canonical TCR rearrangement (Vα14Jα18 in mice and Vα14Jα24 in humans), are the largest NKT cell population and account for the majority of NKT cell-associated activity [173]. iNKT cells respond to various glycolipids, both self and non-self, but the primary molecule used experimentally and clinically to activate iNKT cells is a marine sponge-derived sphingoglycolipid known as α-galactosylceramide, abbreviated α-GalCer or α-GC [174175].

Additional minor subsets of NKT cells that are restricted by CD1d but do not recognize α-GalCer have been identified [173, 176]. These Type II NKT cells have different CD1d-restricted TCRs that recognize other glycolipids and include a subset (Vα9 TCR rearrangement) that recognize sulfatide-containing glycolipids [177, 178]. CD1d-independent NKT-like cells have also been described which are mainly conventional T cells that upregulate NK cell markers following activation [173]. In measuring the relative contributions of Type 1 versus Type II NKT in cancer research, the most effective approach to date has been to assess tumor growth in CD1d-deficient mice lacking Type I and Type II NKTcells versus TCR Jα18 chain-deficient mice lacking Type I NKT cells only [176]. Type II NKT cells may function in an opposing manner to iNKT cells as demonstrated in tumor models showing differences in tumor clearance in $J\alpha18^{-/-}$ vs. $CD1d^{-/-}$ mice [118].

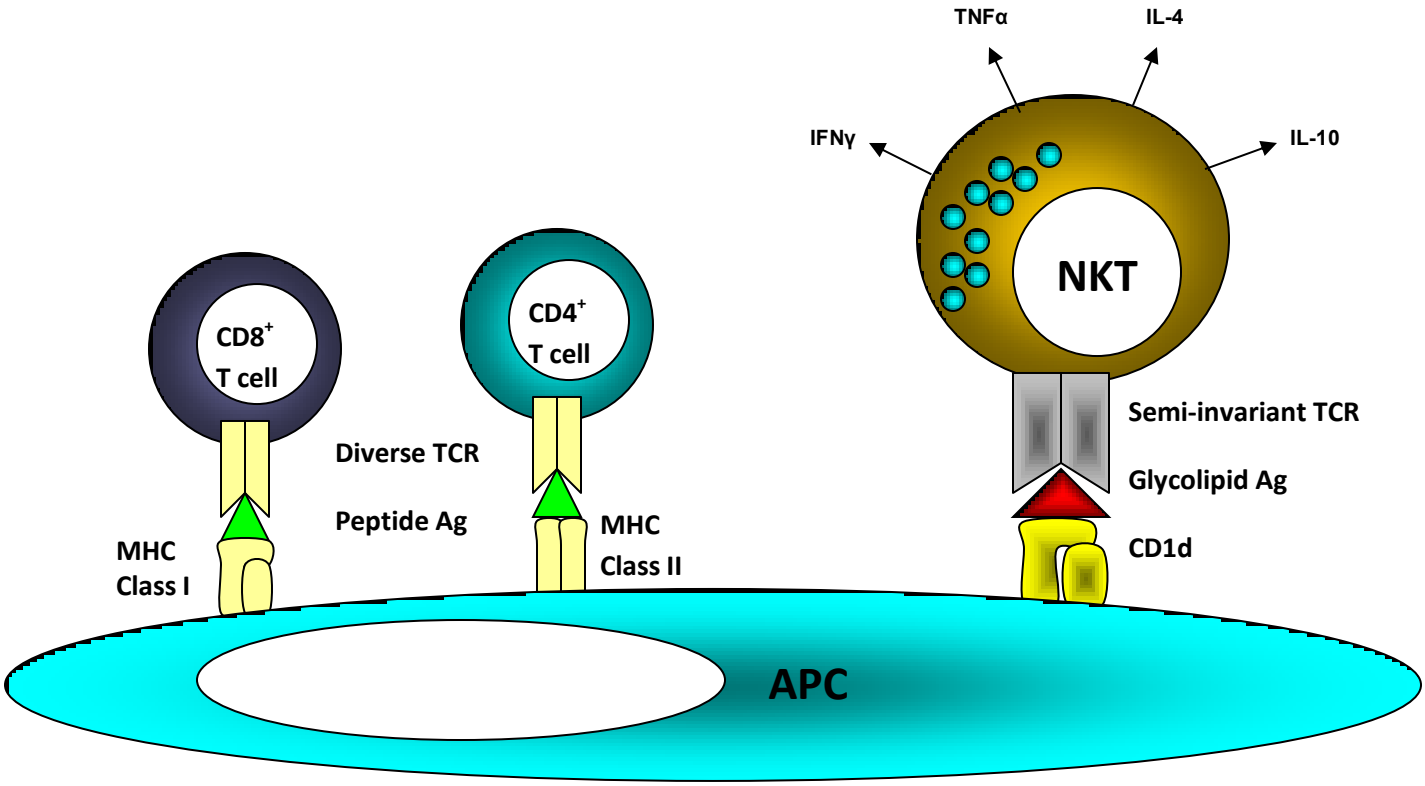

Adapted from E. Tupin *et al*. 2007. *Nat. Rev*. 5: 405-417.

Figure 3: NKT cells via semi-invariant TCRs respond to glycolipid antigen presented by CD1d molecule on APCs. NKT cell activation leads to rapid translation of pre-formed cytokine-encoding mRNAs, leading to a rapid burst of high quantities of immune-modulatory cytokines including IFNγ, TNFα, IL-4, and IL-10. In contrast $CD4^+$ and $CD8^+$ T cells respond via diverse TCRs to peptide antigens presented by MHC Class I and II molecules on APCs.

1.3.1 *iNKT Cells*

iNKT cells are the most well described subset of NKT cells and account for the highest proportion, ~95%, of NKT cells in both humans and mice [179]. iNKT cells are highly conserved between humans and mice [168] (Table 2). Human and mouse iNKT cells express conserved TCR gene rearrangements (Jα14Vα18 in mice and Jα24Vα18 in humans), and can recognize glycolipid presented by CD1d from either species [180]. One key difference is the frequency of hepatic iNKT cells in humans and mice. iNKT cells represent ~30% of the liver lymphocyte population in mice compared to ~1% in humans [168]. Both self and foreign glycolipids are capable of activating iNKT cells; self-glycolipids include β-D-glucopyranosylceramide (β-GlcCer) that plays a role in NKT cell selection, and other endogenous glycolipids that accumulate in humans and mice during infection and in response to Toll-like receptor agonists [181]. Foreign glycolipids include glycolipids derived from bacteria and parasites such as glycosphingolipids derived from *Sphingomonas* species [181]. NKT cells contain large numbers of preformed mRNAs encoding cytokines such as IL-4 and IFN-γ [182]. Upon activation, iNKT cells will rapidly translate and produce a variety of Th1, Th2, and Th17-type cytokines (Figure 3). iNKT cells can be activated via multiple pathways; activation can be caused by inflammatory cytokines and/or self-antigen presented by CD1d, or by presentation of microbial glycolipids by CD1d [183]. From this point iNKT cells will be referred to simply as NKT cells, given their high frequency within the NKT cell grouping and dominant function among NKT cell subgroupings.

The array of NKT cell subsets in humans include $CD4^+CD8^-$, $CD4^-CD8^+$, and $CD4^-CD8^-$ cell types (Table 2). Mice lack the $CD4^-CD8^+$ subset [168]. In humans these subsets vary in overall cytokine expression levels, with $CD4^-CD8^-$ and $CD4^-CD8^+$ subsets preferentially producing Type I cytokines such as IFNγ and TNFα, and the $CD4^+CD8^-$ subset preferentially producing Type II cytokines such as IL-4 and IL-10 [184]. These differences are less distinct in mice although the $CD4^-CD8^-$ subset is associated with better IFNγ-dependent anti-tumor responses [199].In mice, a subset of $NK1.1^-$ NKT cells generates the Th17 type cytokine IL-17. This subset makes up 5-15% of NKT cells in peripheral sites but represents the majority of NKT cells in peripheral lymph nodes [185].

Experimental activation of NKT cells typically involves either the injection of free glycolipids or the adoptive transfer of glycolipid-loaded DCs. A major issue associated with the administration of free glycolipid for the treatment of diseases is that B cell and macrophage

mediated presentation of glycolipid to NKT cells induces anergy, associated with the up-regulation of the cell-surface protein PD-1 [186, 187, 188]. Up-regulation of PD-1 on NKT cells persists for more than a month following *in vivo* free glycolipid activation [189]. Targeting the PD-1L: PD-1 interaction using blocking antibodies against PD-1, PD-1L and PD-2L prevented NKT cell anergy in the B16 melanoma metastasis model, allowing for consecutive successful NKT cell activations and overall enhanced anti-metastatic effects [189]. Another strategy is to transfer DCs loaded with glycolipid as this has been shown to ameliorate anergy and make NKT cells responsive to subsequent glycolipid stimulations [182]. It is thought that free glycolipid treatment allowing for multiple APC types to present glycolipid to NKT cells does not lead to optimal presentation of glycolipid by DCs to NKT cells [172], and therefore the potential activation levels of NKT cells following α-GC administration are limited as compared to DC-based activation.

NKT cells are capable of mediating direct cell-cell cytotoxicity through the use of perforins, granzymes, Fas/FasL and TRAIL [190]. Indirect cytotoxicity is mediated through activation of downstream effector cells including NK cells, $CD8^+$ CTLs and DCs [191]. Optimal NKT cell activation is achieved through reciprocal activation of NKT cell and DCs as a result of co-stimulatory interactions between NKT cells and DCs, including CD40-CD40L, TCR-Ag-CD1d, CD28-B7.1/B7.2, and soluble molecules such as IL-12 [192].

iNKT cells have been shown to play an important anti-tumor role in cancer patients and in animal models of cancer [174, 193, 194, 195 , 196] (Discussed in section 1.3.3). NKT cell-dependent anti-tumor immunosurveillance has been noted in murine methylcholanthrene (MCA)-induced tumor models, where tumor development was enhanced in $J\alpha18^{-/-}$ mice compared to wild type mice [197, 198]. Similarly, $p53^{+/-}$ mice lacking NKT cells exhibited increased tumor incidence, adding further support for the anti-cancer role of NKT cells [176]. Although NKT cells are capable of directly killing tumor cells [197], NKT cell-based anti-cancer effects are primarily indirect, occurring through the activation of NK cells and CTLs following NKT cell IFNγ production and NKT cell-induced IL-12 production by DCs [191, 199]. IL-12 production by DCs enhances IFNγ production by NKT cells following glycolipid activation [200].

Despite a clear anti-tumor role for iNKT cells, the function of Type II NKT cells remains somewhat unclear, exhibiting tumor promoting roles in some models and no role in others. Type II NKT cells like iNKT cells are CD1d-restricted and produce Th1 and Th2 cytokines, but unlike iNKT cells have more diverse TCRα chains and respond mainly to sulfatide-based glycolipids

[118]. Tumor promoting properties of Type II NKT cells have been demonstrated in several tumor models where tumor growth was compared in Jα18$^{-/-}$ mice lacking iNKT cells and CD1d$^{-/-}$ mice lacking all CD1d-restricted NKT cells [118]. Demonstrating the pro-tumor role of Type II NTK cells – specific activation of either iNKT cells with α-GC or Type II NKT cells with sulfatide-based glycolipids in the murine CT26 lung metastasis showed complete abrogation of tumors following iNKT cell activation while Type II NKT cell activation led to enhanced tumor burden [116]. In contrast, it was found that both p53$^{+/-}$ CD1d$^{-/-}$ and p53$^{+/-}$ Jα18$^{-/-}$ mice had similar overall tumor incidence and survival time, suggesting no tumor-promoting effect associated with Type II NKT cells [176]. Furthermore, CD1d$^{-/-}$ and Jα18$^{-/-}$ mice exhibited similar susceptibility to MCA-induced sarcoma development [176]. Although iNKT cells play a clear anti-tumor role, the understanding of the role played by Type II NKT cells in cancer remains incomplete and it may be the case that this role varies depending on the model used and context of cellular activation.

Table 2: Comparison of iNKT cell properties between humans and mice.

Characteristic	Human	Mouse
TCR	Vα24Jα18 / Vβ11	Vα14Jα18 / Vβ8/7/2
CD1d-restricted TCR	Yes	Yes
Mature NKT cell subsets	$CD4^+CD8^-$, $CD4^-CD8^-$, $CD4^-CD8^+$	$CD4^+CD8^-$, $CD4^-CD8^-$
Cytokine production	IFNγ, TNF, IL-4, IL-10, IL-13, IL-17, GM-CSF	IFNγ, TNF, IL-2, IL-4, IL-10, IL-13, IL-17, IL-21, IL-22, GM-CSF
Responsive to α-GC	Yes, and α-GC analogues	Yes, and α-GC analogues
% Leukocytes		
Blood	Typically 0.01-0.5%	0.2-0.5%
Liver	~1%	~30%
Spleen and bone marrow	0.01-0.5%	0.2-0.5%
Thymus	<0.001-0.01%	0.2-0.5%
Lymph node	0.01-0.5%	0.1-0.2%

Adapted from Berzins *et al*. *Nat Rev Immunol*, 2011.

1.3.2 *α-Galactosylceramide and Analogues*

α-Galactosylceramide, also known as KRN7000, is a glycolipid molecule that was originally isolated from the Okinawan marine sponge *Agelas mauritianus* by researchers at the Kirin Brewery Company of Japan [201]. α-Galactosylceramide, commonly abbreviated as α-GC or α-GalCer, is now synthetically produced rather than derived from its' original source [202]. The full chemical name for α-Galactosylceramide is (2S,3S,4R)-1-O-(alpha-D-galactosyl)-N-hexacosanoyl-2-amino-1,3,4-octadecanetriol (Figure 4).

Many chemical modifications of α-GC have been performed to produce an array of synthetic glycolipids with varying abilities to activate NKT cells *in vivo* and skew their responses towards Th1 or Th2. Overall, work being done to enhance, produce and discover new NKT cell activating glycolipids involves work with glycolipids of bacterial origin, various α-GC analogues and variations of α-GC such as sulfatide containing molecules [203]. Of course, many of the modifications to α-GC produce molecules incapable of stimulating NKT cells. For example, the alkylation of galactosylthiol produces α-*S*-galactosylceramide, a molecule incapable of activating NKT cells *in vitro* or *in vivo* [204].

Two α-GC analogues were used in this body of work, α-C-GC and OCH, due to their abilities to skew the NKT cell cytokine response towards Th1 and Th2, respectively. The α-C-GC analog has a carbon-based glycosidic linkage (Figure 4) which decreases its affinity for both the NKT cell TCR and APC CD1d molecule as compared to α-GC in the ternary antigen presentation complex [177]. This reduced affinity leads to a decreased period of antigen presentation in the presence of α-C-GC and related C-glycoside ligands [205]. The prolonged Th1-biased immune response associated with these C-glycoside ligands, however, is a characteristic desired in activating downstream anti-cancer effector cells. OCH, the first identified Th2-skewing analog of α-GC, has shortened acyl and sphingosine chains (Figure 4), resulting in a decreased half-life of binding to CD1d and a lower TCR avidity than the α-GC/CD1d complex [206]. The main difference in skewing towards Th1 and Th2 cytokine production for α-C-GC and OCH is likely related to the stability of these glycolipids in the CD1d binding cleft [206]. The Th1 skewing effect of α-C-GC is a result of a more stable, pH-resistant association with CD1d molecules and vice versa for OCH [206].

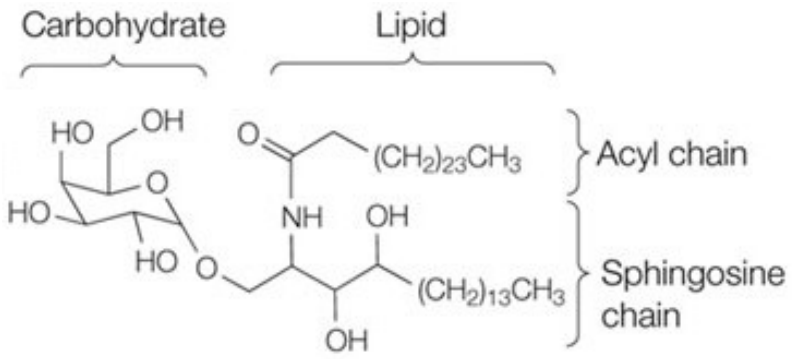

α-GalCer

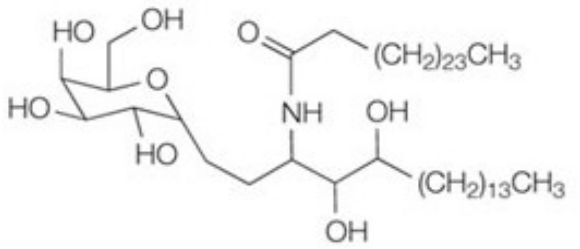

α-C-GalCer

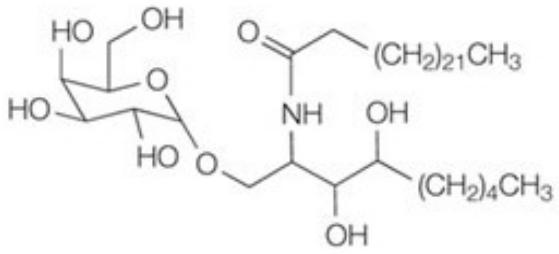

OCH

Adapted from Van Kaer, *Nat Rev Immun*, 2012.

Figure 4: NKT cell-activating glycolipids.

Experimental activation of NKT cells is mediated by α-galactosylceramide and analogous molecules. Activation of NKT cells with α-galactosylceramide induces the production of a mixture of Th1 and Th2 cytokines. The C-glycoside analogue of α-GC (α-C-GC) has a carbon-based glycosidic linkage and induces a Th1-skewed cytokine response. OCH has shortened acyl and sphingosine chains and induces a Th2-skewed cytokine response.

1.3.3 *Anti-tumor NKT Cell Activity*

Jα18$^{-/-}$ mice which lack Vα14 NKT cells develop MCA-induced fibrosarcoma earlier and at a rate ~70% greater than that observed in wild type mice [197]. This effect is partly due to direct lytic activity of NKT cells towards MCA-induced cancer cells, as it was shown that in addition to being able to lyse a number of cancer cell lines such as YAC-1 and EL4-S3 to levels similar to NK cells, NKT cells also have the ability to target and lyse the MCA-induced cancer cell line MCA-1 [197]. Direct toxicity against TAMs has been demonstrated in mouse models of neuroblastoma and is associated with decreased immune suppression and enhanced anti-tumor immunity [212]. Following α-GC activation, NKT cells are capable of eliciting perforin-dependent and independent anti-tumor cytotoxicity *in vitro* and *in vivo* [174, 193].

Treatment of mice bearing oncogene- and chemical-dependent cancers with α-GC has been shown to both delay the establishment of tumors and decrease overall tumor growth [213]. In this study, cancers included MCA-induced sarcomas, mammary sarcomas in Her-2/neu transgenic mice, and spontaneous sarcomas in p53$^{-/-}$ mice. The use of α-GC combined with anti-DR5 and anti-4-1BB mAbs has been shown to induce tumor rejection in mouse models of renal cell and mammary carcinoma [214]. Multiple downstream anti-tumor pathways are activated following NKT cell activation and elicit an indirect NKT cell mediated anti-tumor effect. One component of this indirect anti-tumor mediated by NKT cells in humans may be their ability to enhance the effector activity of T cells such as Vγ9Vδ2 T cells. Vγ9Vδ2 T cells cultured in the presence of activated NKT cells are activated through NKT cell TNFα production to produce enhanced levels of IFNγ and increased degranulation in the presence of tumor cells [113].

Consistent with their role in controlling cancer, NKT cell infiltration into colorectal carcinomas and neuroblastomas is associated with a favorable prognosis [210, 211], while a low level of circulating NKT cells in the peripheral blood is associated with poor survival of patients with acute myeloid leukemia [208]. Similarly, low circulating levels of IFNγ-secreting NKT cells have been noted in the peripheral blood of patients with diverse cancers, including colon, breast and renal cell carcinomas [207], and NKT cells from cancer patients also exhibit an impaired proliferative response to α-GC compared to cells from healthy volunteers [209]. This suggests that optimal endogenous NKT cell activity is impaired in cancer patients, indicating that NKT cell activating therapies may be beneficial.

1.3.4 *NKT Cell Activation in Human Clinical Trials*

In addition to the substantial evidence for NKT cell mediated anti-cancer activity in mouse models of cancer, NKT cell-based immunotherapies have also generated positive outcomes in phase I/II human clinical trials for head and neck carcinomas and non-small cell lung carcinomas [175, 194, 195, 196, 215].

NKT cell-based immunotherapy has thus far been safely implemented in a number of anti-cancer and anti-viral Phase I and Phase II clinical studies. Veldt et al. (2007) [216] performed a dose-escalating randomized placebo-controlled phase I/II trial performed and looked at the effect of injecting free α-GC at doses ranging from 0.1μg/kg to 10μ/kg into 40 chronic hepatitis C patients. Although one patient possessing high baseline iNKT cell levels responded with a transient 1.3 log decrease in HCV-RNA, treatments in general had no significant effect on HCV-RNA levels. αGC was however proven to be safe for human administration, with no noted adverse side-effects to the treatment.

In a 2005 phase I study, eleven patients with advanced non-small cell lung cancer or recurrent lung cancer received intravenous injections of $5 \times 10^7 - 1 \times 10^9$ /m^2 autologous α-GC-pulsed DCs [194]. No severe adverse side-effects were observed and one patient receiving the highest dose of 1×10^9 DCs demonstrated a dramatic expansion in peripheral Vα24 NKT cells [194]. This indicated that NKT cell activation and expansion could be elicited in cancer patients.

A phase I-II study conducted in 2009 examined treatment with α-GC-pulsed PBMCs in 17 patients with advanced non-small cell lung cancer [195]. Treatments were administered intravenously four times and no serious adverse side-effects to treatment were noted. Elevated IFNγ-producing cell numbers were detected in the peripheral blood of 10 of 17 patients following treatment. Five cases remained as stable disease while the other 12 demonstrated progressive disease. The median survival time among the 10 patients with increased IFNγ-producing cell numbers 31.9 months as compared to 9.7 months for the 7 poor-responding patients [195].

Positive clinical outcomes were also observed in a 2008 Phase I clinical study using autologous α-GC-pulsed DCs injected into the nasal submucosa of nine patients with unresectable or recurrent head and neck cancer [196]. Again, no serious adverse effects were observed. Following treatments, four of nine patients demonstrated increased NKT cell numbers and eight of nine patients demonstrated enhanced natural killer cell activity [196]. Of the nine

patients, one demonstrated a partial response with a reduction in the primary tumor mass from 22 to 7 mm, five patients exhibited no change in existing disease status, and three patients exhibited continued disease progression [196].

A phase I clinical trial performed in 2009 involved the use of intra-arterial infusions of *in vitro*-expanded NKT cells combined with sub-mucosal injections of α-GC-loaded-APCs to treat eight patients with head and neck squamous cell carcinoma [175]. Treatments induced elevated numbers of NKT cells and IFNγ-producing cells in 7 of 8 patients. Minor grade 1-2 toxicity was observed in 7 patients associated with anti-tumor responses. Three of eight patients demonstrated significant clinical outcomes; four patients had stable disease and one patient exhibited progressive disease following treatment [175]. In 2011, a phase II clinical study was performed on 10 patients with head and neck squamous cell carcinomas using *ex vivo*-expanded NKT cells and α-GC-pulsed APCs [215]. Seven of the ten patients demonstrated increases in NKT cell numbers with five of these patients also demonstrating tumor regression, associated with elevated NKT cell numbers [215].

Preclinical models and clinical trials involving the administration of α-GC-loaded DCs have proven to be successful in promoting strong anti-cancer responses, targeting metastatic disease and promoting progression-fee survival. Furthering upon the success observed in clinical trials, it would be valuable to assess α-GC-loaded DCs as a post-surgical intervention in breast cancer, specifically targeting metastatic disease through NKT cell activation following primary tumor resection.

1.4 Post-Surgical NKT Cell Activation Model

Clinical data from phase I trials for head and neck cancer using adoptively transferred α-GC-loaded APCs showed that NKT cell activation is capable of causing primary tumor regression in a small number of patients [196]; however, the main effect observed in α-GC-based clinical trials is that NKT cell activation leads to longer survival times despite a lack of primary tumor regression [195, 196]. These findings are consistent with results found using NKT cell activation in animal models of cancer and suggest that the effects of clinical NKT cell activation work best to target metastatic disease. Rather than causing regression of macroscopic tumor masses, treatments in animal cancer models have decreased systemic metastasis [90, 112, 217, 218]. This makes sense, as metastatic foci are typically smaller than the primary tumor mass. Clearance of

CTCs and overall systemic anti-cancer effects following NKT cell activation are also likely reasons for the ability of this treatment to limit metastatic disease. As a result of inherent factors in tumor cells or selective pressure imposed by chemotherapies, the effects of chemotherapies in promoting cancer regression can become limited over time [219]. Reasons for this include access of the drug to the target site and anti-drug resistance mechanisms developed among metastatic cells such as up-regulation of efflux pumps to pump out chemotherapeutic agents and down-regulation of cell membrane transport proteins involved in the uptake of the drugs [219, 220]. The combination of low toxicity and strong systemic effects make the use of NKT cell-activating therapies a promising anti-metastatic treatment option as compared to conventional chemotherapeutic agents.

Previous work with the 4T1 model has involved excision of the primary tumor mass, followed by administration of anti-cancer therapeutics such as anti-S100 protein Abs to target the effects of MDSCs [105]. Given that in most cases of breast cancer, the primary mammary tumor can be surgically removed and that this post-surgical system has been demonstrated in mice, it is possible that an effective anti-cancer treatment can be established by resecting the primary tumor and then providing NKT cell-activating therapeutics to selectively target systemic metastases. Removing the primary tumor mass not only eliminates the main source of CTCs, but also eliminates the main source of induction of tumor-associated immune suppression (Figure 5). Upon removal of the primary tumor mass, immune system recovery is expected as immunosuppressive cell populations including MDSCs, TAMs and Tregs dissipate (Figure 5). This immune recovery is vital, as NKT cell activating treatments are not only dependent on NKT cell function, but also downstream activation of NK cells and effector T cells.

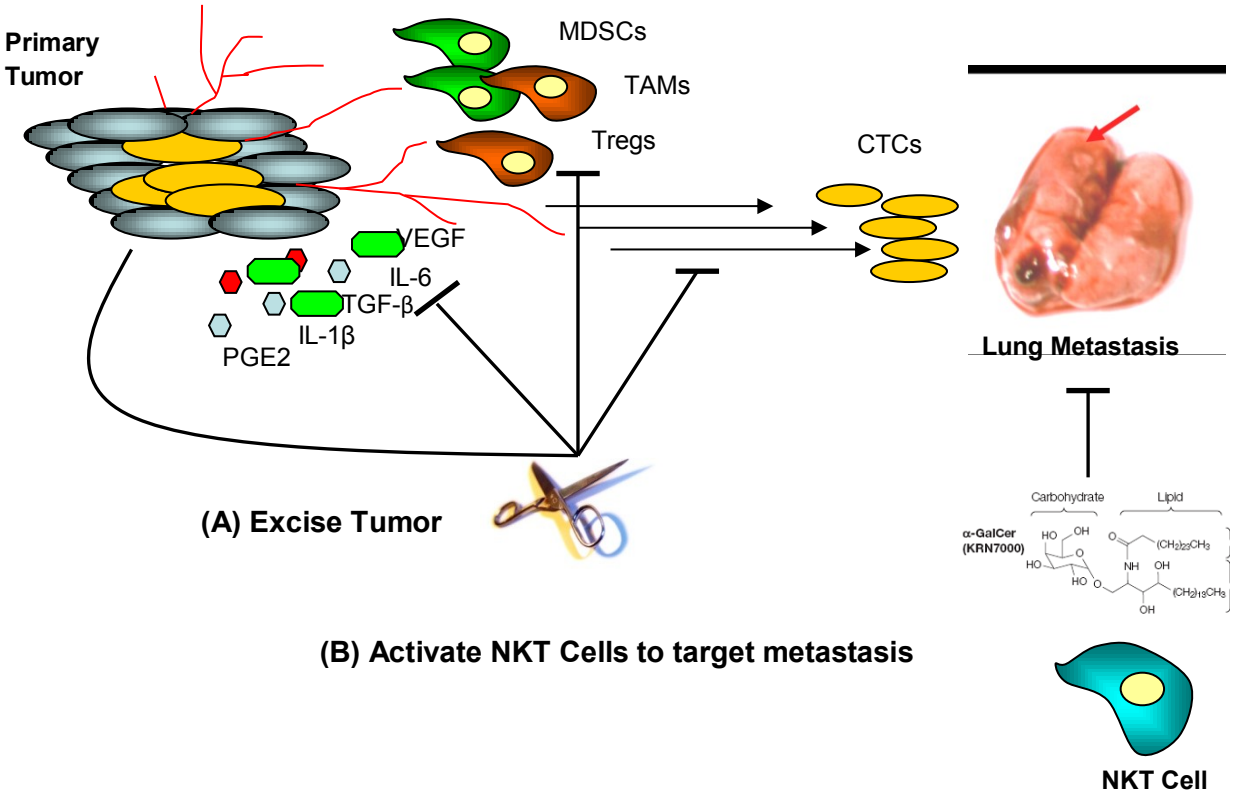

Figure 5: NKT cell activation as a post-surgical treatment for metastatic breast cancer. The primary tumor microenvironment is highly immunosuppressive as a result of the production of molecule such as PGE2, IL-1β, and TGF-β which induce pro-tumor immunosuppressive cell types like MDSCs, TAMs and Tregs. **(A)** Primary tumor excision accomplishes three things; the primary tumor mass is removed and this also results in the main source of immunosuppression and circulating metastatic tumor cells (CTCs) being removed. **(B)** Elimination of the primary tumor mass and diminished immune suppression allows for optimal targeting of metastatic foci through systemic anti-tumor immune response activation via NKT cell-activating glycolipids.

1.5 Objective

Given that 90% of cancer-related deaths are due to metastatic disease, therapies targeting metastasis are of vital importance for the future of cancer treatment. The ability of NKT cell-activation based immunotherapy to target metastatic lesions in both human and murine systems provides a basis for developing NKT cell-based immunotherapy strategies to treat metastasis associated with advanced cancers. Typically, cancers are treated using chemotherapeutic drugs, surgical resection or ionizing radiation to either kill or remove malignancies. However, given the ability of an activated immune system to respond to and destroy cancer cells under various circumstances, and the fact that α-GC-based treatments have already been approved for use in clinical trials, there is good potential for the use of NKT cell activation strategies in a system representative of clinical treatments for patients being treated for metastatic breast cancer. Thus, this research implemented murine models of metastatic breast cancer, where metastasis primarily occurs to the lung tissue. By removing the primary tumor after allowing establishment of metastatic disease, NKT cells could then be activated to target the lung-associated metastasis. It is hypothesized that this post-surgical NKT cell-based treatment system will allow for significant decreases in systemic metastasis and tumor-associated immune suppression, leading to enhanced disease-free survival outcomes.

The first aim was to target metastasis using intraperitoneal injections of free glycolipid, including α-GC and two altered analogs, α-C-GC and OCH. Based on these experiments, glycolipids to be used for subsequent adoptive cell transfer experiments could be determined. The second aim was to use adoptive transfers of glycolipid-loaded DCs to improve upon the effects of free glycolipid injections. α-GC-loaded DC transfers decrease the likelihood of inducing Th2 type responses or NKT cell anergy, and promote enhanced NKT cell activation compared to free glycolipid. DC transfers can therefore be expected to allow for multiple activations and an improved patient response and survival outcome. The third aim was to use adoptive transfer of expanded NKT cells in addition to glycolipid-loaded DCs to bypass the effects that cancer has on NKT cell frequency and function as a result of tumor-associated immune suppression. The effects of all three treatment options were assessed by examining the effects of treatments on NKT cell activation levels, metastatic tumor burden, tumor associated immune suppression, and overall survival.

Chapter 2: Materials and Methods

2.1 Post-Surgical Treatment Model

The general model system and treatment methods used in my studies are outlined in Figure 6. Mice were injected sc. in the fourth mammary fatpad on day 0 with 2 x 10^5 4T1 or EO771 mammary carcinoma cells. The primary mammary tumor developed and was excised at day 12 after it had reached ~200mm^3. The next day, mice were given NKT cell-activating treatments consisting of free glycolipid, adoptively transferred glycolipid-loaded DCs or adoptively transferred NKT cells. Some groups of mice receiving NKT cells also received glycolipid-loaded DCs or free glycolipid stimulation at 14 days post-tumor cell injection (see sections 2.11, 2.12, and 2.14). To measure the effects of treatments, mice were sacrificed at days 21, 28, 35 and 150 days post-tumor cell injection and their lungs plated with 6-TG selection to assess metastatic burden in the lung tissue (see section 2.7). Serum cytokine samples we taken following activation to assess the extent of Th1 and Th2 type cytokine production and gauge the overall immune response (see section 2.18). Blood PBL Gr-$1^+$$CD11b^+$ levels were assessed long term as a prognostic indicator of health. The effects of NKT cell activation on blood MDSC frequency and immunosuppressive function were measured using FACS analysis and T cell proliferation assays (see section 2.19). Overall survival was assessed up to the experimental endpoint of 150 days.

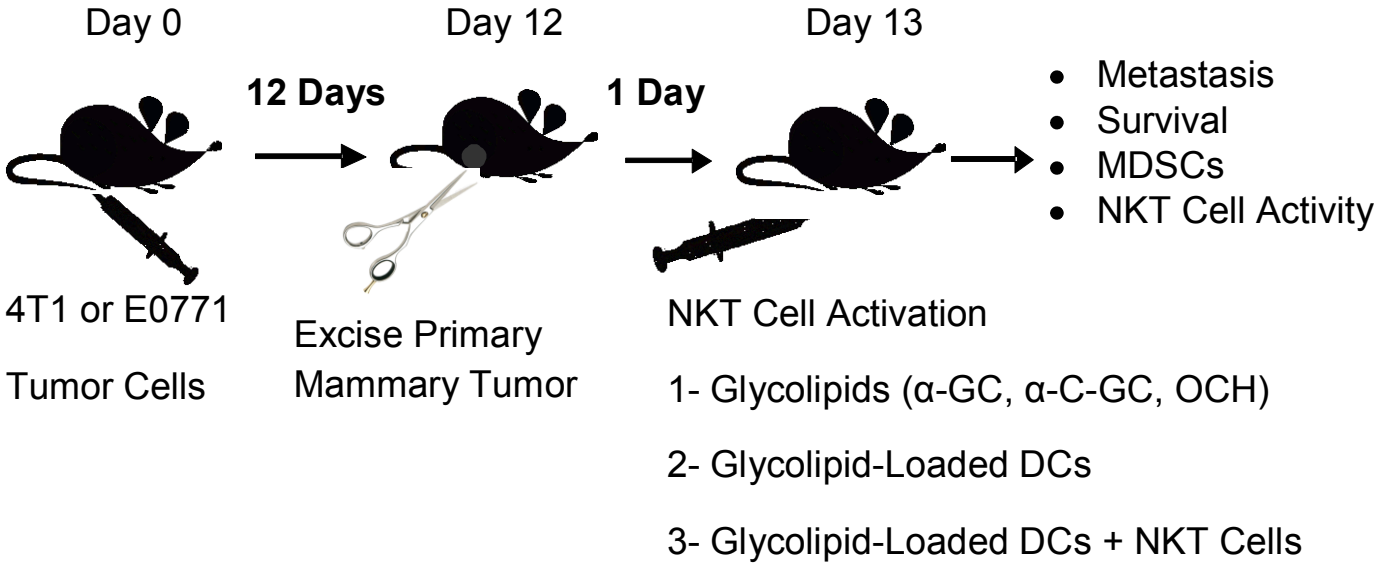

Figure 6: Schematic of post-surgical treatment protocol. Mice are injected with (sc. 2 x 10^5) mammary tumor cells on day 0. Twelve days post-tumor cell injection, the primary mammary tumors are resected. Thirteen days post-tumor cell injection, NKT cell activation is performed via free glycolipid injection, adoptive transfer of glycolipid-loaded DCs, or adoptive transfer of glycolipid-loaded DCs and *in vivo* expanded NKT cells. Serum samples are taken at 2, 6, 24 and 48 hours post-activation. NKT cell activity, MDSC frequency and functional activity, metastatic tumor burden and anti-tumor immune response are measured at set time points subsequent to NKT cell activation. Overall survival is assessed up to a 150 day experimental endpoint.

2.2 Media and Solutions

Iscove's Modified Dulbecco's Medium (IMDM) containing L-Glutamine and HEPES, Hank's Balanced Salt Solution (HBSS) without calcium or magnesium, high glucose Dulbecco's Modified Eagles Medium (DMEM) containing L-glutamine and without sodium pyruvate, RPMI-1640 containing L-glutamine, 10X phosphate buffered saline (PBS) diluted to 1X using Millipore filtered distilled water, fetal bovine serum (FBS), 10,000U/ml Penicillin-10,000µg/ml Streptomycin (PS), and 0.25% Trypsin-EDTA were all purchased from Invitrogen-Life Sciences (Burlington, ON) or Thermo Scientific-HyClone (Logan, UT). Puromycin dihydrochloride was purchased from BioShop Canada (Burlington, ON) and diluted to 1mg/ml with Millipore filtered distilled water. Methylene blue was purchased from BioShop and diluted to a 0.03% solution with Millipore filtered distilled water. 6-Thioguanine was purchased from Alfa Aesar (Ward Hill, MA) and diluted to a 60mM stock solution with Millipore filtered distilled water. Saline solution (0.9% sodium chloride) was purchased from B. Braun Medical Inc. (Irvine, CA). DC media was prepared using 500µl of a 10mM stock of β_2-Mercaptoethanol (Sigma Aldrich, Oakville, ON), 1ml of 100x MEM non-essential amino acids (Invitrogen) and 1ml of 100x sodium pyruvate (Invitrogen) in 98ml of RPMI-1640 containing 10% FBS and 1% P/S. All media and solutions were stored at 4^{o}C with the exception of FBS, PS and Trypsin-EDTA (-20^{o}C), and methylene blue (25^{o}C).

2.3 Glycolipid Compounds

α-GC ((2A,3S,4R)-1-O-(α-D-galactipyranosyl)-N-hexacosaoyl-2-amino-1,3,4-octadecanetriol) was purchased from Alexis Biochemicals (San Diego, CA) and reconstituted at a concentration of 1 mg/ml in a saline solution containing 0.5% Tween-20. Once dissolved, it was aliquoted and stored at 4^{o}C. OCH ((2S,3S,4R)-1-(α-$_{D}$-galactopyranosyl)-2-tetracosanoylaminononan-3,4-diol) was obtained from the National Institutes of Health Tetramer Core Facility (Emory University, Atlanta, GA) and reconstituted with 1ml of cell culture grade water purchased from HyClone. α-C-GC ((2S,3S,4R)-1-1CH_2-(α-$_{D}$-galactopyranosyl)-2-(*N*-hexacosanoylamino)-1,3,4-octadecanetriol) was obtained from the National Institutes of Health Tetramer Core Facility and dissolved in 1ml of DMSO (Sigma-Aldrich) and warmed to 50^{o}C along with sonication. Aliquots of 10µl were stored at -20^{o}C. Prior to use, glycolipid compounds were sonicated at 50^{o}C for 20 minutes.

2.4 Mice and Cell Lines

C57BL/6 and BALB/c wild type mice were acquired form Charles River (Lasalle, QC) or Jackson Laboratories (Bar Harbour, ME). Jα18$^{-/-}$ knockout C57BL/6 mice were provided by Dr. Masaru Taniguchi (RIKEN Research Center for Allergy and Immunology, Kanagawa, Japan) [221]. Mice were maintained according to institutional guidelines in the Carleton Animal Care Facility (Halifax, NS). Experimental procedures were approved by the University Committee on Laboratory Animals. Tumor experiments were performed with female C57BL/6 mice from 8-12 weeks of age and female BALB/c mice from 6-8 weeks of age.

4T1 tumor cells syngeneic to BALB/c mice and E0771 cells syngeneic to C57BL/6 mice were obtained from Dr. Jean Marshall (Dalhousie University). 4T1 cell cultures were periodically grown with 30μM 6-TG selection to assess for maintenance of drug resistance. GFP-expressing 4T1 tumor cells were generated using the Phoenix^{TM} Retroviral Expression System provided by Dr. Craig McCormick and purchased from Gentaur (Santa Clara, CA). Puromycin-resistant and 6-thioguanine-resistant E0771 cells were generated by serial passaging of E0771 cells in 2μg/ml puromycin dihydrochloride or 30μM 6-TG respectively, followed by selection and expansion of resistant clones. E0771 cell cultures were maintained in media containing either 2μg/ml puromycin dihydrochloride or 30μM 6-TG to ensure maintenance of drug resistance.

2.5 Tumor Cell Injections

When tumor cell cultures reached ~80% confluency, the media was aspirated and the cells were detached with 5ml of trypsin-EDTA for 10min at 37^{o}C. Media containing serum (5ml) was added to the cells to inactivate trypsin and cells were centrifuged for 10min at 300xg. After removing the media, cells were washed with 5ml saline and centrifuged as before. Cells were resuspended in 1-2ml of chilled saline, counted, and diluted further in saline to a concentration of 2 x 10^5 cells/100μl saline. Tumor cells, either 4T1 or E0771, were injected subcutaneously into the fourth mammary fat pad of isoflurane-anesthetized BALB/c and C57BL/6 mice respectively, at a dose of 2 x 10^5 cells per mouse in 100μl of saline. Injections were performed using 1ml syringes and 27 gauge needles.

2.6 Primary Mammary Tumor Resection

Primary mammary tumors were resected 12 days post-tumor cell injection, when the primary tumors reached ~200m^3 as described by Pulaski and Ostrand-Rosenberg [55]. The abdominal fur was shaved with Oster small animal trimmers with 2-3cm margins. The mice were anesthetized with inhaled isoflurane and kept under anesthetic for the duration of the surgery. The shaved area was wiped with 70% ethanol, followed by iodine and again with 70% ethanol. The skin superficial to the tumor, the subcutaneous tumor, and any tumor invasive to the peritoneal lining was surgically resected. The skin was sutured together using 5-0 polypropylene sutures purchased from Ethicon (Somerville, NJ). The mice were given 10µl buprenorphine analgesic (BCM Corporation; Bloomingdale, NJ) purchased from McGill Universityin 500µl saline injected sc. in the dorsal subcutaneous cavity. Mice were allowed to recover on a heating pad for 4-5 hours post-surgery.

2.7 Clonogenic Assays for Tumour Cell Metastasis

At set time points post-tumor cell injection, the lungs of the mice were removed and assayed to assess the numbers of metastatic cells present in the tissue. On days 14, 21, 28 and 35 post-tumor cell injection, groups of mice were sacrificed using isoflurane inhaled anesthetic followed by cervical dislocation. The clonogenic assays were performed as previously described by Pulaski and Ostrand-Rosenberg [55], with some modifications. Briefly, the lungs were removed, rinsed in 2ml HBSS, minced with scissors into a 1.5ml microcentrifuge tube containing 1ml of HBSS, and then transferred to a 40µm nylon mesh filter in a 50ml conical tube. The tissue was forced through the mesh with a 1ml syringe plunger and then rinsed through with 3ml of HBSS. Different volumes (1ml, 500µl, and 200µl) of the cell suspension (4 ml total) were plated in 10ml of IMDM containing either 60µM 6-TG for the BALB/c 4T1 model or 1µg/ml puromycin for the C57BL/6 E0771 model. Plates were incubated for 10-14 days at 37^{o}C with 5% CO_2. At this point the media was poured off and the plates fixed with 100% methanol for 5 minutes. Plates were rinsed with 5ml distilled water and stained for 5 minutes with 0.03% methylene blue. Plates were rinsed again with 5ml of distilled water, and dried prior to counting the number of colonies. Colony forming units in whole lung tissue were calculated as: (4 x # colonies on 1ml plate + 8 x # colonies on 500µl plate + 20 x # colonies on 200µl plate)/3. It is

likely that colony forming units were underestimated in some plates with extensive colony coverage.

2.8 Retroviral Transduction

The Phoenix^{TM} Retroviral Expression System is a product of Gentaur (Santa Clara, CA) and in generating GFP-expressing 4T1 tumor cells, was used according to the manufacturer's protocol for transduction of adherent cell lines. Briefly 5 x 10^5 4T1 cells per well were seeded into a 6-well plate (Cellstar®). After 16 hr, the culture supernatant was removed and 3ml of infection cocktail added to each well. The 3ml cocktail consisted of 1ml of GFP-expressing virus stock, 2μg/ml polybrene, and 2ml of DMEM containing 10% FBS and 1% P/S. Serial dilutions of the virus stock down to 10^{-5} were used for the 6 wells. Plates were centrifuged at 500xg for 90min. After 3 hours incubation at 37^{o}C and 5% CO_2, the supernatant was removed and 5ml fresh media was added. After a further 24 hours of incubation, the media was replaced with 5ml media containing 1μg/ml puromycin dihydrochloride to select for cells transduced with the viral vector. Cells were left to incubate, with selective media replacement every 48 hours and analysis of GFP expression by fluorescence microscopy every 24 hours. GFP-expressing cells were sorted by FACS and expanded in selective media prior to freezing down 3 x 10^6 cell aliquots under liquid nitrogen or orthotopic injections of 2 x 10^5 cells into BALB/c mice.

2.9 Fluorescence Microscopy

Green fluorescence expression in transduced cell lines was assessed using a Leica Microsystems LEICA DM5000 fluorescence microscope (Richmond Hill, ON) and images analyzed using Velocity 5.5.1 software (PerkinElmer, Woodbridge, ON).

2.10 Tissue Imaging

Organ and tissue imaging was performed using a Leica S6D stereozoom microscope and QCapture software (QImaging, Surrey, BC).

2.11 Glycolipid Treatment Experiments

Mice received free glycolipid treatments ip. in doses of 1μg, 4μg, or 20μg one day after primary tumor excision. Stock 1μg/μl preparations of α-GC, α-C-GC, and OCH were diluted

into 1xPBS to make final injection volumes of 100µl per mouse. α-C-GC and OCH were only used at a dose of 4µg per mouse.

2.12 Dendritic Cell Culture and Adoptive Transfer

Dendritic cell isolation and adoptive transfer were performed under sterile conditions. Strain-appropriate mice were sacrificed via cervical dislocation under isoflurane-induced anesthesia. Mice and surgical tools were sterilized with 70% ethanol. Femurs and tibias from one BALB/c mouse per NKT cell transfer experiment were removed and washed in 70% ethanol followed by DC media. The ends of the bones were cut with scissors and the marrow pushed through into a 40µm nylon cell strainer in a 50ml conical tube using a 30-gauge needle and 10ml syringe containing 10ml of DC media. The marrow was forced through the cell strainer with the 10ml syringe plunger and washed through with the remainder of the 10ml of DC media. The resulting cell suspension was centrifuged at 300 x g for 10min. The supernatant was aspirated and the cells resuspended in 5ml 0.8% ammonium chloride solution for erythrocyte lysis. After 5 min 5ml of DC media was added to stop the lysis and the previous centrifugation step was repeated. The supernatant was removed and the cells resuspended in 30ml DC media containing 12µl GM-CSF (0.1µg/ml). This cell solution was distributed evenly into a 6 well cell culture plate and incubated at 37^{o}C with 5% CO_2 for 3 days. After 3 days, 5ml of fresh DC media containing 2µl GM-CSF was added to each well. After another 3 days of incubation at 37^{o}C, non-adherent cells were harvested by pipetting into a 50ml tubes. Wells were rinsed with 2ml of DC media and this rinse added to the 50ml conical tubes. Cells were then centrifuged at 300xg for 10min. DCs were resuspended in 30ml DC media containing 6µl GM-CSF and distributed evenly into a 6 well plate. The next day, 2µg αGC was added to each well except for control unloaded wells. The following day, nonadherent cells (via aspiration) and adherent cells (via trypsin treatment), were harvested into 50ml tubes and centrifuged at 300 x g for 10min. Cells were then rinsed in 10ml DC media, centrifuged, and resuspended in 1X PBS for counting with a hemocytometer. Cells were diluted in 1X PBS as required and injected into mice iv. at a dose of $2 \times 10^4 - 3 \times 10^6$ cells in 100ul 1X PBS per mouse. α-GC-loaded-DCs were also transferred (iv. 6×10^5) into some mice to allow for *in vivo* expansion of liver NKT cells to be used for therapeutic adoptive transfer treatments. DCs being given to mice for the purpose of *in vivo* NKT cell expansion were loaded with 1µg α-GC per well.

2.13 Liver Lymphocyte Isolation

BALB/c mice received α-GC-loaded DCs (iv. 6 x 10^5) for *in vivo* NKT cell expansion. After 3 days, mice were anaesthetized using inhaled isoflurane and then sacrificed by cervical dislocation. All remaining procedures were performed under sterile conditions. The abdominal region was sprayed with 70% ethanol. Livers were surgically harvested and the gall bladders removed. In a 60mm cell culture dish (Corning Inc., Lowell, MA) livers were minced with scissors in 5ml of HBSS containing 5% FBS. The tissue was then forced through 40μm wire mesh into a 15ml BD® Falcon tube using the plunger from a 1ml syringe (BD) and washed with 5ml HBSS containing 5% FBS. Samples were centrifuged at 500 x g for 10 min at RT. The cells were then washed with 10ml HBSS + 5% FBS and again centrifuged at 500 x g for 10 min at RT. Pellets were transferred into a 37.5% Percoll solution consisting of 9.4ml Percoll (GE Healthcare, Baie d'Urfe, QC), 2.5ml 10X PBS and 13.1ml dH_2O. Samples were then centrifuged at 700xg for 15 min at 20^oC. Erythrocyte lysis was then performed by re-suspending the pellets in 5ml Ammonium Chloride lysis buffer (Sigma-Aldrich) for 5 min. To stop lysis, 7ml HBSS + 5% FBS was added followed by centrifugation at 300xg for 10 min. Cells were resuspended in 1.5ml 1XPBS + 2% FBS and counted using a hematocytometer. Expanded NKT cells were isolated by staining cells with FITC-labeled anti-TCRβ antibody (clone H57-197; eBioscience, San Diego, CA) and APC-labeled α-GC-loaded CD1d tetramer (NIH Tetramer Core Facility) for cell sorting using a BD FACSaria sorter.

2.14 NKT Cell Isolation and Adoptive Transfer

FACS-sorted *in vivo* expanded NKT cells were resuspended in saline and their numbers verified with a hematocytometer count. NKT cells were adoptively transferred iv. into BALB/c mice at a dose of 2 x 10^5 to 1 x 10^6 cells in a total volume of 100μl per mouse. Some groups of mice receiving iNKT cells also received ip. 4μg α-GC or iv. 5 x 10^5 DCs.

2.15 Blood Leukocyte Cytospins

Blood (50μl) from female BALB/c tumor-resected mice (day 35 following tumor inoculation) and control unchallenged mice was used for cytospins and subsequent staining and imaging. Red blood cells were lysed by adding 2ml of ddH_2O for 1min followed 30 seconds later by the addition of 2ml of 2xPBS. Samples were centrifuged at 300xg for 5min and

leukocytes were resuspended in 400µl HBSS. Cytospins were performed using a Cytospin 3 from Shandon (Bohemia, NY). Silinated slides (Ultident; St. Laurent, QC) were centrifuged at 500xg for 2min with 50µl HBSS loaded to pre-wet the slides. Prepared blood samples (300µl; ~ 1 x 10^5 – 3 x 10^5 cells) were centrifuged with low acceleration for 5min at 300xg. Slides were allowed to dry overnight at room temperature. Samples were fixed for 3 hours in 10% acetate buffered formalin. Samples were stained with hematoxylin and eosin (H&E) by Histology and Research Services (Department of Pathology, Dalhousie University). Slides were examined and photographed with a Zeiss Axioplan 2 imaging microscope and AxioVision 4.8 software (Toronto, ON) at 1000x magnification.

2.16 Blood Lymphocyte Isolation for Flow Cytometry

Blood lymphocyte isolation was performed as follows: 4-10 drops of blood were collected in 5ml BD® Falcon tubes containing 20µl of 10,000U/ml heparin (Sigma-Aldrich). Samples were vortexed briefly followed by the addition of fluorochrome-conjugated antibodies, followed by another brief vortex and 35min incubation at room temperature. Following staining, the samples were resuspended in 2ml of ddH_2O added. After 30 sec, 2ml of 2xPBS was added to stop lysis and the samples were centrifuged for 10 min at 300xg. The supernatant was aspirated and the lysis procedure was repeated. Samples were resuspended in 300µl 1%PFA for flow cytometric analysis.

2.17 Flow Cytometry

Antibodies were titered for optimal staining using isolated splenocytes. Cultured GFP-expressing 4T1 cells (0.5-3 x 10^6) were isolated using trypsin treatment and transferred to a solution of 1x PBS containing 5% FBS. These cells were sorted using a FACSAria flow cytometer (BD Biosciences, Mississagua, ON) and CellQuest software (BD Biosciences), gating cells using the Fluorescein isothiocynate (FITC) channel. To examine MDSCs, blood samples were stained with a Phycoerythrin (PE)-labeled anti-CD11b (clone M1/70) antibody purchased from eBioscience (San Diego, CA) and a Peridinin chlorophyll protein (PerCP)-labeled anti-Gr-1 (Ly6G and Ly6C) (clone RB6-8C5) purchased from BD Biosciences. Some blood samples were also stained in combination with one or more of the following antibodies to differentiate granulocytic and monocytic MDSCs: FITC-labeled anti-CD11c (clone N418), Allophycocyanin

(APC)-labeled anti-Ly6G (clone RB6-8C5) and APC-labeled anti-F4/80 (clone BM8) all from eBioscience, APC-labeled anti-CD115 (clone AFS98) and PE-labeled Ly6C (clone HK1.4) from BioLegend (San Diego, CA), and/or anti-CX3CR1 Goat IgG and PE-labeled anti-goat IgG from R&D Systems (Minneapolis, MN). Expanded liver leukocytes (~1.8 x 10^8) for adoptive transfer experiments were isolated from BALB/c mouse livers and stained with FITC-labeled anti-TCRβ (clone H57-597) from eBioscience and APC-labeled α-GC-loaded mCD1d tetramers (NIH Tetramer Core Facility) for sorting NKT cells.

2.18 Serum Cytokine Assays

Blood samples were taken from mice via submandibular puncture at 2, 6, 24 and 48hr after ip. injection of α-GC, α-C-GC, OCH, or iv. injection of α-GC-loaded DCs, or iv. injection of expanded iNKT cells. Samples were collected in 1.5ml microcentrifuge tubes containing 20µl 10,000U/ml heparin. The samples were centrifuged at 2300 x g for 5 minutes and the serum was extracted and stored at -80^{o}C. Cytokine levels for IFNγ and IL-4 were measured using IFNγ and IL-4 ELISA kits (eBioscience) according to manufacturer specifications. Samples were measured using a BioTeck® Epoch Microplate Spectrophotometer (Winooski, VT) with BioTeck® Gen 5 Data Analysis Software and analyzed using SoftMax Pro software from Molecular Devices (Sunnyvale, CA).

2.19 Functional Suppression Assay

At day 35, 100µl of blood was drawn into FACS tubes containing 20µl 10,000U/ml heparin solution from the submandibular vein of naïve mice, tumor-resected mice receiving no DC therapy, and mice treated on day 13 with 2 x 10^5 α-GC-loaded DCs. RBC lysis was performed as per section 2.15 and samples were resuspended in 200µl RPMI. Responder cells for the assay were isolated from the spleens of naïve mice. Spleens were pressed through 40µm wire mesh into 15ml BD® Falcon and washed with 5ml RPMI. RBC lysis was performed using 5ml ammonium chloride solution for 5 min, followed by the addition of 5ml RPMI. Cells were pelleted at 500xg for 10 min at RT and re-suspended in RPMI. Cells from naïve spleens were stained with Oregon Green (Invitrogen) as per the manufacturer's protocol and 2 x 10^5 T cells were combined with blood in a 1:1 ratio in 200µl RPMI. Anti-CD3/anti-CD28 beads (Invitrogen) were added at a ratio of1 bead: 2 cells and samples were incubated at 37^{o}C 5% CO_2

for 72hr. Responder cell proliferation was assessed by flow cytometry gating on T cells stained with APC-conjugated anti-CD4 (clone RM4-5, ebiosciences) and PE-conjugated anti-TCRβ (clone H57-597, ebiosciences). Cell division was assessed by dilution of Oregon Green staining [222].

2.20 Statistical Analysis

All data are expressed as mean ± standard error of mean (SEM) of pooled data sets, unless otherwise noted. All statistical analysis was performed using an unpaired approach using GraphPad Instat or GraphPad Prism 5 software (Graphpad Software Inc.; La Jolla, CA). Statistical analysis for multiple comparisons was performed by one-way analysis of variance (ANOVA) followed by Bonferroni post-hoc test, or a nonparametric Kruskal-Wallis test, followed by Dunn's post-hoc test. Statistical analysis for comparisons performed between two groups was performed using a parametric two-tailed t-test with Welch correction or a Mann-Whitney nonparametric two-tailed test. Statistical significance was set at p values less than 0.05. Significant differences are indicated in each figure. The data were not considered significantly different unless indicated.

Chapter 3: Results

3.1 The BALB/c 4T1 Model

Primary mammary 4T1 tumors could be detected in BALB/c mice within 3-4 days of (sc.) 2 x 10^5 tumor cell injection and grew at a highly consistent rate. At day 12, tumors had reached approximately 200mm^3 in size (Figure 7A). To model human breast cancer treatment, primary tumors were excised at 12 days post-tumor cell injection. This included removal of both the primary tumor tissue and the adjacent inguinal lymph node (Figure 7B).

Approximately 8 days following (sc. 2 x 10^5) mammary fat pad injection of 4T1 tumor cells, metastatic colony forming 4T1 cells could be detected in the lung tissue based on 6-TG plating assays (Figure 8). By 12 days post-tumor cell injection, when the primary mammary tumors are surgically resected, hundreds of 4T1 colony-forming units (CFU) could be detected in the lung tissue (Figure 8). At time points of 21, 28, and 35 days post-tumor cell injection, >1000, >10,000, and >100, 000 CFU respectively could be detected in the lung tissue by clonogenic 6-TG plating assays (Figure 8). Around 35 days post-tumor cell injection, untreated mice died from respiratory failure associated with accumulation of metastatic cells in the lungs.

(A)

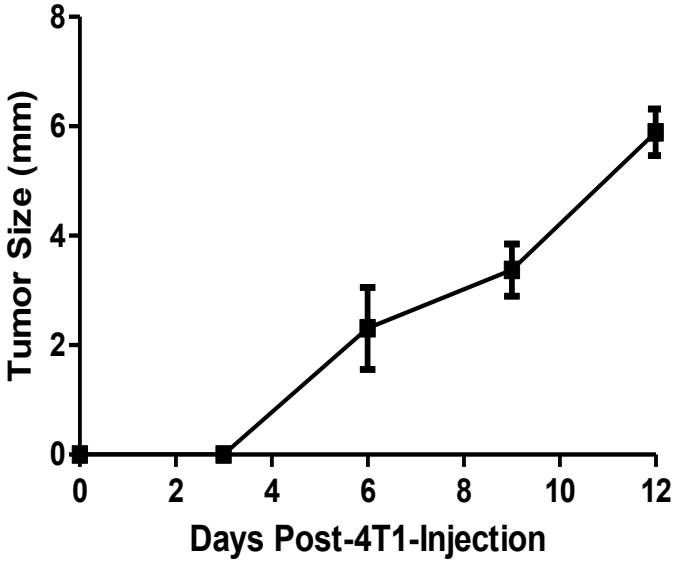

(B)

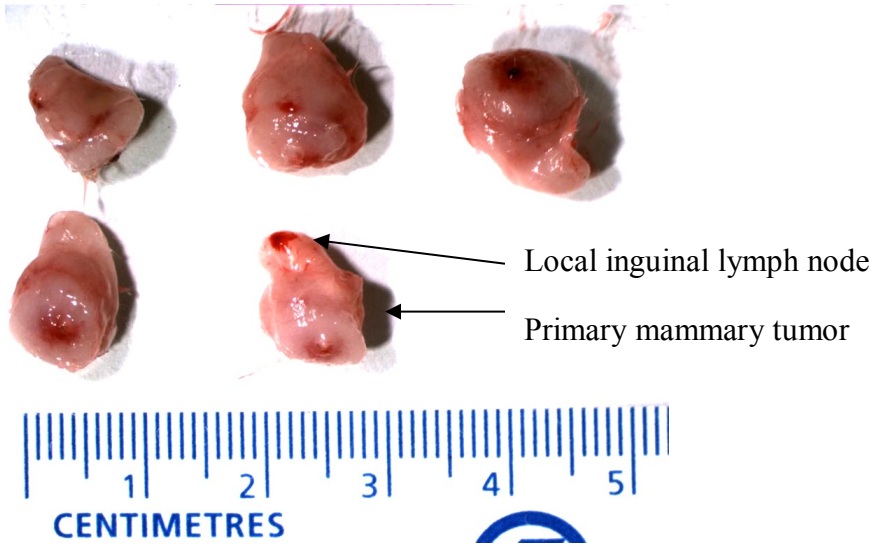

Figure 7: **Consistent primary mammary tumor growth is observed in BALB/c mice receiving (sc. 2 x 10^5) 4T1 cells.** **(A)** Tumor growth curve from days 0-12 post-tumor cell injection. Mean tumor diameter shown (n = 10). **(B)** Primary mammary 4T1 tumors and local inguinal lymph nodes resected 12 days post-tumor cell injection. Tumor size is recorded as the average of the longest and shortest horizontal dimensions.

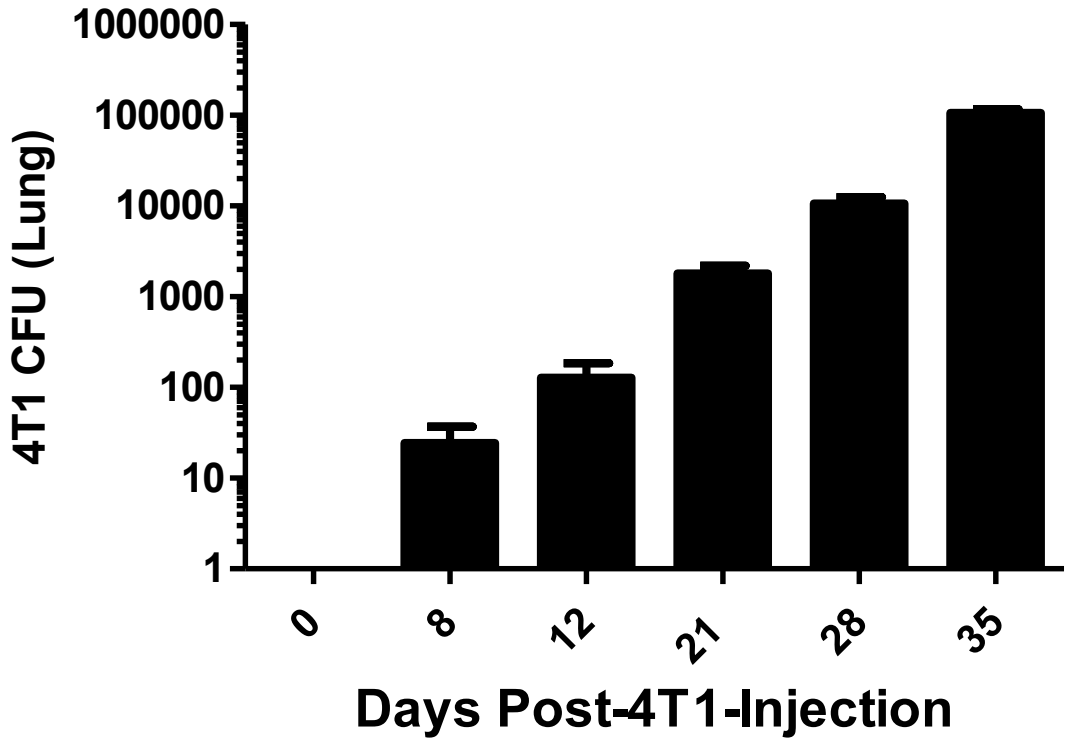

Figure 8: Lung metastasis kinetics for the BALB/c 4T1 model. Mice received (sc. 2 x 10^5) 4T1 tumor cells in the fourth mammary fatpad and the primary mammary tumor was resected at day 12. Mice were sacrificed and metastasis was measured by selecting for tumor cells on 6-TG (n = 3-7 per time point).

3.1.1 GFP-Expressing 4T1 Cells

GFP-expressing 4T1 cells generated using the Phoenix™ retroviral transduction system were screened and sorted by FACS using the FL-1 channel (Figure 9A). GFP-expressing cells were also screened for GFP expression using fluorescence microscopy (Figure 9B). BALB/c mice were injected in the mammary fatpad with 2 x 10^5 GFP-expressing 4T1 cells. The primary tumors exhibited a very consistent growth profile (Figure 9C), resembling what was observed with normal 4T1 tumor cells (Figure 7A). Tumors were resected at day 12 and lung tissue plated at day 21 following day 13 treatment with either saline or α-GC. Consistent with the observations with 4T1 cells, α-GC treatment caused a significant reduction in day 21 lung metastasis with GFP-4T1 cells (Figure 9D). However, FACS was unable to detect significant numbers of GFP positive cells from lung tissue at this time point. Either the clonogenic assay is more sensitive for metastatic cells or transduced 4T1 cells are losing GFP *in vivo*.

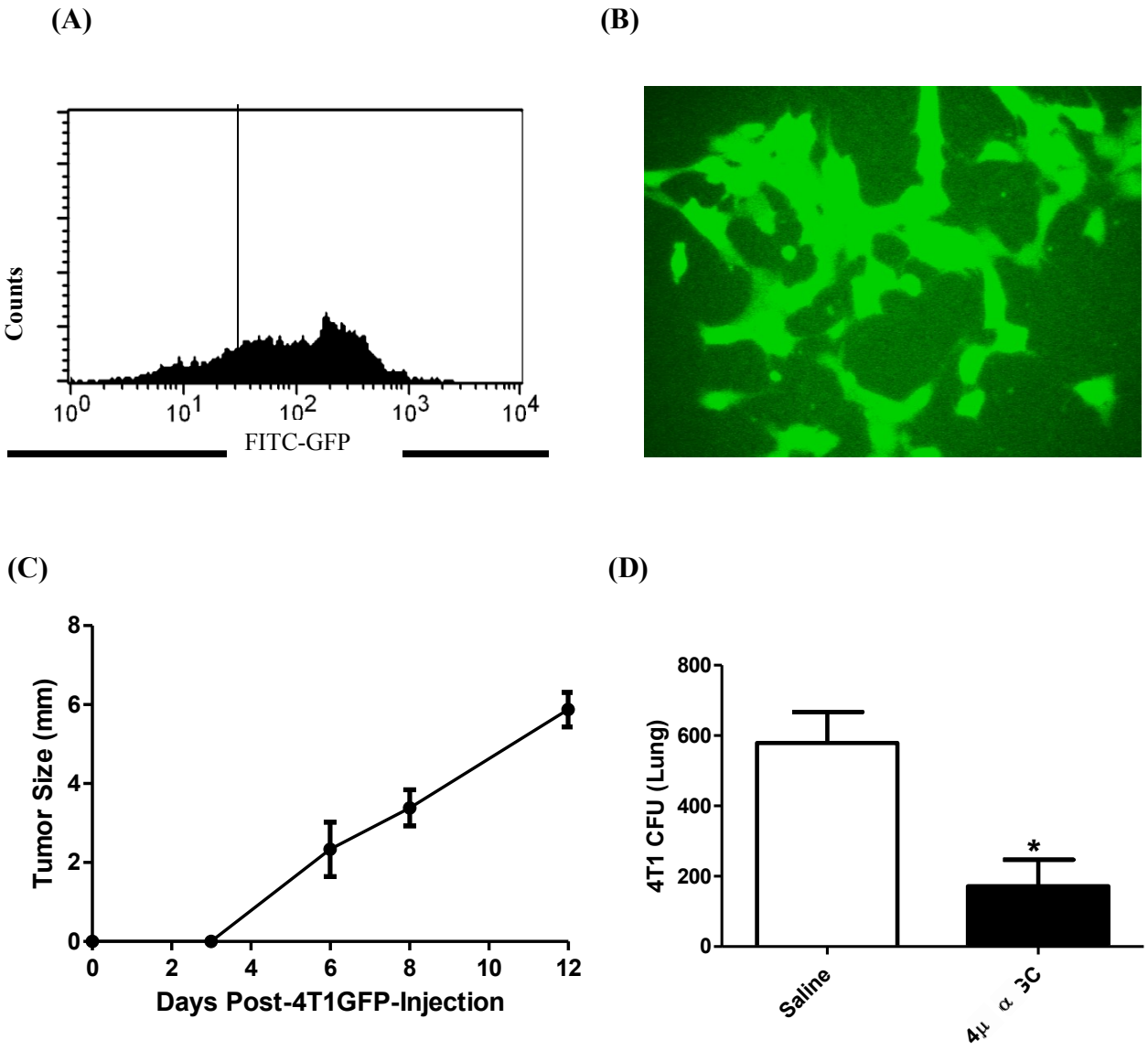

Figure 9: GFP-expressing 4T1 tumor cells were generated and their growth kinetics assessed *in vivo*. (A) Histogram demonstrating 4T1 tumor cell populations positive for GFP expression. **(B)** Fluorescence microscopy imaging of GFP-expressing 4T1 cells. **(C)** Growth profile of primary mammary tumors in BALB/c mice receiving (sc. 2 x 10^5) GFP-expressing 4T1 cells. **(D)** Clonogenic GFP-4T1 cells in lungs of saline versus (ip. 4μg) α-GC treated mice 21 days post-4T1 injection (n = 4-6 per group). * $p < 0.05$

3.2 Free Glycolipid Treatments (BALB/c 4T1 Model)

On day 13 (the day following primary tumor resection), groups of mice were treated with saline (control) or α-GC (ip. 4μg) to activate NKT cells. On day 21, the lung tissue was plated using 6-TG^R clonogenic plating assays. There was a significant decrease in lung metastatic 4T1 cells in α-GC-treated compared to saline-treated mice (Figure 10A and C). The number of lung CFU at 21 days showed no correlation with primary mammary tumor size (Figure 10B) indicating that a ~4mm range in primary tumor size at day 12 did not influence the extent of lung metastasis at day 21. Despite the significant reduction in day 21 lung metastasis in α-GC treated mice, the effect of free α-GC treatment was lost by day 28 with no significant difference in lung metastasis of α-GC and saline treated mice at day 28 or day 35 (Figure 11A). Macroscopic lung metastases at day 21 were few in number and limited to small clear lesions, making differences between the lungs of control and treatment group mice difficult to detect with the naked eye (Figure 11B). By day 35 extensive tumor burden was observable in the lung tissue of both α-GC and control treated mice (Figure 11C).

The α-GC analogues OCH and α-C-GC, which have been shown to enhance Th2 and Th1 polarization *in vivo* respectively [206, 217], were also given as post-surgical free glycolipid treatments. Mice receiving α-GC or α-C-GC exhibited a significant decrease in day 21 lung metastasis (Figure 12A). OCH treatment tended to reduced day 21 lung metastasis, but this effect did not reach significance (Figure 12A). α-GC treatment generated a peak serum IFNγ level under 2000 pg/ml at 24 hr post-treatment and a peak IL-4 level near 250 pg/ml at 6 hr post-treatment (Figure 11B). α-C-GC treatment induced a peak IFNγ level near 2000 pg/ml at 24 hr post-treatment and a peak IL-4 level near 400 pg/ml at 6hr post-treatment (Figure 12C). OCH-induced serum IFNγ levels peaked at just over 500 pg/ml at 6hr, and high IL-4 levels of around 1500 pg/ml were observed from 2hr to 6hr post-treatment (Figure 12D). To assess the extent of Th1 versus Th2 cytokine responses following treatment with α-GC, α-C-GC and OCH, IFNγ:IL-4 ratios were determined for 2h, 6h and 24h time points. Similar trends were observed for α-GC and α-C-GC, with 2h and 6h ratios of 0.46-2.60 and 24h ratios of 28.03 and 32.12, respectively (Figure 12E). In contrast, the Th2 skewing effects of OCH resulted in 2h, 6h and 24h ratios of 0.07, 0.55 and 9.63, respectively (Figure 12E).

Mice receiving α-GC (ip. 4μg) treatment following day 12 mammary tumor resections exhibited a small but significant increase in survival time compared to untreated mice (Figure

13A). A similar trend was observed when α-GC was given on day 13 and resections were performed on day 16 (Figure 13A), but this did not reach significance.

To determine whether tumor dose affected the response, some groups of mice were inoculated with 2 x 10^4 4T1 cells with tumor resections on day 12. Mice survived longer with the lower dose of 4T1 (Fig. 14A vs. Fig. 13A), but α-GC (ip. 4μg) treatment did not enhance survival (Figure 14A). When resections were delayed to day 21 survival times were reduced compared to mice receiving day 12 resections, regardless of α-GC treatment (Figure 14 A and B).

In a dose response experiment using 1, 4, and 20μg α-GC given on day 13 following day 12 tumor resection, no survival advantage was observed with the 1 and 4μg doses (Figure 15A). Mice receiving 20μg α-GC had mixed responses with some mice dying early, likely due to α-GC-related toxicity [223, 224, 225, 226], some dying at the expected 35-45 day range. However, 40% of mice survived for over 120 days. Overall, no significant survival advantage was acheived using the elevated α-GC dose (Figure 15A). Increasing the α-GC dose sequentially increased the 24hr serum IFNγ levels from under 1000 pg/ml up to over 4000 pg/ml (Figure 15B). In contrast, serum IL-4 levels at 24hr levels decreased with increasing α-GC dose (Figure 15B).

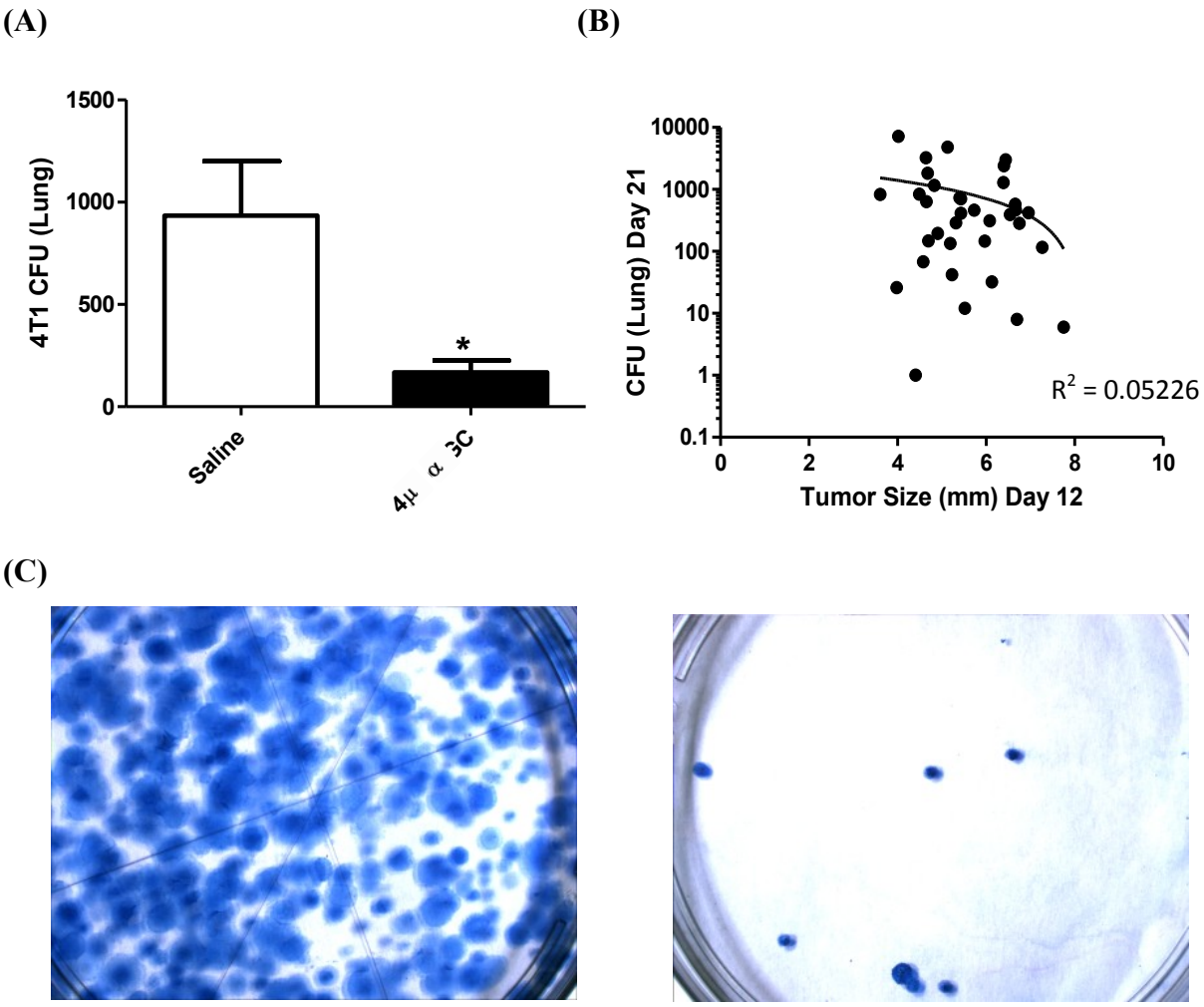

Figure 10: Post-surgical α-GC treatment leads to significant reductions in lung metastasis by day 21 post-tumor cell injection. (A) Clonogenic 4T1 cells in whole lung tissue of saline and α-GC (ip. 4μg) treated BALB/c mice (n = 20-25). * $p < 0.05$ compared to saline control. **(B)** Correlation between tumor size 12 days post-4T1 tumor cell injection and lung 4T1 CFU at 21 days post-4T1 tumor cell injection. **(C)** Sample 4T1 clonogenic assay plates from lung tissue 21 days post-tumor cell injection in saline control (left) and α-GC treated mice (right).

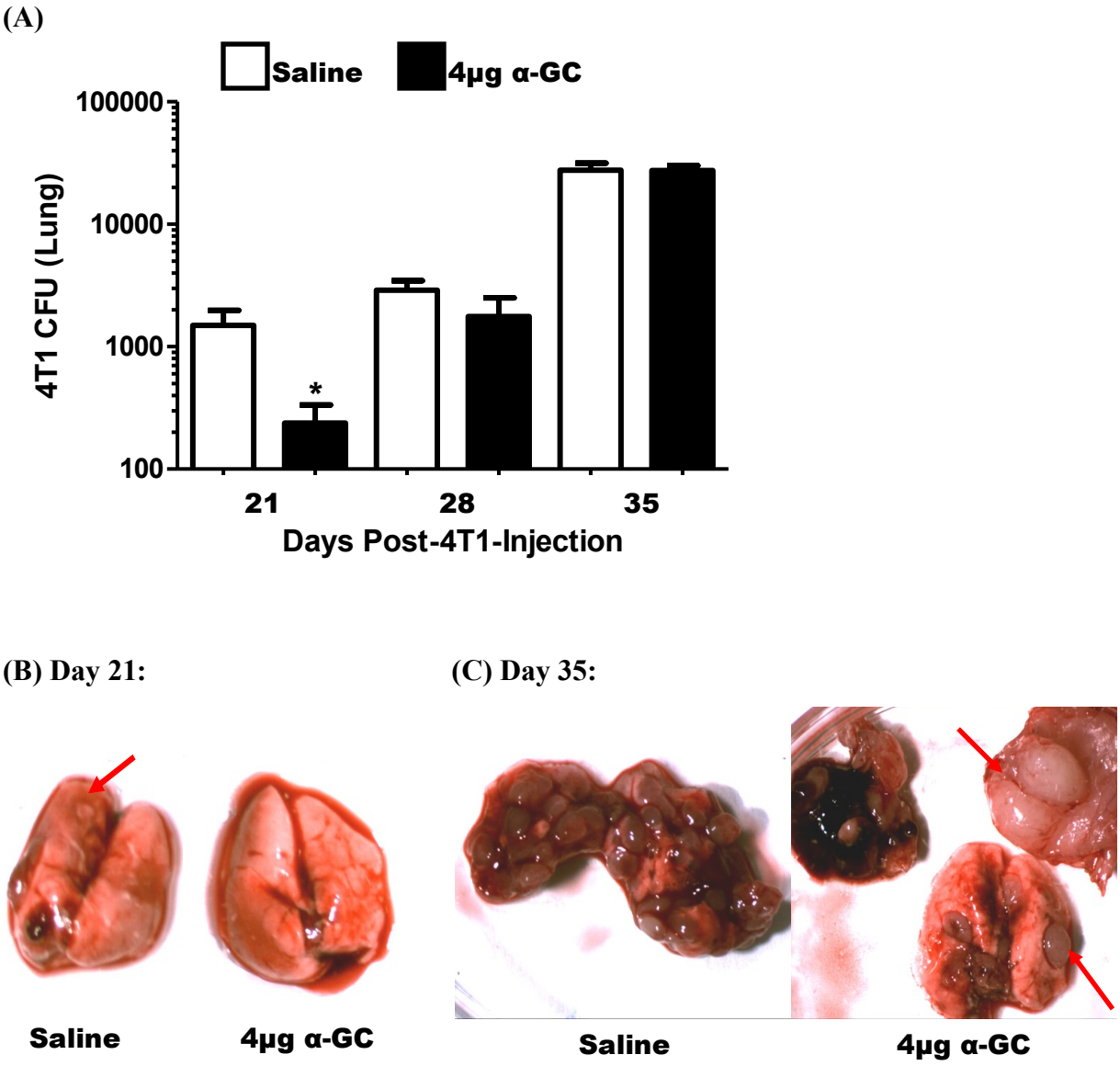

Figure 11: The anti-metastatic effects of free glycolipid treatment are transient.

(A) Clonogenic 4T1 cells in lungs of saline versus α-GC (ip. 4µg) treated mice 21, 28 and 35 days post-4T1 injection (n = 7-25 per group). * $p < 0.05$ compared to saline control.

(B) Representative lung tissue 21 days post-4T1 tumor cell injection in mice receiving day 12 saline versus α-GC treatment. **(C)** Representative lung tissue 35 days post-4T1 tumor cell injection in saline versus α-GC treated mice.

(A)

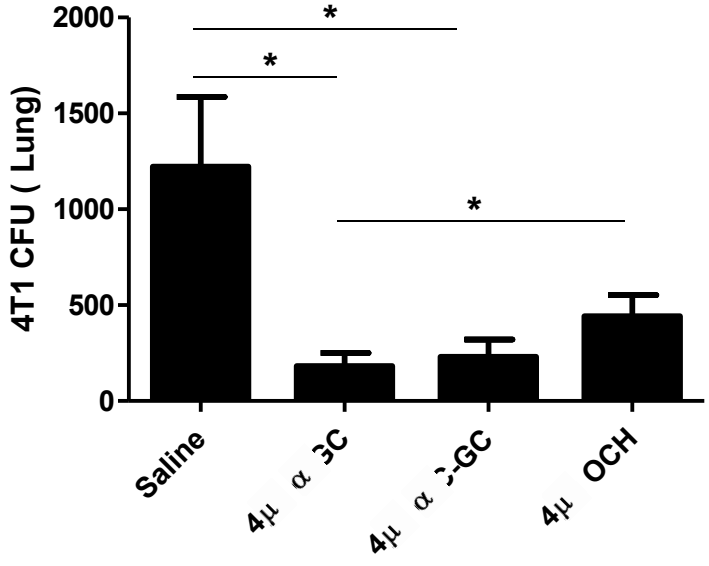

(B) **(C)** **(D)**

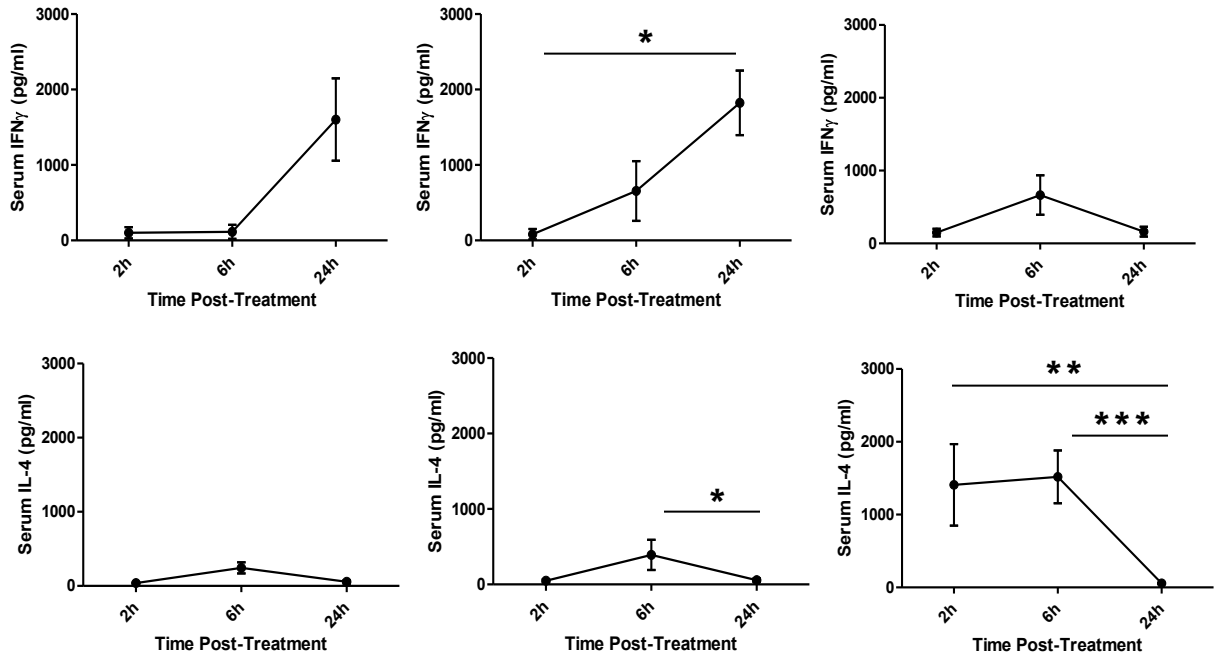

(E)

	α-GC			α-C-GC			OCH		
Time	**2h**	**6h**	**24h**	**2h**	**6h**	**24h**	**2h**	**6h**	**24h**
IFNγ:IL-4	2.60	0.46	28.03	1.71	1.68	32.12	0.07	0.55	9.63

Figure 12: α-GC is the most effective glycolipid in reducing early lung metastasis compared to analogous glycolipids. **(A)** Day 21 lung metastasis for mice receiving day 13 saline or ip. 4μg α-GC, α-C-GC or OCH. (n = 12-25). **(B)** Serum IFNγ and IL-4 levels 2, 6, and 24hr post-α-GC injection. (n = 6). **(C)** Serum IFNγ and IL-4 levels 2, 6, and 24hr post-α-C-GC injection. (n = 3). **(D)** Serum IFNγ and IL-4 levels 2, 6, and 24hr post-OCH injection. (n = 5). **(E)** IFNγ:IL-4 ratios at 2h, 6h and 24h post-activation for α-GC, α-C-GC and OCH.
* $p < 0.05$ ** $p < 0.01$ *** $p < 0.001$

(A)

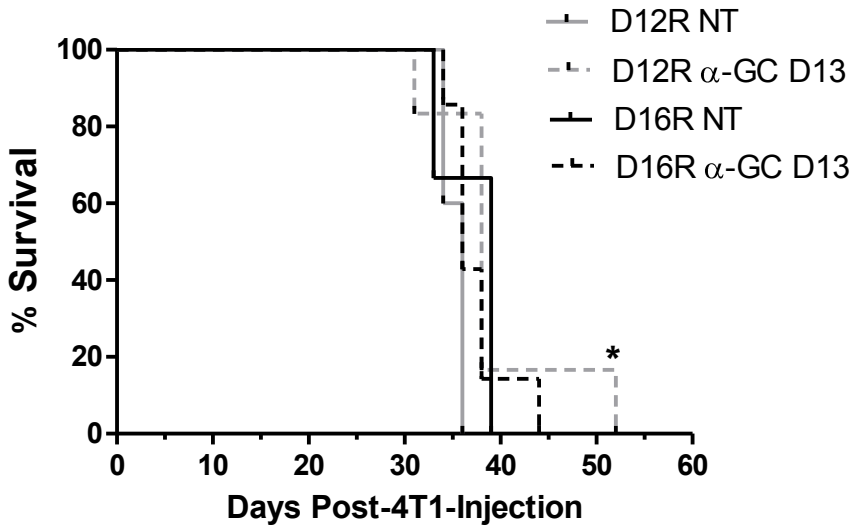
D12R NT
D12R α-GC D13
D16R NT
D16R α-GC D13
% Survival
100
80
60
40
20
0
0
10
20
30
40
50
60
Days Post-4T1-Injection
*

(B)

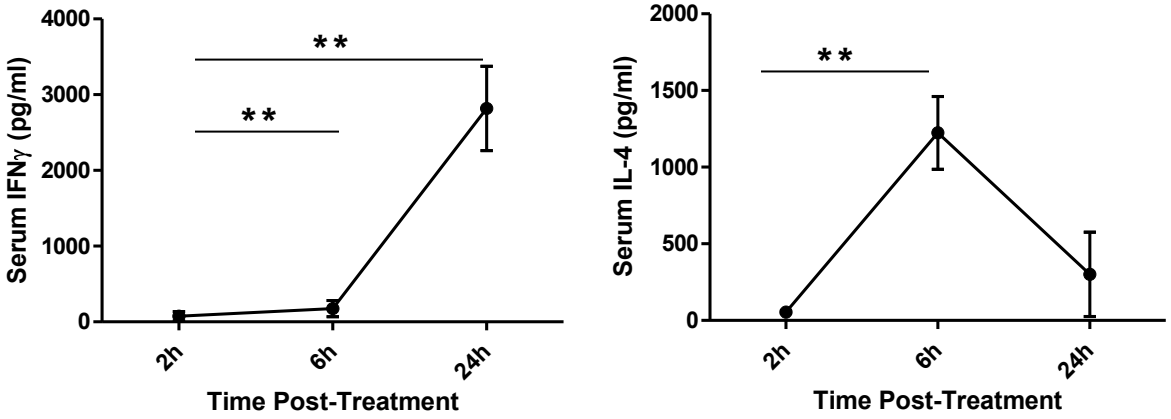
Serum IFNγ (pg/ml)
4000
3000
2000
1000
0
**
**
2h
6h
24h
Time Post-Treatment
Serum IL-4 (pg/ml)
2000
1500
1000
500
0
**
2h
6h
24h
Time Post-Treatment

(C)

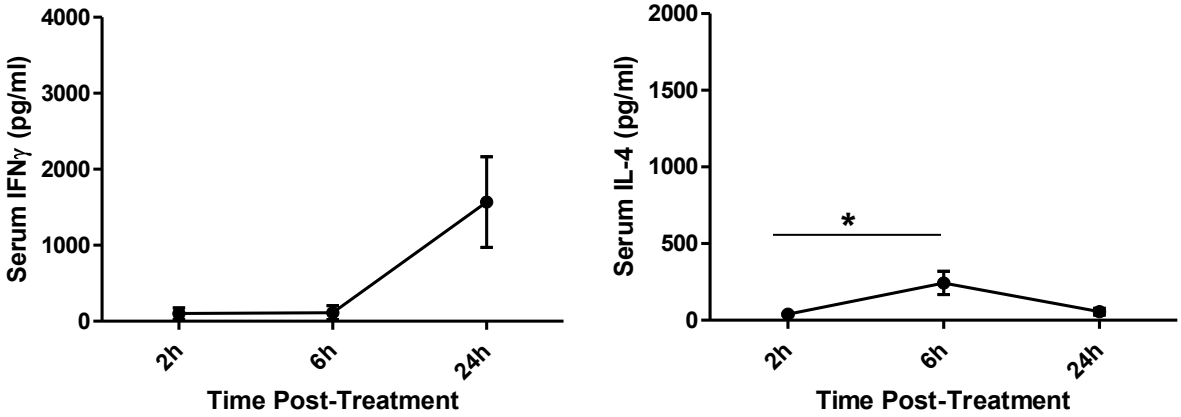
Serum IFNγ (pg/ml)
4000
3000
2000
1000
0
2h
6h
24h
Time Post-Treatment
Serum IL-4 (pg/ml)
2000
1500
1000
500
0
*
2h
6h
24h
Time Post-Treatment

Figure 13: Pre-surgical NKT cell activation leads to stronger cytokine responses.
(A) Survival among four different treatment groups: day 12 resection (D12R) with no treatment (NT), day 12 resection with day 13 α-GC treatment (ip. 4μg), day 16 resection (D16R) with no treatment and day 16 resection with day 13 α-GC treatment. (n = 5-7 per group). * $p < 0.05$ compared to no treatment group. **(B)** Serum IFNγ and IL-4 cytokine levels at 2hr, 6hr and 24hr post-day 13) α-GC treatment in mice receiving day 16 tumor resections. (n = 3) **(C)** Serum cytokine levels 2hr, 6hr and 24hr post-day 13 treatment for mice receiving day 12 tumor resections. (n = 6). * $p < 0.05$ **$p < 0.01$

(A)

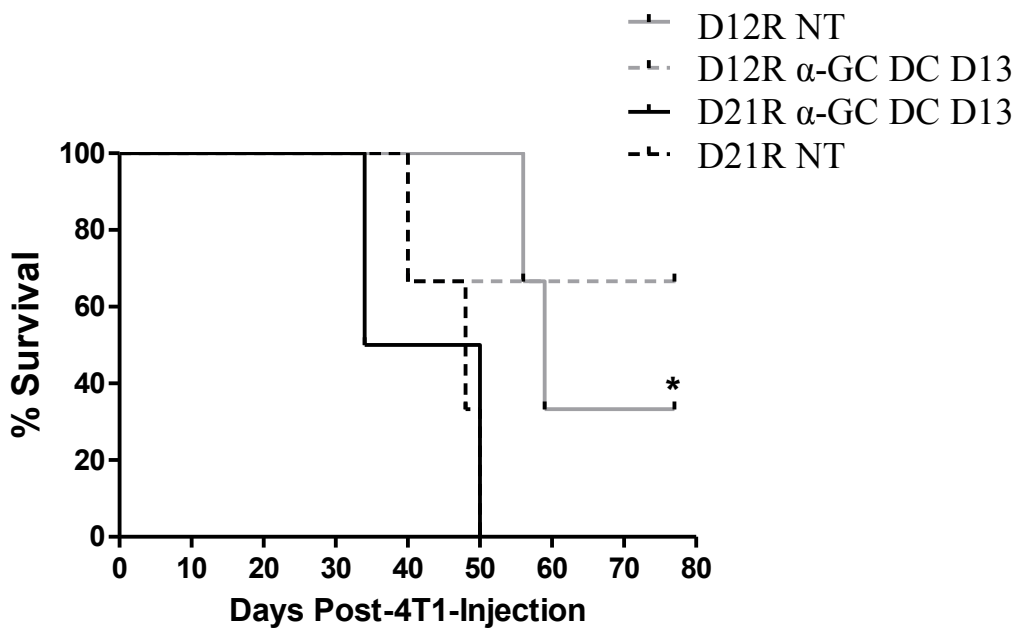
D12R NT
D12R α-GC DC D13
D21R α-GC DC D13
D21R NT
% Survival
Days Post-4T1-Injection
*

(B)

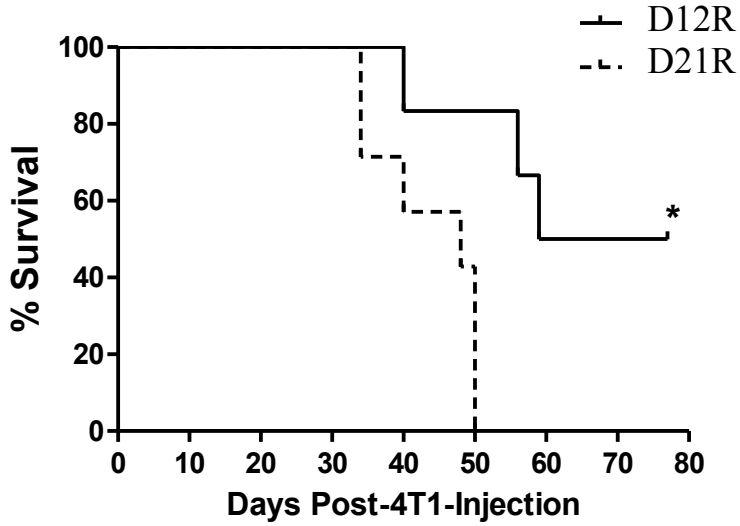
D12R
D21R
% Survival
Days Post-4T1-Injection
*

Figure 14: Delaying tumor resection significantly decreases long term survival. Comparison of survival between mice receiving (sc. 2 x 10^4) 4T1 cells where primary tumor excision occurs 12 or 21 days later with or without day 13 (ip. 4μg) α-GC treatment. **(A)** Survival among four different treatment groups: day 12 resection (D12R) with no treatment (NT), day 12 resection with day 13 α-GC treatment, day 21 resection with no treatment and day 21 resection with day 13 α-GC treatment (n = 3-4 per group). * $p < 0.05$ compared to day 21 NT. **(B)** Combined survival among all mice receiving day 12 resections and all mice receiving day 21 resections. (n = 6-7 per group). * $p < 0.05$ compared to day 21 resection.

(A)

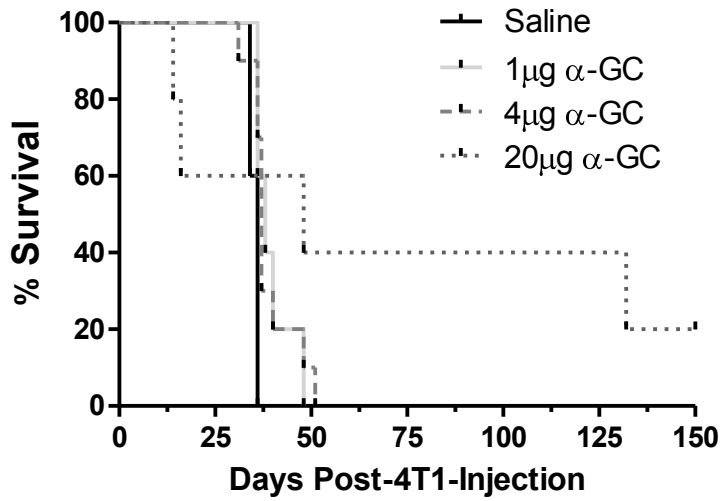

(B)

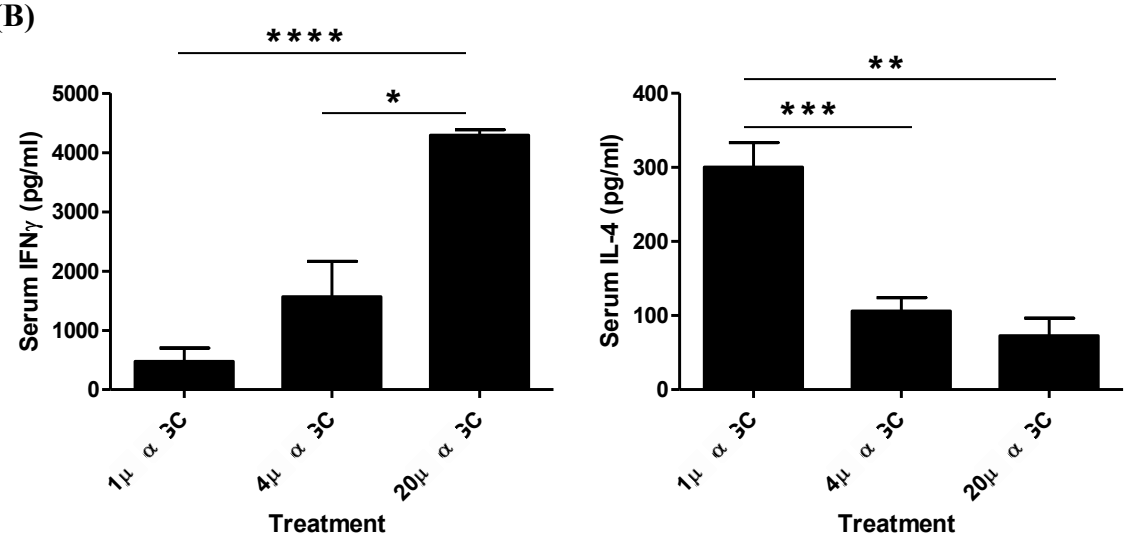

Figure 15: No significant overall survival advantage is observed with varying doses of post-surgical administered α-GC. Survival response and serum cytokine levels in mice receiving (ip. 1μg, 4μg or 20μg) α-GC on the day following day 12 primary tumor resections. **(A)** Survival of mice in the three treatment groups (n = 5-7 per group). **(B)** Serum IFNγ and IL-4 levels 24hr post-NKT cell activation (n = 3-6). * $p < 0.05$ ** $p < 0.01$ *** $p < 0.001$ *** $p < 0.0001$

3.3 DC Treatments (BALB/c 4T1 Model)

As single doses of α-GC were unable to elicit a sustained anti-tumor response (Figure 11A), and multiple treatments with free glycolipids have been linked to anergy induction [186, 187, 188], a different approach was needed. Glycolipid presentation by DCs has been shown to induce potent NKT cell activation without anergy [227]. Therefore, I examined the ability of adoptively transferred α-GC-loaded DCs to control tumors in the 4T1 model. On the day following day 12 primary tumor resections, mice were given adoptive transfers with 5×10^4 to 3×10^6 cells bone marrow derived DCs loaded in culture with α-GC. Serum IFNγ and IL-4 levels were measured 24hr following treatments with 2×10^5 to 3×10^6 cells (Figure 16A). Maximum 24hr IFNγ levels > 2000 pg/ml were observed following the 5×10^5 cell dose, but this level was not significantly different from IFNγ levels elicited by the other doses (Figure 16A). Maximum 24hr IL-4 levels > 400 pg/ml were observed following the 1×10^6 cell dose; this level was significantly greater than the levels found with the 2×10^5 and 5×10^5 cell doses, and tended to be greater than the level observed at the 3×10^6 cell dose (Figure 16A). IL-4 levels doses of 2-5 $\times 10^5$ and 3×10^6 cells were > 200 pg/ml. Twenty-four hour IFNγ:IL-4 ratios were determined for the four doses assessed. In order of increasing dose from 2×10^5 to 3×10^6 cells, the ratios were 12.38, 8.37, 4.01 and 7.25 (Figure 16B). A Th2-skewing effect was noted with increasing dose (Figure 16B) and may be linked to poor survival outcomes with the 1×10^6 and 3×10^6 doses (Table 3). Based on cytokine data (Figure 16A) 2×10^5 α-GC-loaded DCs induced the strongest Th1-skewed cytokine response and this dose was used for subsequent experiments. We examined the complete 2hr, 6hr and 24hr cytokine profile for this dose (Figure 16C). Peak IFNγ levels of ~2500 pg/ml were observed at 24hr post-treatment and peak IL-4 levels of ~400 pg/ml were observed at 6hr (Figure 16C).

Mice were treated with doses of α-GC-loaded DCs ranging from $5 \times 10^4 - 3 \times 10^6$ cells following 4T1 tumor resection and long-term survival was monitored. Mice surviving up to and including 50 days were considered non-responders (NR), while mice surviving 51-150 days were considered partial responders (PR) and mice healthy at 150 days were considered complete responders (CR) and were sacrificed at the 150 day experimental endpoint (Table 3). None of the mice treated with low numbers of α-GC-loaded DCs (5×10^4 or 1×10^5) or the highest number of DCs (3×10^6) responded to treatment with increased survival (Table 3). However, partial and complete responses were observed in mice given more intermediate numbers of α-

GC-loaded DCs. The best responses were observed with the 2-5 x 10^5 doses, consistent with the strongest Th1 polarization induced by these treatments (Figure 16). Combined, these groups had a 70% response rate (14/20) with 35% (7/20) of mice surviving long term (>150 days). Compared to mice receiving a single day 13 treatment with 2 x 10^5 unloaded DCs, mice receiving 2 x 10^5 α-GC-loaded DCs had significantly greater survival, with ~40% of mice having a CR (Figure 17A). Upon sacrifice of CR mice at day 150, lungs were completely clear of macroscopic metastatic lesions (Figure 17B) and no 4T1 cells were detected when lung tissue was plated using clonogenic assays.

Serum cytokine levels were assessed 24hr following consecutive treatments with 3 x 10^6 α-GC-loaded DCs on days 13, 16 and 19. The data demonstrate that sequential NKT cell stimulations lead to diminished responses, with nearly no cytokine response observed following the third stimulation (Figure 18). It is possible that the stimulations were too close together to allow NKT cells to recover, or in contrast to the literature [227, 228], we were inducing anergy in our mice.

To assess the effectiveness of using a single versus multiple post-surgical α-GC-loaded DC treatments, mice were given either a single treatment with 2 x 10^5 α-GC-loaded DCs on day 13, two treatments on day 13 and day 20, or three treatments on days 13, 20 and 27. At day 28, lung metastasis was significantly reduced in single treatment mice compared to mice receiving unloaded DCs; similar reductions were observed in the double and triple treatment groups (Figure 19A). Whole lung tissue in the single treatment group was completely devoid of observable metastatic lesions at day 28 while control mice had readily apparent macrometastases in the lung tissue (Figure 19B).

In mice given 2 x 10^5 α-GC-loaded DC treatments on days 13, 20 and 27, it was observed that 24hr IL-4 responses decreased with each subsequent NKT cell activation (Figure 20). IFNγ levels at 24 hr dropped to baseline levels following the second activation on day 20, but showed a significant increase over baseline levels following the third activation on day 27 (Figure 20). This suggests that two weeks may be required between stimulations for optimal NKT cell activation.

To assess the effects of prophylactic treatment on tumor growth and prevention of metastasis, mice were given a treatment of 2 x 10^5 α-GC-loaded DCs one day prior to tumor cell injection. Treatment with α-GC-loaded DCs initially delayed tumor growth, but the tumors in

control and treated mice began to grow at roughly the same rate ~8 days following tumor cell injection (Figure 21A). Overall, tumor growth was significantly decreased in treated mice compared to saline-treated control mice (Figure 21A). Tumor size in DC treated mice was reduced ~42% compared to control mice at the time of tumor resection on day 12 (Figure 21B). Prophylactic treatment was extremely effective in promoting long-term survival as CRs were observed in 75% of treated mice (Figure 21C).

(A)

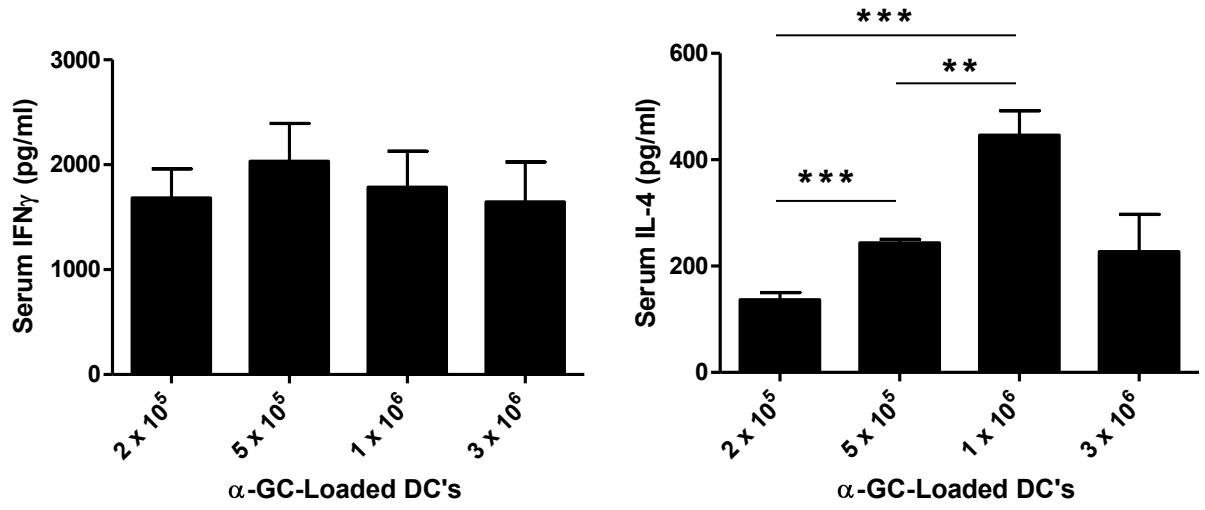

(B)

α-GC-DCs	2 x 10^5	5 x 10^5	1 x 10^6	3 x 10^6
IFNγ:IL-4 (24h)	12.38	8.37	4.01	7.25

(C)

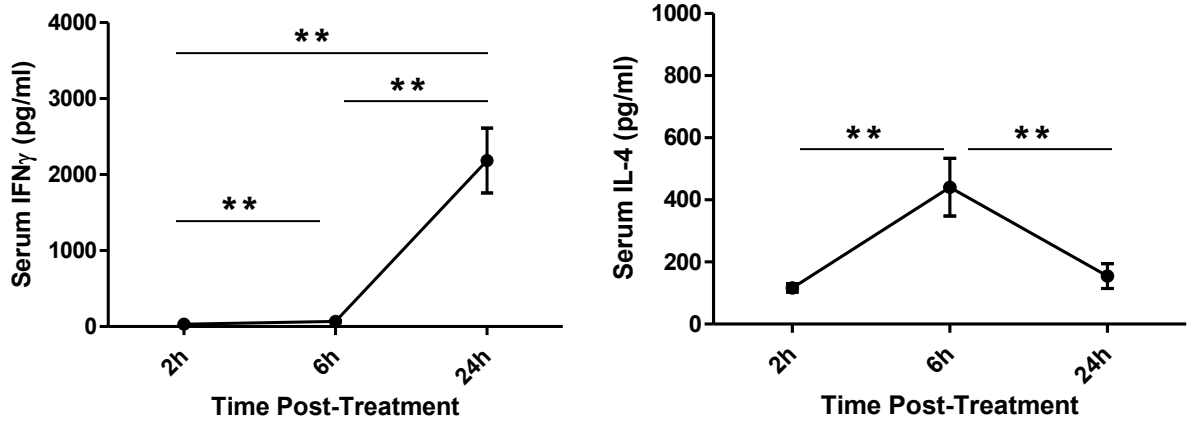

Figure 16: Cytokine responses following post-surgical administration of α-GC-loaded DCs. **(A)** Serum IFNγ and IL-4 cytokine levels from mice 24hr following post-surgical treatment with 2 x 10^5, 5 x 10^5, 1 x 10^6 or 3 x 10^6 α-GC-loaded DCs. (n = 3-8 per group). **(B)** 24h IFNγ:IL-4 ratios for the four treatment groups. **(C)** Serum IFNγ and IL-4 levels 2, 6 and 24hr following (iv. 2 x 10^5) α-GC-loaded DC treatment in tumor-resected mice (n = 8-12 per group).
* $p < 0.05$ ** $p < 0.01$ *** $p < 0.001$

Table 3: Survival outcomes in mice receiving post-surgical α-GC-loaded DCs.

DCs transferred (iv.)	NR	% NR	PR	%PR	CR	%CR
5×10^4	3 (35,36,36)	100%	0	0%	0	0%
1×10^5	3 (34,36,40)	100%	0	0%	0	0%
2×10^5	4 (40,41,48,50)	31%	4 (54,75,67,68)	31%	5 (150)	38%
5×10^5	2 (37,40)	29%	3 (61,63,83)	43%	2 (150)	29%
1×10^6	2 (41,44)	67%	1 (58)	33%	0	0%
3×10^6	5 (33,33,34,35,36)	100%	0	0%	0	0%

NR (non-responder; <51 days post-4T1 cell injection), PR (partial responder; <151 days survival), CR (complete responder; healthy at 150 days post-4T1 cell injection). Numbers in brackets indicate day of death or sacrifice.

(A)

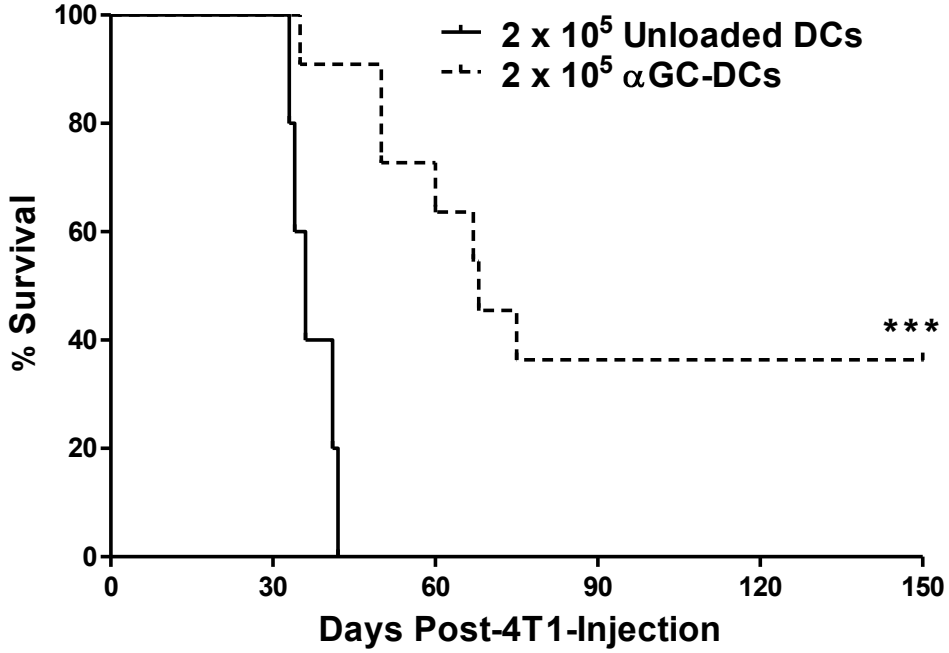

(B)

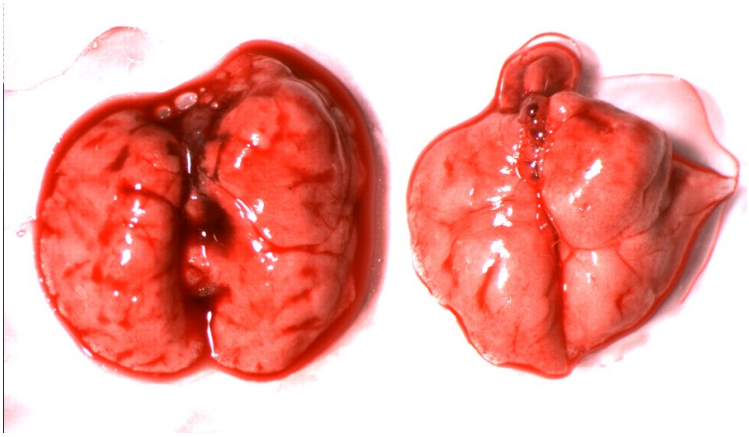

Figure 17: Mice receiving post-surgical α-GC-loaded DCs exhibit complete responses to treatment. (A) Survival of mice receiving either unloaded DCs or (iv. 2 x 10^5) α-GC-loaded DCs one day post-primary tumor resection (n = 5-11 per group). **(B)** Tumor-free whole lung tissue from complete responders 150 days post-tumor cell injection. *** $p < 0.001$ compared to unloaded DC treatment.

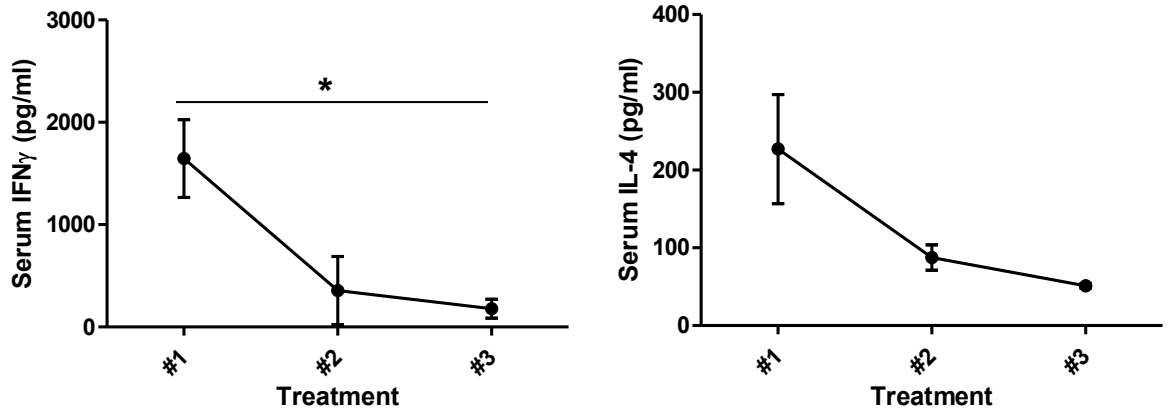

Figure 18: Consecutive transfers of α-GC-loaded DCs lead to significant reductions in cytokine responses. Serum IFNγ and IL-4 levels 24hr following (iv. 3 x 10^6) α-GC-loaded DC treatments on days 13, 16 and 19 post-tumor cell injection (n = 3 per time point). * $p < 0.05$

(A)

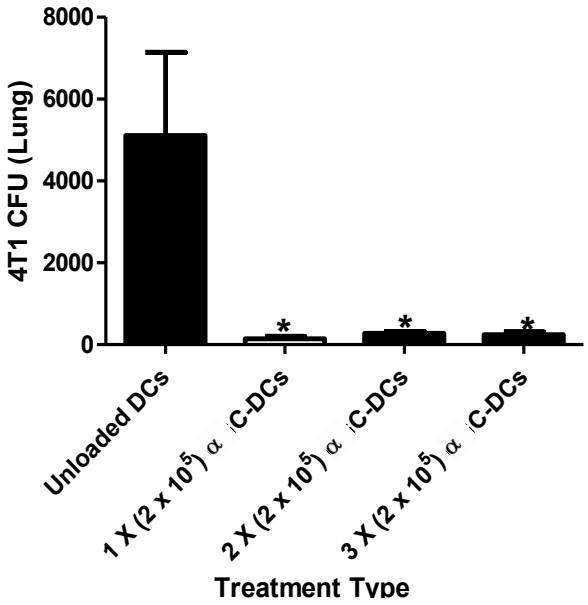

(B)

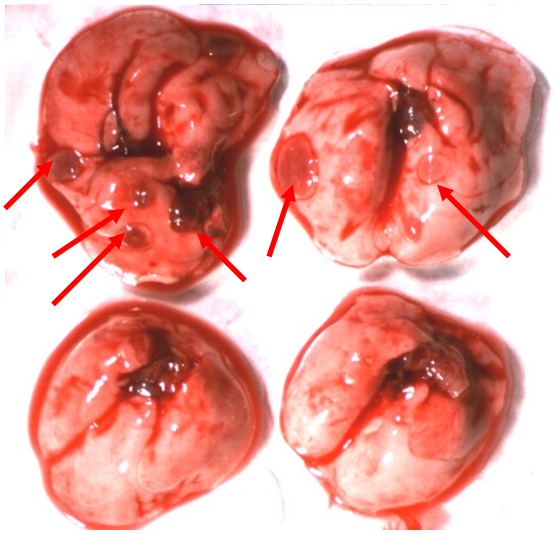

Unloaded DCs

Day 28 Tissue

1X (2 x 10⁵) α-GC-loaded-DCs

Day 28 Tissue

Figure 19: Lung metastasis is reduced at 28 days post-4T1 injection in mice receiving post-surgical α-GC-loaded DCs. (A) 4T1 CFU at 28 days in mice receiving either unloaded DCs on day 13 or 1X, 2X or 3X (iv. 2 x 10^5) α-GC-loaded DC injections on days 13, 13 and 20, or 13, 20 and 27. (n = 3-5 per group) * $p < 0.05$ compared to treatment with unloaded DCs. **(B)** Whole lung tissue from mice receiving either unloaded DCs or 1X α-GC-loaded DCs on day 13. Red arrows indicate macrometastatic lesions.

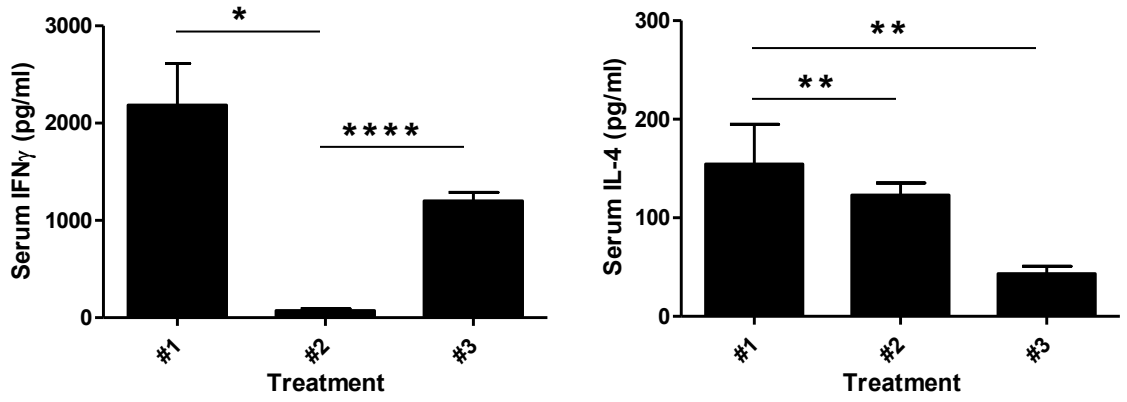

Figure 20: Cytokine responses to multiple post-surgical treatments with α-GC-loaded DCs. Serum IFNγ and IL-4 levels were measured 24hr following sequential treatments with (iv. 2 x 10^5) α-GC-loaded DCs on days 13, 20 and 27 post-tumor cell injection (n = 4-12).

* $p < 0.05$ ** $p < 0.01$ **** $p < 0.0001$

(A)

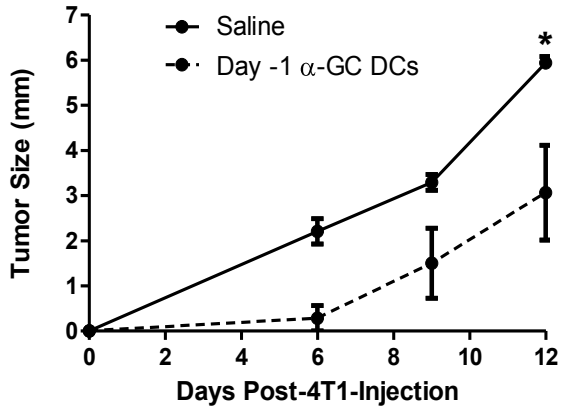
Saline
Day -1 α-GC DCs
*
Tumor Size (mm)
0
1
2
3
4
5
6
7
0
2
4
6
8
10
12
Days Post-4T1-Injection

(B)

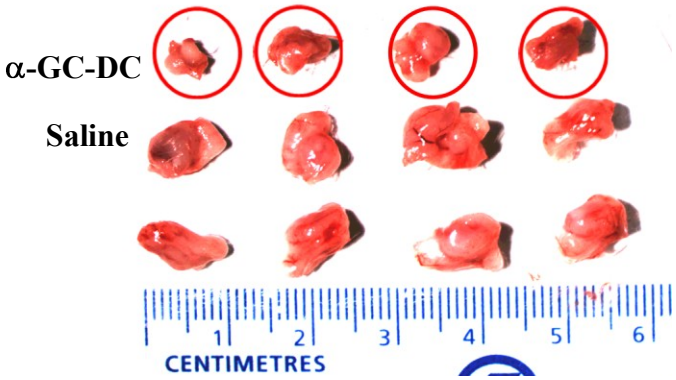
α-GC-DC
Saline
1
2
3
4
5
6
CENTIMETRES

(C)

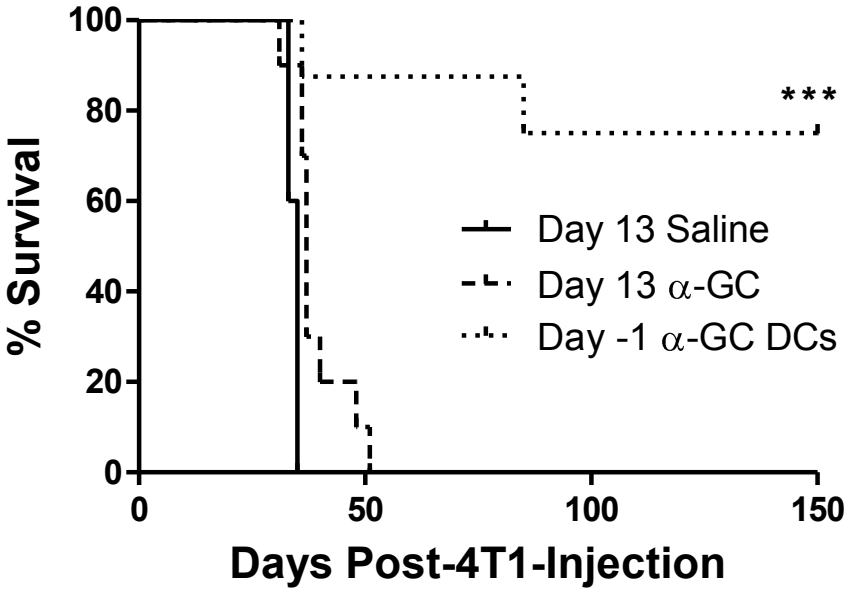
100
80
60
40
20
0
% Survival
***
Day 13 Saline
Day 13 α-GC
Day -1 α-GC DCs
0
50
100
150
Days Post-4T1-Injection

Figure 21: Prophylactic α-GC-loaded DC treatment decreased primary mammary tumor growth and promoted overall survival. **(A)** Growth profile for primary 4T1 mammary tumors in mice receiving either saline or (iv. 2 x 10^5) α-GC-loaded DCs day prior to tumor cell injection. (n = 4-8 per group) **(B)** Primary mammary tumors resected from BALB/c mice 12 days post-4T1 injection with mice having received either α-GC-loaded DCs or saline one day before 4T1 tumor cell injection. **(C)** Survival of mice receiving day -1 α-GC-loaded DC treatment, day 13 saline treatment, or day 13 (ip. 4μg) α-GC. (n = 5-8) * $p < 0.05$ *** $p < 0.01$ compared to saline treatment.

3.4 NKT Cell Treatments (BALB/c 4T1)

In order to compensate for deficiencies in the activity and number of NKT cells noted in patients with various forms of cancer [209, 229, 230], *in vivo* expanded NKT cells were adoptively transferred (iv.) into mice at a range of 2 x 10^5 to 2 x 10^6 cells per mouse on the day following primary tumor resection. Some groups of mice receiving NKT cells also received α-GC or 5 x 10^5 (ip. 4μg) α-GC-loaded DCs (iv. 2 x 10^5 DCs). Poor IFNγ production was noted at 24hr post-treatment in all assessed NKT cell transfer treatment groups except for mice receiving α-GC-loaded DCs in addition to NKT cells (Figure 22). This same trend was also observed for IL-4 levels 24hr post-treatment (Figure 22).

The adoptive transfer of expanded NKT cells alone or in combination with α-GC did not enhance survival of tumor-resected mice (Table 4). Enhanced survival was noted in some mice treated with NKT cells plus α-GC-loaded DCs (Table 4), but the responses were not better than those observed with transfer of α-GC-loaded DCs alone (Table 4).

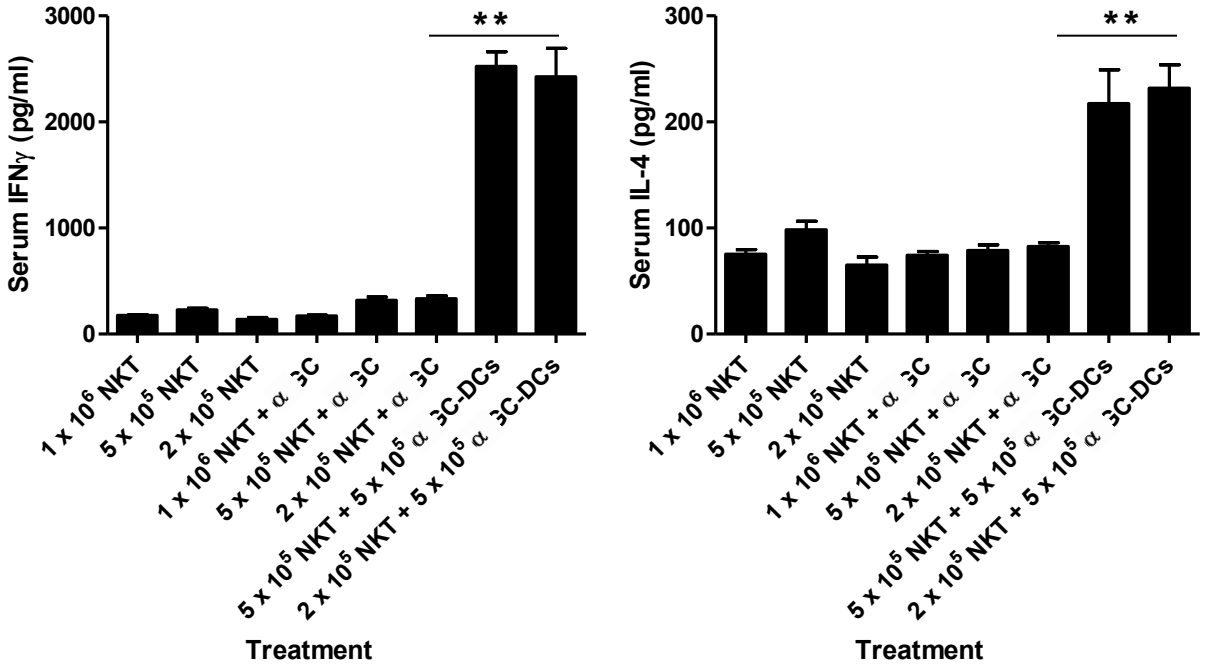

Figure 22: Cytokine responses following adoptive transfer of NKT cells alone, or in combination with α-GC stimulation or α-GC-loaded DCs. Treatment groups were as follows: 1 x 10^6, 5 x 10^5, or 2 x 10^5 *in vivo* expanded NKT cells alone or in combination with α-GC (ip. 4μg); and 2 x 10^5 or 5 x 10^5 NKT cells combined with 5 x 10^5 α-GC-loaded DCs. (n = 3-4 per group) ** $p < 0.01$ comparing groups receiving either 2 x 10^5 NKT cells with α-GC or 2 x 10^5 NKT cells with 5 x 10^5 α-GC-loaded DCs.

Table 4: Complete responses among mice receiving NKT cells are dependent on also receiving α-GC-loaded DCs. Survival outcomes for mice receiving α-GC-loaded DCs, adoptive NKT cell transfer, NKT cell transfer with α-GC, or co-adoptive transfer of NKT cells and α-GC-loaded DCs.

Group	NR	PR	CR
2-5 x 10^5 α-GC DCs	6 (37-50)	7 (54-83)	7 (150 healthy)
1-2 x 10^6 NKT + 2 x 10^5 α-GC DCs	7 (33 - 46)	1 (53)	2 (150 healthy)
5 x 10^5 NKT + 2-5 x 10^5 α-GC DCs	5 (32-46)	4 (56-72)	2 (150 healthy)
1 x 10^6 NKT + α-GC	2 (42 - 46)	1 (94)	0
5 x 10^5 NKT + α-GC	6 (44 - 47)	0	0
1 x 10^6 NKT	3 (39 - 40)	0	0
2-5 x 10^5 NKT	5 (38 - 46)	1 (58)	0

NR (non-responder; <51 days post-4T1 cell injection), PR (partial responder; <151 days survival), CR (complete responder; healthy at 150 days post-4T1 cell injection). Numbers in brackets indicate day of death or sacrifice.

3.5 Myeloid Derived Suppressor Cells

Blood Gr-1$^+$CD11b$^+$ cells were initially assessed by FACS analysis in the 4T1 model to assess the extent to which NKT cell activation would decrease the frequency of MDSCs. As no direct or immediate NKT cell activation-associated effect was observed (data not shown), tracking blood MDSCs for this purpose became unnecessary. However, in tracking the frequency of blood Gr-1$^+$CD11b$^+$ cells over the course of short and long term experiments, the frequency of Gr-1$^+$CD11b$^+$ cells became a useful prognostic indicator of health for mice in the various experimental treatment groups (Figure 23). Naïve mice and mice inoculated in the mammary fatpad with tumor cells 2-3 days prior to analysis had a frequency of ~50% Gr-1$^+$CD11b$^+$ cells in blood (Figure 23). The maximum Gr-1$^+$CD11b$^+$ levels of ~90% were observed around day 14 (Figure 23A), 2 days after primary tumors were resected. Following resection, Gr-1$^+$CD11b$^+$ levels receded to levels slightly above baseline by day 24 (Figure 23B). In mice with advancing metastatic disease, the frequency of blood Gr-1$^+$CD11b$^+$ levels would increase to > 90% of PBLs towards days 30-40 (Figure 23B). Levels climbing back up to ~75-80% at any time following day 24 were a strong indicator that metastatic disease was advancing and that these mice would exhibit symptoms of lung metastasis-associated respiratory distress within a week (Figure 23B). Some mice with partial responses to post-surgical treatment would exhibit near baseline Gr-1$^+$CD11b$^+$ levels for an extended period of time, but the frequency of Gr-1$^+$CD11b$^+$ cells would eventually increase as disease progressed (Figure 23B). In mice exhibiting complete responses to treatment, with no disease progression up to the experimental day 150 endpoint, small increases in Gr-1$^+$CD11b$^+$ levels were observed subsequent to day 24, but levels never increased above ~70% and essentially remained near baseline levels beyond day 80 (Figure 23).

To identify the proportions of PBLs that were lymphocytes, granulocytes, monocytes and immature leukocytes, cytospins were performed using the blood of day 35 mice in groups of tumor-resected mice receiving no treatment or post-surgical 5 x 10^5 or 1 x 10^6 α-GC-loaded DC treatments on day 13. Naïve BALB/c mice having received no tumor challenge were used as a control. Cytospins from the blood of naïve mice had very high percentages of lymphocytes with few granulocytic and monocytic cells observed (Figure 24). In contrast, mice with advanced disease had few to no lymphocytes, but had very high PBL counts with the majority of cells having morphology of immature and mature granulocytic cells (Figure 24). Mice exhibiting a

response to treatment at day 35 had a much lower cell count by comparison and had significantly greater proportion of lymphocytes in peripheral blood (Figure 24).

Day 35 cytospin data was compared to FACS data generated from the same blood samples (Table 5). Based on cytospin analysis, lymphocyte frequencies for non-responding, responding and naïve mice were 5.84 ± 4.27%, 37.21 ± 1.57% and 73.14 ± 3.17%, respectively (Table 5). The frequency of non-lymphocyte cells were 94.16 ± 4.27%, 62.79 ± 11.17% and 26.86 ± 3.81% (Table 5). Based on FACS analysis, lymphocyte percentages were 9.07 ± 4.22%, 37.30 ± 1.96% and 38.07 ± 3.44% (Table 5). Non-lymphocyte percentages were 90.93 ± 5.86%, 62.70 ± 3.12% and 61.93 ± 4.25% (Table 5).

To examine the effects of NKT cell activation therapy on both Gr-1^+CD$11b^+$ cell numbers and immunosuppressive activity, the frequency of Gr-1^+CD$11b^+$ cells was assessed in the blood, lungs and spleens of naïve mice, day 35 resected mice receiving no treatment and day 35 mice responding or not responding to post-surgical 2 x 10^5 α-GC-DC treatment. In addition to extensive lung metastasis, splenomegaly was observed in the spleens of mice that received no therapy and non-responding mice (Figure 25A). Mice responding to DC therapy had normal sized spleens and no observable lung metastasis (Figure 25A). Based on FACS analysis, Gr-1^+CD$11b^+$ cells as a percentage of PBLs in untreated, treated (NR) and treated (R) mice were 97.30, 94.70 and 46.49%, respectively (Figure 25B). Gr-1^+CD$11b^+$ cells as a percentage of splenocytes were 76.21, 71.12 and 25.91% (Figure 25B). Gr-1^+CD$11b^+$ cells as a percentage of lung cells were 67.58, 52.24 and 31.22% (Figure 25B).

Immunosuppressive activity in the blood was assessed by examining the ability to suppress division of Oregon Green-labeled naïve T cells stimulated with anti-CD3/anti-CD28 – coated beads. High T cell proliferation was observed when T cells were incubated with PBLs from naïve mice and mice responding to treatment (Figure 25 B and C). Proliferating cells comprised ~80% of the T cell population in both groups. Little to no T cell proliferation was observed when T cells were incubated with PBLs from mice receiving no NKT cell treatment or mice that did not respond to treatment (Figure 25 B and C). Proliferating cells comprised <5% of the T cell population in these groups.

(A)

Days Post-4T1 Injection:

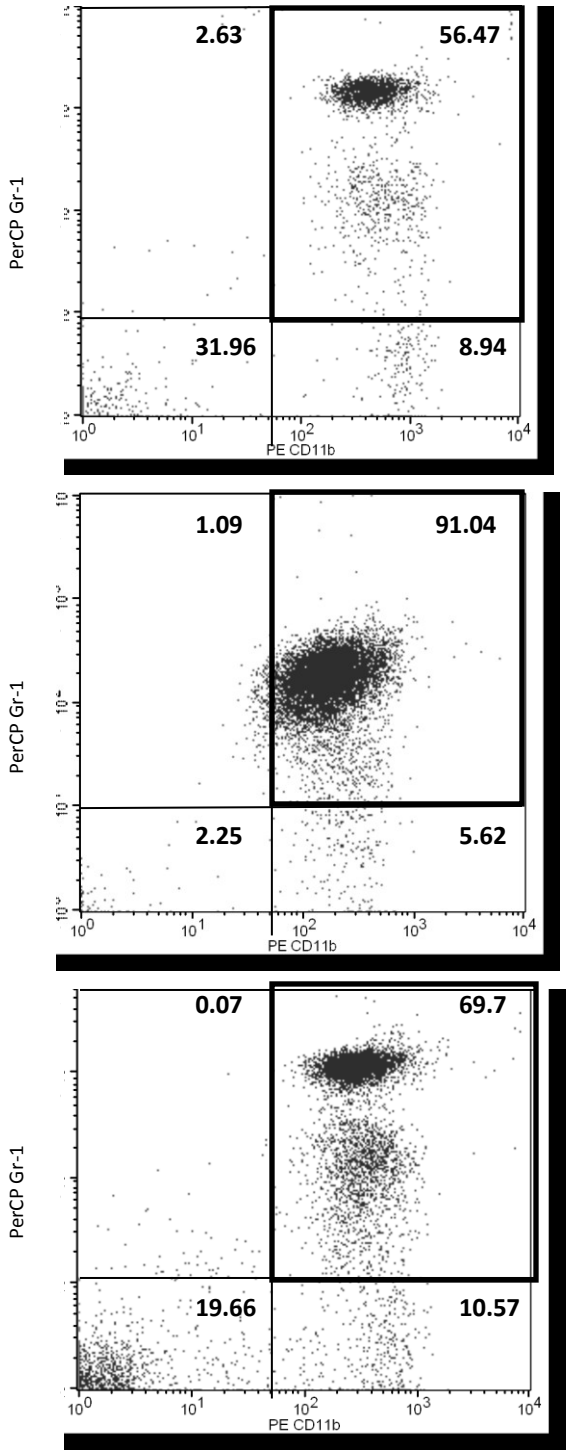

3 Days

14 Days

150 Days

(B)

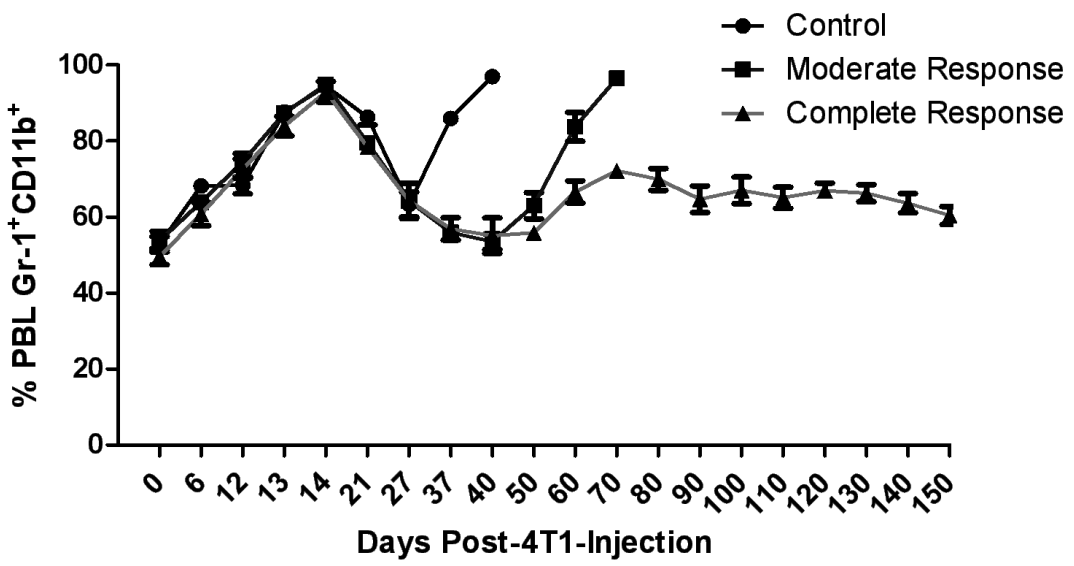

Figure 23: The frequency of blood Gr-1$^+$CD11b$^+$cell levels are a prognostic health indicator in mice surviving long-term following treatment. (A) Representative blood Gr-1$^+$CD11b$^+$ leukocyte proportions at days 3, 14, and 150 days post-4T1 tumor cell injection in mice demonstrating a complete response to day 13 (iv. 2 x 10^5) α-GC-loaded DC treatment. **(B)** The frequency of Gr-1$^+$CD11b$^+$ cells increased with metastatic burden and was predictive of impending mortality. Complete responding mice demonstrate complete clearance of metastatic disease and no significant increase in the frequency of post-surgical Gr-1$^+$CD11b$^+$ cells. Control – Untreated, Moderate Response – responding to α-GC-loaded DC treatment with survival >50 to <151 days, Complete Response – healthy at day 150 with no lung metastasis.

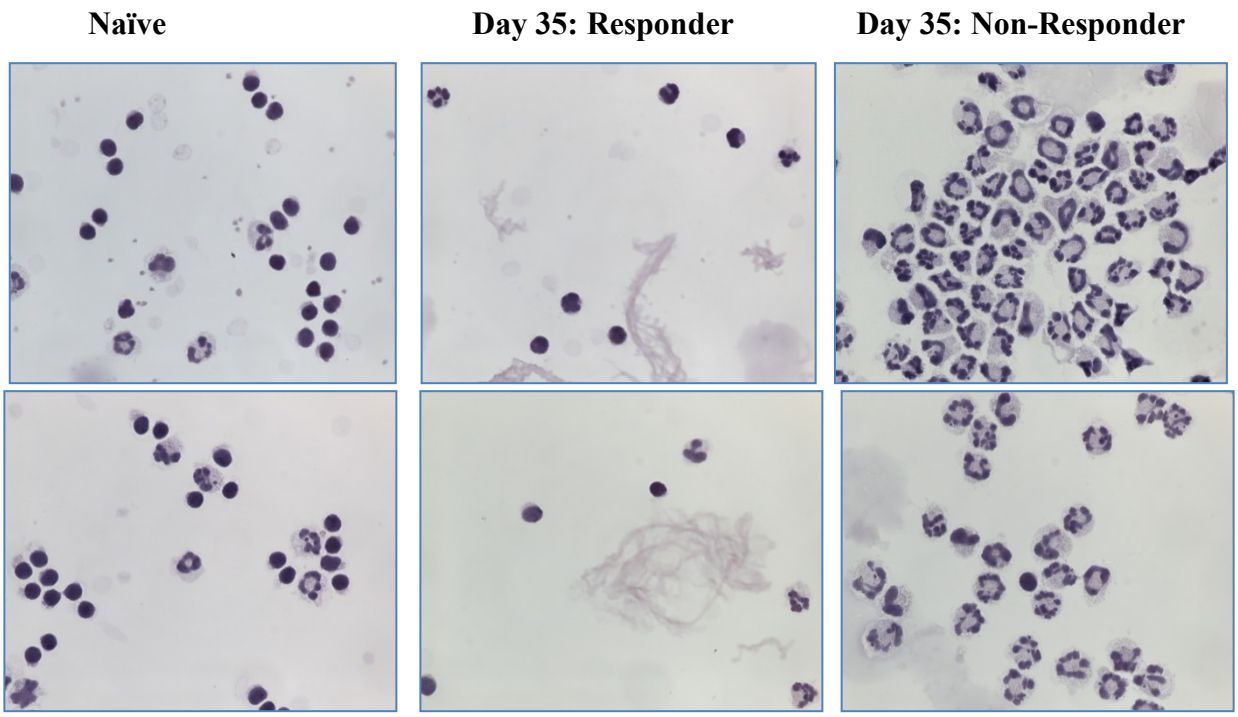

Figure 24: Blood leukocyte cytospins demonstrate high granulocytic leukocyte content in the blood of mice with advanced metastatic disease. Pictures are representative of blood from naïve mice and responding and non-responding mice receiving post-surgical α-GC-loaded DC treatment on day 13.

Table 5: Cytospin and FACS data for blood cells.

Mouse	n	**Lymphocytes**	Monocytes	Band form	Neutrophils	**Non-Lymphocytes**
Values based on Cytospin Analysis						
NR	5	**5.84 ± 4.27**	8.91 ± 2.58	25.09 ± 5.03	60.09 ± 6.04	**94.16 ± 4.27**
Responders*	3	**37.21 ± 1.57**	21.23 ± 6.13	15.98 ± 8.24	25.58 ± 3.28	**62.79 ± 11.17**
Naive	3	**73.14 ± 3.17**	5.05 ± 1.80	7.42 ± 3.99	14.39 ± 5.33	**26.86 ± 3.11**
Values based on FACS Analysis						
NR	5	**9.07 ± 4.22**	-	-	-	**90.93 ± 5.86**
Responders*	3	**37.30 ± 1.96**	-	-	-	**62.70 ± 3.12**
Naive	3	**38.07 ± 3.44**	-	-	-	**61.93 ± 4.25**

Data represents analysis blood from naïve mice and day 35 blood from mice in groups receiving post-surgical α-GC-loaded DC treatment on day 13. *Responders were identified as mice with a blood Gr-1^{+}CD11b^{+} percentage below 65% based on FACS analysis at day 35, and having survived to the experimental 150 day endpoint. Data presented as mean ± SD.

(A)

Untreated **Treated Non-Responder** **Treated Responding**

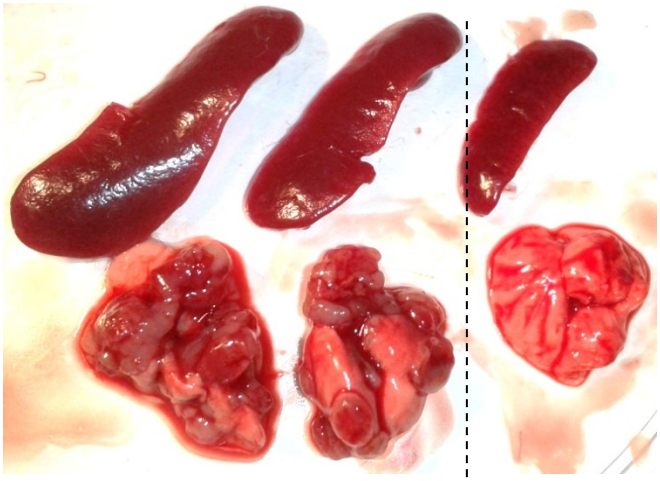

Spleen – Day 35

Lung – Day 35

(B)

	Day 35:% Gr-1^{+}CD11b^{+} cells		
Mouse	**Blood**	**Spleen**	**Lung**
No therapy	97.30%	76.21%	67.58%
DC therapy (Non-Responder)	94.70%	71.12%	52.24%
DC therapy (Responding)	46.49%	25.91%	31.22%

(C)

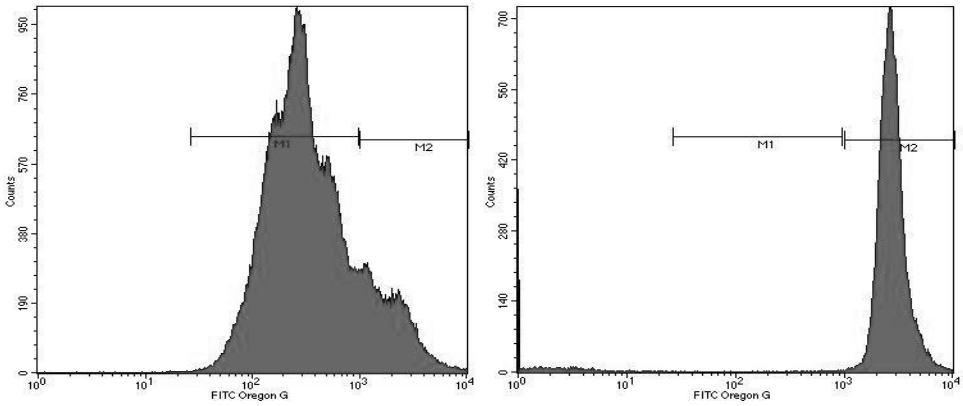

Naïve

No therapy

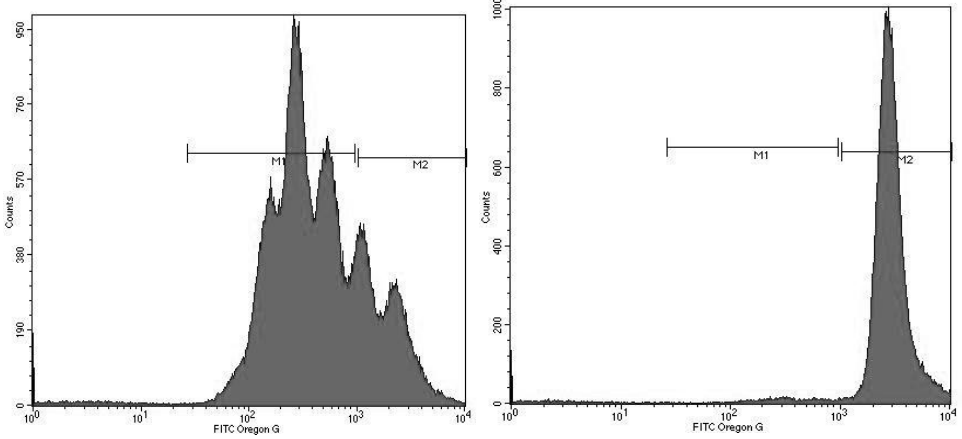

α-GC-DC (R)

α-GC-DC (NR)

(D)

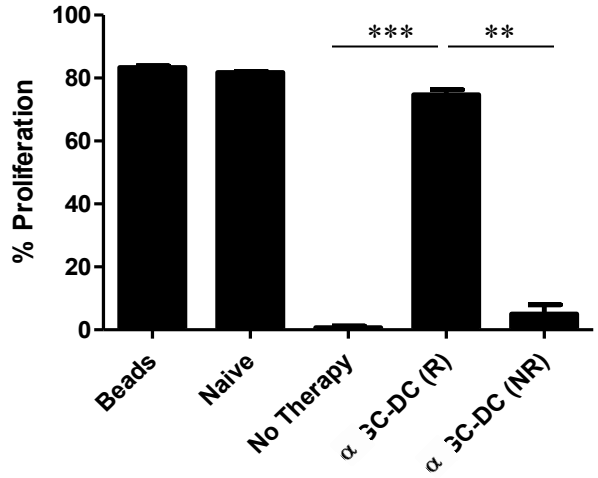

Figure 25: NKT cell-based immunotherapy is effective in controlling MDSC number and immunosuppressive activity. (A) Splenomegaly and extensive lung tumor coverage is observed in mice receiving no DC therapy and non-responding mice at day 35. **(B)** The frequency of tissue MDSCs (Gr-$1^{+}$$CD11b^{+}$ cells) as a total of all non-red blood cells was greater in mice receiving no DC therapy and non-responding mice as compared to mice responding to post-surgical treatment with 2 x 10^{5} α-GC-loaded DCs. **(C)** Representative T cell proliferation following incubation with day 35 blood PBLs from naïve mice, mice receiving no DC therapy, and mice responding (R) or not responding (NR) to post-surgical 2 x 10^{5} α-GC-loaded DC treatment. **(D)** Blood PBLs from mice receiving no DC therapy and mice not responding to treatment exhibit greater levels of T cell suppression compared to blood PBLs from naïve mice and mice responding to DC treatment (n= 2-3/group).** $p < 0.01$ *** $p < 0.001$ Note: Experiments described in Figure 25C and 25D were performed with the help of Simon Gebremeskel.

3.6 Free Glycolipid Treatments (C57BL/6 E0771 Model)

To generate an E0771 cell line that could be used to assess metastasis, puromycin-resistant E0771 cells were generated by serial passaging E0771 cells in 2μg/ml puromycin dihydrochloride followed by selection and expansion of resistant clones.

Eight week old female C57BL/6 mice were injected sc. in the fourth mammary fat pad with 2 x 10^5 $Puro^R$ E0771 cells. Primary mammary tumors developed at a fairly consistent rate, with palpable tumors observed at days 4-5 post-tumor cell injection and tumors reaching ~7mm in diameter by 12 days post-tumor cell injection (Figure 26A). Primary tumors were consistent in size with high levels of vascularization and blood content (Figure 26B).

Tumors were resected at day 12 and mice were treated ip. with saline (control) or 4μg α-GC the next day. Based on puromycin selection plating of 21 day lung tissue, there was a significant reduction in metastasis to the lung in mice receiving α-GC treatments compared to saline controls (Figure 27A).

α-GC treatment induced a moderate elevation in serum IL-4 levels by 2hr post-NKT cell activation, but this transient increase was lost by 6hr post-activation (Figure 27B). Serum IFNγ levels peaked at 6hr post-activation with peak levels being much lower than IL-4 (Figure 27B). IFNγ levels dropped to baseline by 48hr post-NKT cell activation (Figure 27B).

(A)

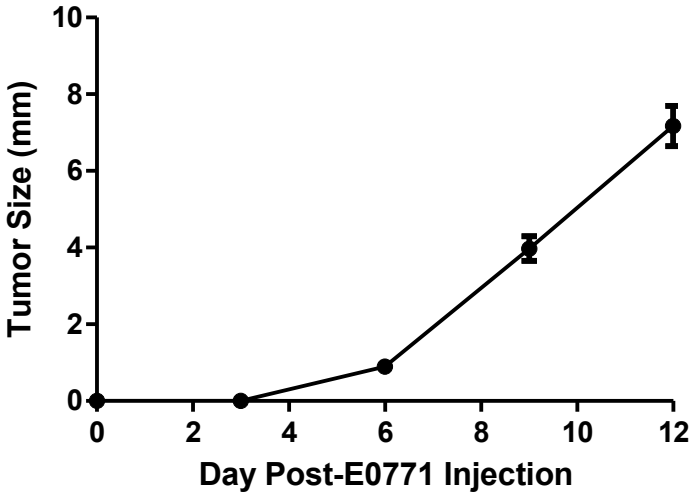

(B)

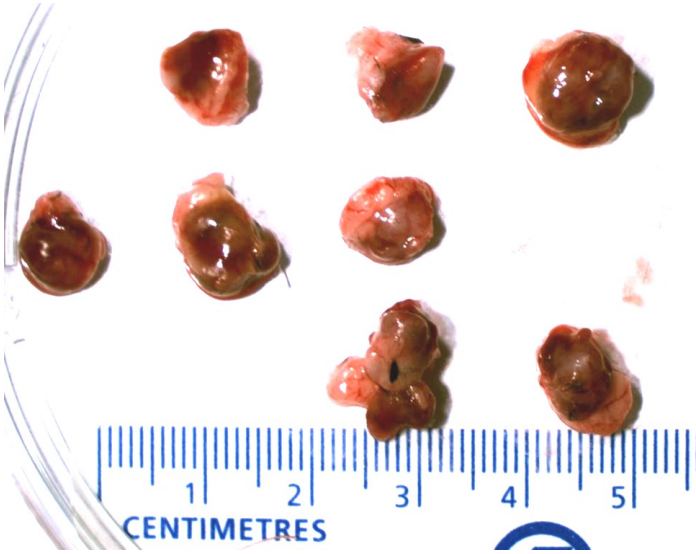

Figure 26: **Growth profile for E0771 primary mammary tumors and primary tumors resected at 12 days post-tumor cell injection.** **(A)** Tumor growth curve for E0771 mammary tumors in mice receiving (sc. 2 x 10^5) E0771 tumor cells (n = 8). **(B)** Resected E0771 mammary tumors. Tumor size recorded as the average of the longest and shortest horizontal dimensions.

(A)

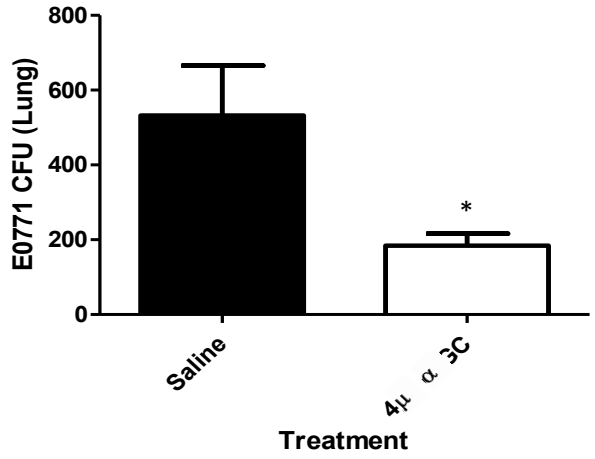

(B)

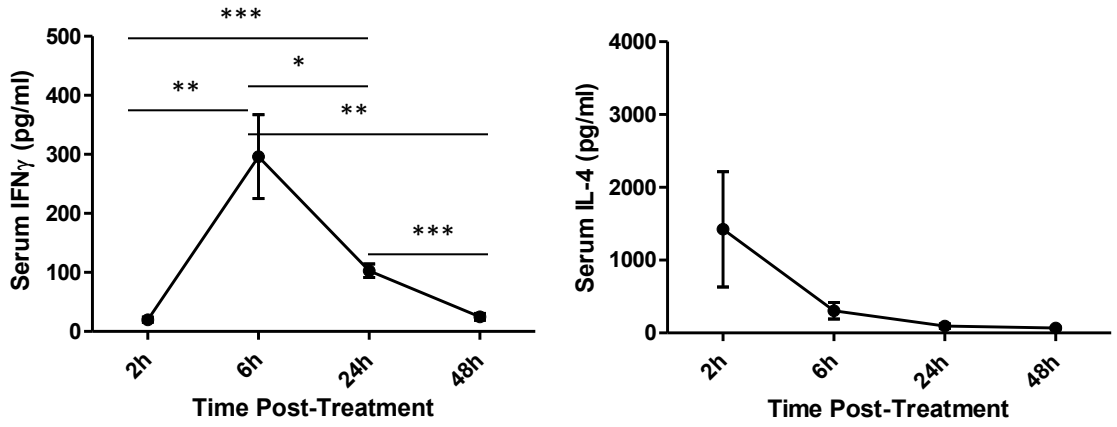

Figure 27: A significant reduction in lung metastasis is observed following post-surgical treatment with α-GC and is associated with low level cytokine responses.

(A) Lung metastasis levels 21 days following (sc. 2 x 10^5) Puro^R-E0771 tumor cell injection in C57BL/6 mice receiving day 13 saline or (ip. 4μg) α-GC (n = 4). * $p < 0.05$ compared to saline treatment. **(B)** Serum IFNγ and IL-4 levels 2, 6, 24 and 48hr following day 13 (ip. 4μg) α-GC injection. (n = 4). * $p < 0.05$, ** $p < 0.01$, *** $p < 0.001$

Chapter 4: Discussion

Given that 90% of cancer-related deaths are due to metastatic disease, therapies targeting metastasis are of vital importance for the future of cancer treatment. The ability of NKT cell-activation based immunotherapy to target metastatic lesions in both human and murine systems provides a basis for developing NKT cell-based immunotherapy strategies to treat metastasis associated with advanced cancers. Typically, cancers are treated using chemotherapeutic drugs, surgical resection or ionizing radiation to either kill or remove malignancies. However, given the ability of an activated immune system to target and destroy cancers cells, and the fact that α-GC-based treatments have already been approved for use in clinical trials, it is logical to use NKT cell activation strategies in a model representative of clinical treatments for patients being treated for metastatic breast cancer.

4.1 BALB/c 4T1 Model

The BALB/c 4T1 model was the main model used in our experiments and proved to be useful as implemented in our post-surgical treatment system. After determining an optimal initial tumor cell injection quantity of 2×10^5 cells, we proceeded to assess metastasis in lung tissue at time points of 14, 21, 28, 35 and 150 days post-tumor cell injection using 6-TG^R plating assays. Tumors were resected at 12 days post-tumor cell injection with NKT cell activation being induced the following day. Treatments included free glycolipids and adoptive transfers of *in vivo* expanded NKT cells and/or bone marrow-derived DCs. Effectiveness of treatments was assessed by examining lung metastasis, long term survival (up to 150 days), cytokine production associated with NKT cell activity and blood MDSC levels. The effects of free glycolipid and adoptive NKT cell transfer treatments were limited, but treatments with α-GC-loaded DCs were highly effective in both clearing lung metastases and promoting long term disease-free survival.

4.1.1 *Primary Tumor Growth*

Initially, 7×10^3 4T1 cells were injected into mice to assess the resulting tumor growth and metastasis profile. This number of 4T1 cells is consistent with what has previously been used in systems using the 4T1 model [55]. Unfortunately, tumor growth was slow and inconsistent, and lung metastasis was minimal. In contrast, primary mammary tumor growth was highly consistent between mice when receiving injections of 5×10^4 or more tumor cells. As shown in

Figure 6, a primary injection with 2 x 10^5 cells, which was used for the majority of our experiments, resulted in consistent primary tumor growth, with tumors reaching ~6mm in diameter 12 days following the initial tumor challenge. Although 4T1 tumor cells primarily spread via the hematogenous route [231], the local inguinal lymph node was also removed to prevent it from acting as a potential source of circulating and trafficking tumor cells (Figure 7B). A low percentage (~10%) of mice given tumor cell injections developed local tumor invasion to the peritoneal lining by the time of primary tumor resection. Overall, this did not influence the outcome of metastasis in these mice, but did result in more extensive surgery to remove tumour from the peritoneal lining and the subcutaneous regions. Another rare problem associated with the tumor cell injections was accidental intravenous injection into blood vessels in the region of the mammary fatpad. When such an injection would occur, mice would develop limited or no primary mammary tumor but would demonstrate systemic metastasis by day 12 and would have to be sacrificed within two weeks of tumor cell injection. Similar effects were observed with accidental injection into the peritoneum, with mice developing rapid onset disease in the peritoneal cavity requiring sacrifice prior to day 12.

4.1.2 *Metastasis*

Lung metastasis was evaluated using 6-TG^R plating assays at 14, 21, 28, 35 and 150 days following tumor cell injection. Metastasis to the lungs was detectable as early as day eight with less than 20 colony forming units (cfu) detected at this time point (Figure 8). This confirms that metastasis is likely occurring very early in conjunction with primary tumor establishment in the mammary fatpad [231]. Detection of metastasis at day eight is important as it indicates that CTCs are present in the blood, and that metastasis is established prior to the primary tumor being removed at day 12. By day 14, two days following primary tumor resection, a few hundred cfu were detectable in the lungs (Figure 8). At days 21, 28, and 35, metastasis to the lungs was detectable at levels of 1000's, 10,000's and 100,000's cfu respectively (Figure 8). The high metastatic tumor burden by day 35 resulted in morbidity and death at or around this time point in mice receiving no further treatment. At various time points, inguinal lymph nodes, blood, and liver tissues were also assessed for metastatic content using the clonogenic assays. However, metastasis to these tissues was inconsistent and tissue films were often an issue with these plates. Limiting dilutions were used to address tissue film formation, but metastatic cells were most

often not detected with the required dilutions. In a group of mice given fewer tumor cells, surgery was performed beyond 20 days post-injection, at which point metastatic lesions could be observed with the naked eye in the lungs, liver, spleen, and kidneys. Using a lower number of tumor cells and later surgery could therefore allow us to implement our post-surgical NKT cell treatment system in a model where a higher level of systemic metastasis is observed, in an attempt to demonstrate the effectiveness of our treatments on systemic disease. The major issue with this would be getting consistent metastasis levels in mice receiving injections with fewer tumor cells.

4.1.3 *GFP-Expressing 4T1 Cells*

In order to develop a comparable standard to the 4T1 clonogenic assays for measuring metastasis and to provide a means of further validating the results of clonogenic assay data, we created green-fluorescent protein-expressing 4T1 cell lines (GFP-4T1). These cell lines were developed using the Pheonix™ retroviral transduction system. Despite the normal growth profile of the primary mammary tumors up to 12 days post-tumor cell injection (Figure 9C), FACS analysis plots of single cell-dissociated lung tissue at 21 and 28 days post-tumor cell injection were difficult to read with respect to pinpointing GFP-expressing cells. This may be partly due to the low numbers of tumor cells present in the lungs at these time points (~100 and ~3000 at days 21 and 28 respectively). One important issue which should have been considered more thoroughly prior to developing the GFP-4T1 cells is the immune response in BALB/c mice towards GFP [232, 233]. The anti-GFP immune response may limit the number of tumor cells in the lungs or select against high GFP-expressing cells, resulting in only low GFP-expressing cells showing up in FACS plots. Although the model could potentially be used for more long term studies where the numbers of GFP-expressing cells in the lungs are sufficient to consistently detect and measure by FACS, there is a high potential for variability between mice in terms of the level to which an anti-GFP immune response is mounted. Due to the results of our initial 4T1-GFP experiments and the information available on the issues associated with using GFP-expressing cells in BALB/c mice, the GFP-expressing 4T1 model was abandoned for subsequent experiments. Future work involving the use of 4T1 cells carrying alternative selection markers could involve using non-immunogenic fluorescent proteins, although these would also present some of the shortfalls encountered when using the GFP expression system. Luciferase-

expressing 4T1 cell lines have already been developed and could be another potential option [57]. The luciferase-expression system would be useful for both quantifying metastatic cells in harvested tissues and tracking *in vivo* metastasis in live animals using live animal imaging equipment.

4.2 Free Glycolipid Treatment Experiment

As a starting point for post-surgical NKT cell activation experiments, free α-GC (ip. 4μg) was given on day 13 following primary tumor resection on day 12. Initially mice were assessed for metastasis to the lungs in saline control and α-GC treated mice at 21 days post-tumor cell injection using 6-TG^R plating assays. Visible metastasis was limited at day 21 and therefore could not be used to assess differences between treatment groups (Figure 11B). α-GC treatment resulted in significant reductions in lung metastasis at day 21 (Figure 10 A and C). Primary tumor size was not influencing the levels of lung metastasis as 21 lung tissue cfu numbers did not correlate with primary tumor size (Figure 10B). Lung tissue from control and α-GC treated mice at days 28 and 35 were also plated. Unfortunately, the protective effect observed at day 21 was lost by day 28, and by day 35 similar levels of lung metastasis were observed in both control and α-GC treated mice (Figure 11A). It is not clear why this is the case, but it is possible that following α-GC-induced targeting of metastatic cells following day 13 treatment, NKT cells could become anergic as a result of B cell and macrophage presentation of α-GC to NKT cells [186, 187]. Induction of NKT cell anergy following the day 13 stimulation would mean that although an initial anti-tumor immune induction phase would occur, no subsequent NKT cell activity would be present to regulate the anti-tumor immune response. If the NKT cell activation is indeed driving the anti-tumor response observed at day 21, then the return of metastasis by day 35 can be inferred to be a result of limiting long-term effects of free glycolipid treatment associated with the induction of NKT cell anergy. It follows as such that multiple free glycolipid activations would not be any more beneficial than a single activation in that NKT cell anergy following the initial activation would not allow for subsequent treatments to have any effect. However, multiple stimulations would be possible with transfer of glycolipid-loaded DCs as DC-based NKT cell activation provides effective co-stimulation to NKT cells without inducing anergy [234].

4.2.1 *Comparison of the Effects of α-GC, α-C-GC and OCH*

Initial experiments compared lung metastasis following treatment with three different glycolipid antigens, α-GC, α-C-GC and OCH. α-GC induces production of both Th1 and Th2 cytokines, while α-C-GC induces a greater Th1 response associated with better tumor clearance in some metastasis models [112, 235]. OCH induces a more Th2 polarized cytokine response [236], but has also been found to protect against metastasis [217]. Significant reductions were observed in day 21 lung metastasis using both α-GC and α-C-GC, but not with OCH (Figure 12A). Despite the observation of an elevated Th1-type skewed response in mice receiving α-C-GC (Figure 12C) and other synthetically produced Th1-skewing α-GC analogues [205, 237], α-GC generated the most consistent reduction in day 21 lung metastasis compared to the other two glycolipids tested (Figure 12A). It has been suggested that α-C-GC has increased stability in the CD1d binding cleft, which may contribute to prolonged signaling that favors a Th1 response [205, 235]. However, the beneficial response with α-GC may be related to the higher affinity for the TCR on NKT cells [177], leading to a greater *in vivo* NKT cell activation response. Still, some work with other Th1 skewing α-GC analogues has shown greater anti-cancer efficacy with modified α-GC analogues in mouse models of cancer [237]. It is thought that these compounds may increase the avidity of the NKT cell TCR interaction.

As mentioned, the immune activation associated with α-C-GC produced the highest serum IFNγ levels at 6 and 24hr post-administration (Figure 12C). While the kinetics were faster, these levels were, matched at 24hr by α-GC administration (Figure 12B). α-C-GC treatment also produced higher serum IL-4 levels than α-GC (Figures 12 B and C) which may be associated with the heightened tendency for a Th2 response in BALB/c mice [238]. Consistent with this, we observed greater Th1 polarization in C57BL/6 mice treated with α-C-GC [235]. The Th2-skewing OCH produced low levels of IFNγ and very high serum IL-4 levels (Figure 12D). Looking at the IFNγ:IL-4 ratios, α-C-GC maintained a Th1-skewed response at all three time points, while α-GC had a small tendency towards a Th2 response at 6hr, but achieved a similar Th1 response by 24hr. OCH induced a strong Th2-skewed response early on, but eventually shifted towards a Th1-type response by 24hr. The Th2-skewed response at 2 and 6h may explain decreased anti-metastatic effects observed using OCH (Figure 12A). The Th1 response observed by 24hr may explain why day 21 anti-metastatic effects were still reasonably strong with OCH treatment (Figure 12A). Unlike α-C-GC and OCH, α-GC has been used in previous clinical

trials making α-GC based treatments more likely to be implemented clinically. It phase I/II trails α-GC induced no profound adverse side-effects, indicating that additional safety studies would not be required for this glycolipid [175, 195]. For these three reasons, α-GC was chosen for use in subsequent experiments involving free glycolipid treatments and glycolipid-loaded DC treatments.

To examine the effects of post-surgically administered α-GC on survival and to compare the effects of delaying primary tumor resection on survival, mice were split into four treatment groups with resections occurring at either day 12 or 16, with saline or α-GC administered on day 13. Only day 12 resection with α-GC treatment significantly increased survival compared to the baseline treatment of resection at day 12 with day 13 saline (Figure 13A). At the time of sacrifice for mice receiving day 16 resections, systemic metastasis was much greater than that observed in mice having received day 12 resections. Observable metastases were visible in the liver, spleen and kidneys in addition to the lungs in some day 16 resected mice. By comparison, mice receiving day 12 resections only had metastases in lung tissue, with no observable systemic metastasis elsewhere. This makes sense, as leaving the primary tumor in longer allows more time for metastatic cells to seed from the primary tumor and lung metastases to other organs prior to tumor resection. The growing primary tumor being present for an additional four days would also enhance tumor associated immune suppression and aid in metastatic spread. Interestingly, mice receiving day 16 resections had much greater serum cytokine responses compared to mice receiving day 12 resections (Figure 13 B and C). IFNγ levels were nearly double and IL-4 levels were nearly five times greater, although only peak IFNγ levels were significant compared to baseline levels. The elevated IL-4 levels compared to IFNγ levels is an important point to consider as this indicates that although cytokine responses are high, they are also Th2-skewed, suggesting a pro-tumor signaling environment. Therefore, rather than a heightened cytokine response being beneficial to anti-metastatic outcomes, the pro-tumor Th2-skewed signaling would likely act as more of a therapeutic hindrance, as it could lead to decreased Th1-based anti-tumor cytotoxic effects.

Since the primary tumor was still present at the time of NKT cell activation in the day 16-resected mice, it was possible that there would be more tumor-associated immune suppression negatively influencing the glycolipid-induced cytokine response. The elevated IL-4:IFNγ ratio

suggests this is the case. However, the fact that higher cytokine responses were observed in the day 16 resection group suggests that overall NKT cell activation was not impaired.

It has been shown that the number of effector NK cells, density of NK cell receptors, and NK cell cytotoxic activity are reduced in breast cancer patients following adjuvant radiotherapy, adjuvant combined chemo-radiotherapy and surgery [239]. It may therefore be useful to delay NKT cell activation in the day 12 resection model to day 14 or 15 rather than day 13 as a means of allowing greater immune recovery prior to NKT cell-activating treatment. It would also be interesting to look at pre-surgical administration in terms of NKT cell cytokine responses and anti-metastatic effects, given the high number of NK cells and NK cell activity in pre-operative patients as compared to post-treatment and control groups [239]. In moving forward with the post-surgical model, there is a balance needed since allowing more time between surgery and NKT cell activation allows more time for metastases to establish and grow, but delaying activation even just by 24hr could be beneficial in allowing for a greater level of immune system recovery following surgery.

In an attempt to enhance systemic metastasis by delaying primary tumor resection, mice were given a lower tumor cell injection of 2×10^4 cells with treatment occurring at day 13 and resections at either days 12 or 21. Survival among mice receiving day 12 resections was significantly greater than mice receiving day 21 resections (Figure 14B). However, in both cases survival was not significantly influenced by treatment with either saline or α-GC (Figure 14A). This data shows further support for the idea that delaying surgery is detrimental in that it allows for substantial increases in metastatic disease as compared to earlier surgery. This also demonstrates the issue with using a lower number of tumor cells for mammary fatpad injections; it is possible that most mice receiving day 12 resections had little to no lung metastasis at the time of sacrifice, as both treatment and control mice survived and were healthy at the experimental endpoint (77 days) of this particular experiment. Mice in day 21 resection groups succumbed to the effects of metastasis around day 50 regardless of treatment type.

Overall, the effects of treatment with 4μg free α-GC were limited in promoting long term survival among the various resection and tumor dose protocols used. Given the shortfalls observed with using the 4μg α-GC, a dose response study was performed using 1μg, 4μg, and 20μg of α-GC. Long term survival was similar for 1μg and 4μg α-GC treatments with mice surviving ~50 days (Figure 15A). The 20μg α-GC dose in contrast was somewhat effective, as

some mice survived to the experimental endpoint of 150 days (Figure 15A). Unfortunately, the 20μg α-GC was also toxic; some mice died within days of treatment, likely as a result of liver toxicity from this treatment dose [223, 225]. As expected, 24hr IFNγ levels increased with increasing dose (Figure 15B). Surprisingly, the inverse was true for 24hr IL-4 levels (Figure 15B). This inverse relationship indicates an increasing Th1-skewed immune response with increasing doses of α-GC. Based on cytokine responses and survival outcomes with increasing doses and issues observed relating to toxicity, it would be most beneficial to titrate an optimal dose of α-GC. However, it is likely that individual human patients would respond to different optimal doses. Furthermore, hepatic toxicity is unlikely to be a critical consideration in human patients due to the smaller number of liver NKT cells compared to mice [168].

Regarding the use of α-GC as a free glycolipid, it can be concluded from these experiments that a small beneficial anti-metastatic effect can be gained by administering post-surgical free α-GC. However, these effects are not long-lasting and do not lead to survival outcomes worthy of using this form of treatment in a clinical setting. Benefits gained from free glycolipid treatment would likely be observed at very high doses, where toxicity could become an issue. Clinical studies using free α-GC confirm our findings. In a dose escalation study involving the intravenous transfer of α-GC into 24 patients with solid tumors, positive biological activity associated with NKT cell activation was noted but no clinical responses were recorded [240].

4.3 Glycolipid-loaded DC Treatment Experiments

Given the limited abilities of post-surgical free glycolipid treatment to promote long-term survival (Figure 13A), and the knowledge that multiple treatments with free glycolipids induce NKT cell anergy [217, 241], a different treatment modality was required. NKT cell activation via the adoptive transfer of glycolipid-loaded DCs is known to induce potent NKT cell activation, with an enhanced IFNγ response [182, 194, 234, 242]. This is associated with better tumor control and prolonged survival in mouse models and human clinical trials [195, 196, 243]. Furthermore, glycolipid-loaded DCs do not induce NKT cell anergy, opening the possibility for repeated treatments [182, 243, 234].

Initially, a dose response study was used to assess the effect of various doses of post-surgically delivered α-GC-loaded DCs ($5 \times 10^4 - 3 \times 10^6$) on long term survival and NKT cell

activation. Serum IFNγ levels did not differ significantly between doses. However, serum IL-4 levels increased significantly with higher doses of DCs (Figure 16A). Based on IFNγ:IL-4 ratios at the given doses, a trend was observed where lower doses of glycolipid-loaded DCs induced a skewed Th1 response while increasing doses induced a skewed Th2 response (Figure 16B). It would therefore be of benefit to use a lower dose to enhance the Th1 skewing effect.

Among all six treatment groups assessed, only doses of 2-5 x 10^5 α-GC-loaded DCs were effective at promoting long-term survival (Table 3). At these doses, partial response rates were observed in 31- 43% of mice in respective treatment groups and complete response rates were observed in 29 - 38% of mice (Table 3). A partial response rate of 33% was observed with the 1 x 10^6 dose (Table 3). The highest doses of 1 x 10^6 and 3 x 10^6 cells however provided limited to no survival advantage and this may be associated with the skewed Th2 response observed with higher doses (Figure 16B).

Based on the survival and cytokine data, the 2 x 10^5 α-GC-loaded DCs dose was the primary dose used for subsequent experiments. With α-GC treatment, it was shown that by day 28, the effects of treatment had worn off and lung metastasis had returned to near control levels (Figure 11A). Consistent with enhanced anti-tumor responses induced by glycolipid-loaded DCs [234, 242, 243], treatment with 2 x 10^5 α-GC-loaded DCs resulted in a sustained reduction in lung metastasis at day 28 (Figure 19A). In contrast to control mice receiving unloaded DCs, lung tissue from mice receiving loaded DCs had no observable metastatic lesions (Figure 18B).

Consistent with the anti-metastatic effects of α-GC-loaded DC treatment observed at day 28, mice receiving 2 x 10^5 α-GC-loaded DCs had significantly greater survival outcomes than mice receiving the same number of unloaded DCs (Figure 17A). As shown in Table 3, a complete response rate of 38% was observed with this treatment. Mice exhibiting complete responses were observed to be healthy and upon sacrifice at the experimental endpoint of 150 days. Lung tissue from these mice had no observable metastatic lesions (Figure 17B) or culturable tumor cfu.

Initial experiments examining the effects of multiple transfers with α-GC-loaded DCs found that 24hr IFNγ and IL-4 levels decreased with consecutive transfers to near-baseline levels following the third activation (Figure 18). These results appear to contrast the reported ability of glycolipid-loaded DCs to prevent NKT cell anergy [182, 234, 243]. However, it is also possible that NKT cells do not recover sufficiently from the first stimulation with only three days between

activations. Previous studies reporting a lack of anergy examined the effect of stimulations that were separated by 28 days [234]. As NKT cells undergo expansion over 3-5 days, followed by a contraction phase [244], it is possible that our repeated treatments overlapped with the contraction phase and failed to induce further activation. In subsequent studies, we began to optimize the spacing of DC treatments.

In contrast to a lack of NKT cell recovery observed when spacing treatments only three days apart (Figure 18), allowing two weeks between activations allowed for NKT cell recovery with IFNγ levels 24hr after day 27 activation reaching approximately half the level observed following day 13 activation (Figure 20). The Th1 cytokine response was near baseline following the second activation on day 20, but recovery was substantial by the time the third treatment was given on day 27. As treatments were spaced equally apart, it would be expected that given a strong response following the third activation, there should also be a reasonably strong response following the second activation. This however was not the case and may be explained by an ineffective second round of treatments. If treatments were indeed the same through all three administrations, then the lack of NKT cell response following the second treatment may point to a mild level of NKT cell anergy being induced following the initial treatment which is greater relieved over a span of two weeks as compared to one. An interesting finding was that IL-4 levels continued to decrease with consecutive transfers, while IFNγ levels rebounded strongly following the third activation (Figure 20). These findings indicate an increasingly Th1-skewed response with consecutive transfers spaced weeks apart. Multiple post-surgical treatments may therefore be a viable option given sufficient space of ~2-3 weeks between treatments. Furthering upon the results of this experiment, mice from treatment groups given multiple post-surgical treatments should be examined in long-term survival experiments to compare the strength of these treatments regimens in promoting long-term disease-free survival compared to a single post-surgical treatment where a 38% complete response rate was observed (Table 3).

As a means of further demonstrating the anti-cancer effects of α-GC-loaded DC treatment, 2 x 10^5 α-GC-loaded DC were transferred on the day prior to tumor cell injection. Primary mammary tumor growth was significantly reduced in treated mice compared to untreated mice (Figure 21 A and B). Survival among treated mice was significantly greater than saline treated mice with 75% of treated mice exhibiting a complete response (Figure 21C). This strong survival response is likely linked to both the prevention of metastases establishment

and clearance of established micrometastases. As to how much of a factor each of these components are playing is not entirely clear, but it can be concluded that as a prophylactic treatment, α-GC-loaded DC treatment is highly effective at reducing primary tumor growth, clearing/preventing metastasis and promoting long-term survival in mice.

4.4 Adoptive NKT Cell Transfer Experiments

The third treatment option to be assessed was the adoptive transfer of *in vivo* expanded NKT cells. NKT cell numbers and/or function are impaired in many cancer patients [207, 208, 230], including breast cancer [207], suggesting that NKT cell responses to DC therapy could be less than optimal. NKT cells were transferred alone or in combination with α-GC or α-GC-loaded DCs in an attempt to counteract cancer-associated NKT cell suppression. In clinical studies, NKT cell adoptive transfer have been derived from cultures of autologous glycolipid stimulated blood cells [175, 215]. Due to issues related to expanding NKT cells and maintaining viable NKT cells *in vitro*, donor mice were given injections of α-GC-loaded DCs to induce *in vivo* NKT cell expansion. Expanded NKT cells were isolated from the livers of stimulated mice and adoptively transferred into recipient mice.

Post-surgical treatments used 2 x 10^5 to 1 x 10^6 NKT cells with or without additional activation with 4μg α-GC, 2 x 10^5 α-GC-loaded DCs or 5 x 10^5 α-GC-loaded DCs. In preliminary experiments, near baseline cytokine responses were observed in all treatment groups where DCs were not given (Figure 22), indicating that although transferred NKT cells may induce low level cytokine production and anti-cancer activity, they did not respond to secondary glycolipid activation and do not induce significant cytokine production post-transfer. Co-adoptive transfers of loaded DCs and NKT cells resulted in 24hr serum cytokine levels similar to those observed previously with similar quantities of DCs (Figure 16A). Although cytokine data was not terribly promising, it was still possible that adoptive NKT transfers could have a long term effect in promoting survival. It may be possible to optimize responses in the future by delaying NKT cell activation to some point after transferred NKT cells are allowed to reset. Alternatively, it may be possible to rest NKT cells in culture prior to transfer.

Mixed results were observed among the 11 different treatments groups in long term experiments. As low numbers of mice were used in these experiments major conclusions cannot be drawn from these experiments. Transfers of NKT cells alone or in addition to α-GC were for

the most part ineffective at promoting survival (Table 4). Positive responses were observed in some mice in groups receiving co-adoptive transfer with loaded DCs, (Table 4), but this was no better than DC transfer alone. Low levels of NKT cells present in mice, even if suppressed may be sufficient to generate a response similar to what is observed with the addition of expanded NKT cells. Repeating these experiments will help to clarify exactly what is the case, but based on preliminary findings, the most effective treatment in our 4T1 model was a single post-surgical transfer 2 x 10^5 α-GC-loaded DCs.

4.5 Measuring MDSCs

MDSCs are a suppressive population of immature myeloid cells that arise from dysregulated myelopoiesis in cancer patients and during infections [245, 246, 247]. NKT cell activation has been shown to cause decreases in the number and immunosuppressive activity of MDSCs in a murine model of Influenza A infection [166]. We therefore proposed that NKT cell activation in murine cancer models could promote a similar effect. We used flow cytometry to assess the effects of NKT cell activation on the frequency of Gr-1^+CD$11b^+$ MDSCs in peripheral blood (Figure 22). The frequencies of Gr-1^+CD$11b^+$ cells were tracked in mice from pre-tumor cell challenge through until the time of death or sacrifice. At baseline, Gr-1^+CD$11b^+$ cells were ~50% of blood cells in naïve BALB/c mice, most likely identifying non-immunosuppressive populations of granulocytes, mainly neutrophils that share the same markers (Figure 23A). It has been shown that in non-tumor challenged mice, Gr-1^+CD$11b^+$ populations are non-immunosuppressive and are therefore not MDSCs but rather consisting mainly of circulating neutrophils [139]. Gr-1^+CD$11b^+$ cells levels reach a maximum of ~90-95% on day 14 (Figure 23A), 2 days after primary tumor resections. Gr-1^+CD$11b^+$ cell levels dropped beyond day 14 to near baseline levels around day 28, consistent with the role of tumor-associated immune suppression in maintaining MDSCs [248, 249, 250]. However, Gr-1^+CD$11b^+$ cell levels before tracked back to levels greater than 90% around days 35-40 in mice that did not receive treatment or failed to respond to treatment (Figure 23B). Some mice exhibiting partial responses to DC treatment had Gr-1^+CD$11b^+$ cell levels near baseline for an extended period of time, but levels tracked up to near 100% as metastatic disease eventually established and built, resulting in death within 12 weeks of tumor cell injection (Figure 23B). Gr-1^+CD$11b^+$ cell levels in mice with complete responses stayed near baseline with no significant increases observed at the experimental

endpoint (Figure 23B). In attempting to demonstrate the immunosuppressive effects of MDSCs in our model, it was not entirely clear what distinctive roles MDSCs and neutrophils were playing. Both populations are negative for the F4/80 macrophage marker, have similar PMN morphology, and exhibit similar expression of the markers CD124, S100A8, S100A9, CD11b, Gr-1, Ly6G and Ly6C [139]. Compared to neutrophils, MDSCs exhibit up-regulation of the markers CD115 and CD244, and genes associated with the cell cycle, autophagy and the CREB pathway [139]. MDSCs have lower phagocytic activity and TNFα production than neutrophils [139]. Both cell types show similar NO production, although MDSCs produce higher levels of myeloperoxidase, ROS and arginase which lead to high levels of T-cell immunosuppressive activity not observed with neutrophils derived from naïve mice [139]. It is apparent that MDSCs and neutrophils are very similar cell populations with some differences in cell surface marker expression and gene expression. The main difference which is most relevant to diseases such as cancer is the immunosuppressive activity of MDSCs. In attempting to track MDSC populations, it is therefore not as important to know what effects neutrophils are having compared to MDSCs. The granulocytic population in advanced cancer will be mostly derived of highly immunosuppressive MDSC populations which would be targeted by very similar if not the same treatments used to target a theoretical population of immunosuppressive neutrophils.

In an attempt to characterize the granulocytic population of MDSCs and identify the proportions of MDSCs which are mature neutrophils, cytospins were used to analyze PBL populations from non-tumor challenged mice and mice at various stages following tumor challenge. Naïve mice, as expected, had large numbers of lymphocytes in the peripheral blood with few monocytes and neutrophils (Figure 24). Mice receiving no DC treatments and non-responding mice had very large numbers of leukocytes in the peripheral blood, consisting mainly of cells with granulocytic morphology (Figure 24). Partially responding mice had low PBL numbers containing a mixture of granulocytes and lymphocytes (Figure 24). Unfortunately, it was very difficult to find any morphological distinctions between granulocytes observed in the peripheral blood of naïve and diseased mice. This supports the findings of previous studies showing limited differences in PMN morphology between MDSCs and neutrophils [139]. As a control, the frequency of blood MDSCs was also determined by flow cytometry (Table 5). Cytospin analysis identified higher percentages of lymphocytes than non-lymphocytes as

compared to FACS analysis, but this was likely due to misidentification of monocytes as lymphocytes.

Naïve, day 35 untreated, day 35 treated (responding) and day 35 treated (non-responding) mice were used to determine the effects of post-surgical treatment with glycolipid-loaded DCs on Gr-1^+CD$11b^+$ cell frequency and functional activity. In an immunosuppression assay using naïve T cells stimulated with anti-CD3/CD28 coated beads, significant T cell proliferation was observed when blood from naïve and responding mice was added (Figure 25 C and D). In contrast, little to no proliferation was observed when blood from mice receiving no therapy and non-responding mice was added (Figure 25 C and D). These results are only preliminary, but indicate that as expected, MDSCs comprise a high percentage of PBLs in untreated and non-responding mice and are highly immunosuppressive. It is promising to see that responding mice in addition to showing no physical signs of disease, also have MDSC/CD$11b^+$Gr-1^+ frequencies and activities similar to those observed in naïve mice. It is apparent that blood MDSC/CD$11b^+$Gr-1^+ frequencies can be useful as a prognostic indicator in using the BALB/c 4T1 model. Rather than having to sacrifice animals at given time points to assess metastasis, established values for MDSC/CD$11b^+$Gr-1^+ frequencies over a given time course can be correlated with the level of lung metastasis over the same time course. Indeed, this is what we have done with our long-term survival experiments. Excessive use of mice can be prevented by assessing blood MDSC/CD$11b^+$Gr-1^+ frequencies periodically over the span of an experiment to determine the correlated disease extent, allowing for tracking of treatment responses and aiding in the assessment of the appropriate times to sacrifice mice.

4.6 C57BL/6 E0771 Model

The E0771 model presented a number of unique challenges not encountered with the more established 4T1 model. First, E0771 tumor cells are not drug-resistant [62], meaning that measuring metastasis in a clonogenic assay was not possible in this model. To solve this problem, we attempted to transduce E0771 cells with a Pheonix^{TM} GFP-expressing retrovirus. Puromycin selection of transduced cells eventually resulted in a small number of puromycin-resistant colonies that were expanded under puromycin selection and used to select monoclonal cell lines. However, there was no detectable GFP expression in these lines by flow cytometry and they did not contain detectable retroviral construct by PCR. Puromycin-resistant E0771 cells

were used in Figures 26 and 27. Growth kinetics of the primary tumor masses were highly consistent between tumor cell challenged mice (Figure 26). The major issue with these cells was their lack of consistency in metastasizing to the lungs. Only data from mice with clear lung metastasis (based on plating assays) could be used in data analysis as lung metastasis rates were less than 20%, with absence of metastasis apparent in both control and treated mice. This lack of consistency in metastasis also prevented survival analysis as there were limited numbers of mice dying of metastatic disease, with no common cause of death or time of death observed between mice. However, preliminary experiments involving the E0771-Puro^R model did show similar results to the 4T1 model using (ip. 4μg) α-GC treatment, with a roughly 68% decrease in day 21 lung metastasis (Figure 27A).

Compared with the 4T1 model in BALB/c mice, there was little consistency in blood MDSC levels between mice in the C57BL/6 mice E0771 tumor model. This may again relate to the variability we observed in this model.

Future experiments using this model may require delaying primary tumor excision until later time points to allow time for metastasis to occur. The number of cells used to challenge mice could be reduced to allow for slower tumor growth and provide more time for metastasis prior to the primary tumor becoming such a burden to the mouse. Another possibility would be to isolate metastatic tumor cells from the lungs and generate a new monoclonal population that has a higher probability of trafficking to the lungs [251].

It can be noted that as compared to BALB/c mice where GFP is highly immunogenic, GFP in C57BL/6 mice has been shown to have very little immunogenicity [252, 253], indicating that it may be useful to generate GFP-expressing E0771 cells for the measurement of E0771 cell metastasis. We have developed 6-TG-resistant E0771 cell lines with resistance to 6-TG at concentrations of over 120μM. This is the same drug used for screening metastatic 4T1 cells and thus allows for an overlap in screening procedures between the two models. These 6-TG^R E0771 cells will be used in future experiments to assess their growth and metastasis profile *in vivo* and used for optimization of an E0771 breast cancer lung metastasis model.

Chapter 5: Conclusion

5.1 Summary of Major Findings

Post-surgical free glycolipid treatment using α-GC, α-C-GC or OCH (4μg ip.) was effective at decreasing lung metastasis in both the 4T1 and the E0771 models at 21 days post-tumor cell injection but did not provide lasting protection. Cytokine data showed that α-C-GC produced the most Th1 skewed response with elevated IFNγ output levels compared to α-GC, while OCH produced the most Th2 skewed response with elevated IL-4 compared to α-GC. Despite the increased Th1 type response in α-C-GC treated mice, metastasis reductions at 21 days post-tumor cell injection were similar between both α-GC and α-C-GC treated mice. OCH treatment tended to reduce day 21 lung metastasis but this reduction was not significant. α-GC did not improve overall survival in mice as compared to saline treated mice. Survival experiments using OCH and α-C-GC were not performed, but would not be expected to improve upon the results observed with α-GC, as α-C-GC has been shown to have reduced in vivo activity compared to α-GC and OCH induces a Th2-skewed immune response.

Treatments with glycolipid-loaded DCs were better tolerated than free glycolipid and improved survival compared to either glycolipid treated mice or mice treated with unloaded DCs. Mice treated with 2×10^5 α-GC-loaded DCs initially showed some inadvertent responses associated with the treatment, but overall the effect of this treatment was quite dramatic. Mice showed significant reductions in lung metastasis several weeks post-4T1 injection and a number of mice exhibited partial or complete responses to treatment.

Multiple NKT cell activation treatments when given days apart resulted in limited to no secondary cytokine responses. When treatments were spaced apart by two weeks, significant recovery of the cytokine response was observed, suggesting a starting point for further development of DC therapy where treatments would therefore have to be spaced weeks apart in order to see significant anti-cancer effects associated with cytokine signaling pathways.

Blood Gr-1^+CD$11b^+$ levels in the 4T1 model correlated with the level of functionally immunosuppressive MDSCs and provided a good prognostic indicator of overall health and cancer state for mice in the various treatment groups. This will provide a good way to evaluate mice over time without having to sacrifice animals at separate time points.

5.2 Clinical Implications

Effective treatments for advanced metastatic disease are currently lacking. In recent clinical trials, NKT cell activation therapies have been shown to extend survival, but do not typically cause regression of the primary tumor [114, 196]. Given the known anti-metastatic effects of NKT cell activation and what has been shown in this body of research, the prospects are good for using NKT cell activation as part of a post-surgical treatment option for patients diagnosed with metastatic breast cancer. Breast cancers, unlike many other solid cancers, typically allow for effective surgical removal of the primary tumor. This makes breast cancer an ideal situation in which to implement anti-metastatic NKT cell therapies. We have shown here that by removing the primary mammary tumor and then targeting distant metastasis via post-surgical NKT cell activation, metastatic breast cancer can be cured in mice. This was accomplished using various doses of α-GC-loaded DCs. Multiple treatments will likely be required in humans in the event of extensive disease. We have established that administering treatments several weeks apart allows for recovery of NKT cell responses which is a good sign that multiple treatments may be effective in at least controlling disease long enough for other treatments to have an effect. Further possibilities include combining NKT cell activating treatments with chemotherapeutics and other forms of treatment to extend survival.

Based not only our positive findings using this post-surgical NKT cell activation system in mice, but also positive outcomes in other murine cancer models and in various clinical trials involving adoptive α-GC-loaded DC transfers [114, 115, 194, 195, 196, 254, 255], we remain optimistic that this form of treatment could be advantageous in human cases of metastatic breast cancer.

5.3 Future Directions

It is apparent based on our findings that post-surgical NKT cell-activating therapy holds potential for the treatment of metastatic breast cancer. Free glycolipid treatment was not effective unless toxic doses were used, and the adoptive transfer of NKT cells appeared to required high numbers to induce any level of protection. In contrast, a single dose of 2×10^5 α-GC-loaded DCs was highly effective in targeting and eliminating lung metastases. The most effective treatments involved using either a single low-dose transfer of α-GC-loaded DCs or a combined transfer of α-GC-loaded DCs with a large number of NKT cells.

To further verify and extend our findings, it will also be important to implement post-surgical treatments at later time-points to assess whether these NKT cell activating treatments can be curative when metastatic lesions have become better developed and more widespread. This may mean decreasing the initial tumor cell injection quantity to allow for slower growth of the primary tumor while the metastases are being established. Decreasing the tumor cell inoculation will decrease the consistency at which primary tumors and metastases grow, but will allow for systemic metastasis to occur prior to surgical resection of the primary tumor mass and subsequent NKT cell activation therapy. MDSC screening may be a suitable way to screen mice for tumour metastasis prior to treatment. Maintaining the tumor cell inoculations at 2×10^5 cells and delaying the surgery and treatment by a few days would also provide a means of achieving higher metastasis. However, surgeries become more extensive as the primary tumors are allowed to grow further, leading to a higher potential for surgical complications. The surgery could be kept at day 12 and the NKT cell activation extended to day 15-18 since it appears as though maximum MDSC levels are reached at day 14 and immune recovery occurs thereafter. Unfortunately, delaying NKT cell-activating therapy also allows further time for metastases to become established. In a clinical setting a balance would be needed between how quickly after the surgery optimal immune system recovery occurs versus the build-up of metastases.

NKT cell anergy is a major barrier to overcome if free glycolipid treatments are to be given in a clinical setting. This anergy which is thought to result from non-selective presentation of α-GC by B cells, prevents multiple free glycolipid injections from being effective [256]. If only a single dose is to be given, it must be powerful enough to cause complete regression of malignant tissue or at least promote regression to the extent that other therapies such as chemotherapy can eliminate the remaining cancerous tissue. We have demonstrated that optimal responses to α-GC-loaded DC transfer are achieved at intermediate to low dose ranges in mice. In further optimizing DC treatments, it could also be useful to change the amount of α-GC that *in vitro* cultured DCs are cultured with to optimize *in vivo* α-GC presentation from the DCs to host NKT cells. Further experiments could implement the loading of DCs with non-α-GC NKT cell activating glycolipids which are currently being developed. Synthetic analogues of α-GC show promise in that they demonstrate improved Th1-skewed responses compared to α-GC; although, analogues have not yet demonstrated improved anti-cancer activity compared to α-GC *in vivo*.

As we are currently only assessing the effects of adoptively transferred α-GC-loaded DC's when transferred intravenously, it may also be useful to assess responses and survival outcomes when DC's are transferred intraperitoneally or directly into the primary mammary tumor. Injecting α-GC intradermally has been shown to decrease anergy induction compared to intravenous injection [227]. In clinical trials comparing intravenous versus intradermal administration of α-GC-loaded DCs to patients with various forms of metastatic malignancies, greater immunological responses were observed with intravenous treatment as a result of poor trafficking from the injection site with intradermal treatment [228]. The intradermal route did however result in greater NKT cell memory and a quicker response to secondary activations as compared to the intravenous route [228]. The use of immature DCs lacking CCR7 in this study likely reduced DC trafficking from the injection site with intradermal injection [228], indicating that there is still potential for intradermal treatment to be beneficial given a different DC subset selection and a malignancy in a region near the site of injection.

Some DC subsets are better suited to activating NKT cells than others. For example, $CD8^+$ DCs are better activators of NKT cells than other subsets [172, 257]. Similarly, we have found that DCs expressing high levels of the chemokine CXCL16 provide a co-stimulatory signal to NKT cells that enhances IFNγ production (Veinotte and Johnston, unpublished). In future experiments, specific DC subsets will be isolated and assessed for their ability to improve upon the results obtained in the 4T1 model using heterogeneous DC populations. NKT cells use cell surface-expressed CXCR6 during activation to optimally respond to DC presented CXCL16 and to accumulate in tissue sites including the liver and lungs [258, 259]. In mouse models of liver metastasis, enhanced metastasis was noted in the absence of CXCR6 expression and when using CXCL16 neutralizing antibody [217], further indicating the importance of these cell surface molecules in both NKT cell homing and activation, and their importance in the NKT cell-initiated anti-cancer response. Thus, purifying $CXCL16^{high}$ DCs out of heterogeneous populations and using them in α-GC-loaded DC therapies could be another useful step forward in optimizing this form of treatment.

As NKT cell-based therapies will likely not be used on their own as a means of anti-cancer therapy in a clinical setting, it is of great importance to determine which combination of therapies would be of greatest benefit to patients. Thus, combining radiation therapy and or various chemotherapeutic agents with NKT cell activation therapy should be assessed. It has

been demonstrated that both gemcitabine treatment [110] and local radiation therapy [260] have no negative effect on NKT cell number and function. Cyclophosphamide treatment has also been shown to have no negative influence on NKT cell populations [261].

Despite the poor results obtained using GFP-expressing 4T1 cells in BALB/c mice, it would still be nice to have a secondary means of measuring metastasis in the cancer models we have been using. As GFP has been shown to be immunogenic in BALB/c mice, limiting consistency of metastasis and selecting against high GFP-expressing 4T1 cells, it could be useful to transfect cells with plasmids expressing genes for other fluorescent proteins such as cherry red or blue fluorescent protein. Immunogenicity of these proteins would have to be assessed in BALB/c and C57BL/6 mice if they are to be used with the 4T1 and E0771 models. Alternatively, cells could be made to express human CD2 or a congenic mouse marker that could be detected by FACS. Generating these cell lines would not be a priority, but for future experiments could prove to be very valuable tools.

There are a number of murine metastatic breast cancer models available, although in most models it is difficult to accurately assess the level of metastasis and therefore the effects treatments are having on metastasis. The 4T1 model is an exception in that 4T1 tumor cells have been selected for have resistance against 6-TG [55]. Having generated 6-TG-resistant E0771 cells in our lab through serial passaging with 6-TG selection, we will now proceed to assess *in vivo* tumor growth and metastasis kinetics with these cells in C57BL/6 mice. Further work using the E0771 6-TG^R model, once established, will involve using free glycolipid treatment and treatments involving the use of expanded NKT cells and α-GC-loaded DCs as per what we have done using the 4T1 model. As E0771 cells are ER$^+$, in contrast to 4T1 cells which are ER$^-$ [64, 262], there is the possibility for using targeted hormone therapies such as tamoxifen, Evista or Fareston in combination with NKT cell activation therapy.

Work with the 4T1 model has led to our use of the blood MDSC population as a prognostic indicator of health throughout experiments. It is still not clear however, what fraction of the Gr-1$^+$CD11b$^+$ the population we see in the blood are truly MDSCs or simply neutrophils. We have performed functional assays with blood MDSC populations to compare against FACS data, and clearly the Gr-1$^+$CD11b$^+$ populations in the blood of mice with tumor burden are immunosuppressive. What remains uncertain, and moreover remains uncertain in the field of MDSC research, is the classification and complete characterization of these immunosuppressive

cell types. Further work remains to be done in phenotypically and functionally distinguishing MDSCs from neutrophils. The immunosuppressive contribution of MDSCs in the 4T1 model as compared to other cell types such as Tregs, Bregs and TAMs has been addressed [59, 109, 263, 264, 265, 266], but remains incompletely understood. This holds true not only in the 4T1 model, but also in other breast cancer models, cancer models in general, and in human cancers. As MDSCs are not the only cell type playing a role in tumor-associated immune suppression, it would be useful to look at other suppressive leukocyte populations such as Tregs, Bregs and type 2 macrophages. The activity of Tregs in the 4T1 model has been shown to be a requirement for lung metastasis [264]. Also in the 4T1 model, it was shown that tumor-evoked Bregs (tBregs) induce TGF-β-dependent conversion of resting $CD4^+$ T cells to $FoxP3^+$ Tregs [263]. Depletion of Bregs using anti-B220 prevented lung metastasis by limiting $CD4^+$ T cell to Treg conversion [263]. Characterization of Breg and Treg subsets in addition to macrophage and other immunosuppressive cell populations in the 4T1 model will be assessed. Additionally, the effects of NKT cell activation on these cells will be addressed in future experiments.

References:

1. Sinha P, Clements VK, Fulton AM, Ostrand-Rosenberg S. Prostaglandin E2 promotes tumor progression by inducing myeloid-derived suppressor cells. Cancer Res 2007 May 1;67(9):4507-13.

2. Hanahan D, Weinberg RA. The hallmarks of cancer. Cell 2000 Jan 7;100(1):57-70.

3. Visvader JE. Cells of origin in cancer. Nature 2011 Jan 20;469(7330):314-22.

4. Dimaras H, Kimani K, Dimba EA, Gronsdahl P, White A, Chan HS, Gallie BL. Retinoblastoma. Lancet 2012 Apr 14;379(9824):1436-46.

5. Kang E, Park SK, Yang JJ, Park B, Lee MH, Lee JW, Suh YJ, Lee JE, Kim HA, Oh SJ, et al. Accuracy of BRCA1/2 mutation prediction models in korean breast cancer patients. Breast Cancer Res Treat 2012 Mar 22.

6. Smith KL, Isaacs C. BRCA mutation testing in determining breast cancer therapy. Cancer J 2011 Nov-Dec;17(6):492-9.

7. Kane EV, Newton R. Benzene and the risk of non-hodgkin lymphoma: A review and meta-analysis of the literature. Cancer Epidemiol 2010 Feb;34(1):7-12.

8. Vineis P, Xun W. The emerging epidemic of environmental cancers in developing countries. Ann Oncol 2009 Feb;20(2):205-12.

9. Thun MJ, Hannan LM, Adams-Campbell LL, Boffetta P, Buring JE, Feskanich D, Flanders WD, Jee SH, Katanoda K, Kolonel LN, et al. Lung cancer occurrence in never-smokers: An analysis of 13 cohorts and 22 cancer registry studies. PLoS Med 2008 Sep 30;5(9):e185.

10. Anand P, Kunnumakkara AB, Sundaram C, Harikumar KB, Tharakan ST, Lai OS, Sung B, Aggarwal BB. Cancer is a preventable disease that requires major lifestyle changes. Pharm Res 2008 Sep;25(9):2097-116.

11. Monk M, Holding C. Human embryonic genes re-expressed in cancer cells. Oncogene 2001 Dec 6;20(56):8085-91.

12. Kramarova E, Stiller CA. The international classification of childhood cancer. Int J Cancer 1996 Dec 11;68(6):759-65.

13. Hanahan D, Weinberg RA. Hallmarks of cancer: The next generation. Cell 2011 Mar 4;144(5):646-74.

14. Tiwari N, Gheldof A, Tatari M, Christofori G. EMT as the ultimate survival mechanism of cancer cells. Semin Cancer Biol 2012 Jun;22(3):194-207.

15. McConkey DJ, Choi W, Marquis L, Martin F, Williams MB, Shah J, Svatek R, Das A, Adam L, Kamat A, et al. Role of epithelial-to-mesenchymal transition (EMT) in drug sensitivity and metastasis in bladder cancer. Cancer Metastasis Rev 2009 Dec;28(3-4):335-44.

16. Sykes SM, Mellert HS, Holbert MA, Li K, Marmorstein R, Lane WS, McMahon SB. Acetylation of the p53 DNA-binding domain regulates apoptosis induction. Mol Cell 2006 Dec 28;24(6):841-51.

17. Halazonetis TD, Gorgoulis VG, Bartek J. An oncogene-induced DNA damage model for cancer development. Science 2008 Mar 7;319(5868):1352-5.

18. Ebos JM, Lee CR, Kerbel RS. Tumor and host-mediated pathways of resistance and disease progression in response to antiangiogenic therapy. Clin Cancer Res 2009 Aug 15;15(16):5020-5.

19. Gabrilovich D, Ishida T, Oyama T, Ran S, Kravtsov V, Nadaf S, Carbone DP. Vascular endothelial growth factor inhibits the development of dendritic cells and dramatically affects the differentiation of multiple hematopoietic lineages in vivo. Blood 1998 Dec 1;92(11):4150-66.

20. Gabrilovich DI, Ishida T, Nadaf S, Ohm JE, Carbone DP. Antibodies to vascular endothelial growth factor enhance the efficacy of cancer immunotherapy by improving endogenous dendritic cell function. Clin Cancer Res 1999 Oct;5(10):2963-70.

21. Ohm JE, Shurin MR, Esche C, Lotze MT, Carbone DP, Gabrilovich DI. Effect of vascular endothelial growth factor and FLT3 ligand on dendritic cell generation in vivo. J Immunol 1999 Sep 15;163(6):3260-8.

22. Bequet-Romero M, Morera Y, Ayala-Avila M, Ancizar J, Soria Y, Blanco A, Suarez-Alba J, Gavilondo JV. CIGB-247: A VEGF-based therapeutic vaccine that reduces experimental and spontaneous lung metastasis of C57Bl/6 and BALB/c mouse tumors. Vaccine 2012 Feb 27;30(10):1790-9.

23. Langley RR, Fidler IJ. The seed and soil hypothesis revisited--the role of tumor-stroma interactions in metastasis to different organs. Int J Cancer 2011 Jun 1;128(11):2527-35.

24. Coughlin TA, Nyasavajjala SM, Pereira M, White TJ, Hurst NG, Reynolds JR, Semeraro D. Hamartomatous polyposis in a middle-aged female subject with rare colonic adenomatous spread. Colorectal Dis 2010 Oct;12(10 Online):e341-2.

25. Chiang AC, Massague J. Molecular basis of metastasis. N Engl J Med 2008 Dec 25;359(26):2814-23.

26. Fidler IJ. Metastasis: Guantitative analysis of distribution and fate of tumor embolilabeled with 125 I-5-iodo-2'-deoxyuridine. J Natl Cancer Inst 1970 Oct;45(4):773-82.

27. Fidler IJ, Yano S, Zhang RD, Fujimaki T, Bucana CD. The seed and soil hypothesis: Vascularisation and brain metastases. Lancet Oncol 2002 Jan;3(1):53-7.

28. Gupta GP, Nguyen DX, Chiang AC, Bos PD, Kim JY, Nadal C, Gomis RR, Manova-Todorova K, Massague J. Mediators of vascular remodelling co-opted for sequential steps in lung metastasis. Nature 2007 Apr 12;446(7137):765-70.

29. Fokas E, Engenhart-Cabillic R, Daniilidis K, Rose F, An HX. Metastasis: The seed and soil theory gains identity. Cancer Metastasis Rev 2007 Dec;26(3-4):705-15.

30. Wu D, Zhau HE, Huang WC, Iqbal S, Habib FK, Sartor O, Cvitanovic L, Marshall FF, Xu Z, Chung LW. cAMP-responsive element-binding protein regulates vascular endothelial growth factor expression: Implication in human prostate cancer bone metastasis. Oncogene 2007 Aug 2;26(35):5070-7.

31. Talmadge JE, Fidler IJ. AACR centennial series: The biology of cancer metastasis: Historical perspective. Cancer Res 2010 Jul 15;70(14):5649-69.

32. Diel IJ, Solomayer EF, Bastert G. Treatment of metastatic bone disease in breast cancer: Bisphosphonates. Clin Breast Cancer 2000 Apr;1(1):43-51.

33. Ruiterkamp J, Ernst MF. The role of surgery in metastatic breast cancer. Eur J Cancer 2011 Sep;47 Suppl 3:S6-22.

34. Canadian Cancer Statistics 2012 [Internet]; c2012. Available from: http://www.cancer.ca/Canada-wide/Publications/Alphabetical%20list%20of%20publications/~/media/CCS/Canada%20wide/Files%20List/English%20files%20heading/PDF%20-%20Policy%20-%20Canadian%20Cancer%20Statistics%20-%20English/Canadian%20Cancer%20Statistics%202012%20-%20English.ashx.

35. Forouzanfar MH, Foreman KJ, Delossantos AM, Lozano R, Lopez AD, Murray CJ, Naghavi M. Breast and cervical cancer in 187 countries between 1980 and 2010: A systematic analysis. Lancet 2011 Oct 22;378(9801):1461-84.

36. Al-Ejeh F, Smart CE, Morrison BJ, Chenevix-Trench G, Lopez JA, Lakhani SR, Brown MP, Khanna KK. Breast cancer stem cells: Treatment resistance and therapeutic opportunities. Carcinogenesis 2011 May;32(5):650-8.

37. Haque R, Ahmed SA, Inzhakova G, Shi J, Avila C, Polikoff J, Bernstein L, Enger SM, Press MF. Impact of breast cancer subtypes and treatment on survival: An analysis spanning two decades. Cancer Epidemiol Biomarkers Prev 2012 Oct;21(10):1848-55.

38. Cancer Genome Atlas Network. Comprehensive molecular portraits of human breast tumours. Nature 2012 Oct 4;490(7418):61-70.

39. Woodward WA, Strom EA, Tucker SL, McNeese MD, Perkins GH, Schechter NR, Singletary SE, Theriault RL, Hortobagyi GN, Hunt KK, et al. Changes in the 2003 american joint committee on cancer staging for breast cancer dramatically affect stage-specific survival. J Clin Oncol 2003 Sep 1;21(17):3244-8.

40. Barse PM. Issues in the treatment of metastatic breast cancer. Semin Oncol Nurs 2000 Aug;16(3):197-205.

41. Sherry MM, Greco FA, Johnson DH, Hainsworth JD. Metastatic breast cancer confined to the skeletal system. an indolent disease. Am J Med 1986 Sep;81(3):381-6.

42. Sherry MM, Greco FA, Johnson DH, Hainsworth JD. Breast cancer with skeletal metastases at initial diagnosis. distinctive clinical characteristics and favorable prognosis. Cancer 1986 Jul 1;58(1):178-82.

43. Huang HJ, Neven P, Drijkoningen M, Paridaens R, Wildiers H, Van Limbergen E, Berteloot P, Amant F, Vergote I, Christiaens MR. Association between tumour characteristics and HER-2/neu by immunohistochemistry in 1362 women with primary operable breast cancer. J Clin Pathol 2005 Jun;58(6):611-6.

44. Osborne CK, Yochmowitz MG, Knight WA,3rd, McGuire WL. The value of estrogen and progesterone receptors in the treatment of breast cancer. Cancer 1980 Dec 15;46(12 Suppl):2884-8.

45. Slamon DJ, Clark GM, Wong SG, Levin WJ, Ullrich A, McGuire WL. Human breast cancer: Correlation of relapse and survival with amplification of the HER-2/neu oncogene. Science 1987 Jan 9;235(4785):177-82.

46. Slamon DJ, Godolphin W, Jones LA, Holt JA, Wong SG, Keith DE, Levin WJ, Stuart SG, Udove J, Ullrich A. Studies of the HER-2/neu proto-oncogene in human breast and ovarian cancer. Science 1989 May 12;244(4905):707-12.

47. Spector NL, Blackwell KL. Understanding the mechanisms behind trastuzumab therapy for human epidermal growth factor receptor 2-positive breast cancer. J Clin Oncol 2009 Dec 1;27(34):5838-47.

48. Saini KS, Azim HA,Jr, Metzger-Filho O, Loi S, Sotiriou C, de Azambuja E, Piccart M. Beyond trastuzumab: New treatment options for HER2-positive breast cancer. Breast 2011 Oct;20 Suppl 3:S20-7.

49. Piccart-Gebhart MJ, Procter M, Leyland-Jones B, Goldhirsch A, Untch M, Smith I, Gianni L, Baselga J, Bell R, Jackisch C, et al. Trastuzumab after adjuvant chemotherapy in HER2-positive breast cancer. N Engl J Med 2005 Oct 20;353(16):1659-72.

50. Romond EH, Perez EA, Bryant J, Suman VJ, Geyer CE,Jr, Davidson NE, Tan-Chiu E, Martino S, Paik S, Kaufman PA, et al. Trastuzumab plus adjuvant chemotherapy for operable HER2-positive breast cancer. N Engl J Med 2005 Oct 20;353(16):1673-84.

51. Pohlmann PR, Mayer IA, Mernaugh R. Resistance to trastuzumab in breast cancer. Clin Cancer Res 2009 Dec 15;15(24):7479-91.

52. Hortobagyi GN, Holmes FA. Optimal dosing of paclitaxel and doxorubicin in metastatic breast cancer. Semin Oncol 1997 Feb;24(1 Suppl 3):S4-7.

53. Perry MC, Kardinal CG, Korzun AH, Ginsberg SJ, Raich PC, Holland JF, Ellison RR, Kopel S, Schilling A, Aisner J. Chemohormonal therapy in advanced carcinoma of the breast: Cancer and leukemia group B protocol 8081. J Clin Oncol 1987 Oct;5(10):1534-45.

54. Aslakson CJ, Miller FR. Selective events in the metastatic process defined by analysis of the sequential dissemination of subpopulations of a mouse mammary tumor. Cancer Res 1992 Mar 15;52(6):1399-405.

55. Pulaski BA, Ostrand-Rosenberg S. Mouse 4T1 breast tumor model. Curr Protoc Immunol 2001 May;Chapter 20:Unit 20.2.

56. Bove K, Lincoln DW, Tsan MF. Effect of resveratrol on growth of 4T1 breast cancer cells in vitro and in vivo. Biochem Biophys Res Commun 2002 Mar 8;291(4):1001-5.

57. Tao K, Fang M, Alroy J, Sahagian GG. Imagable 4T1 model for the study of late stage breast cancer. BMC Cancer 2008 Aug 9;8:228.

58. Vora A, Mitchell CD, Lennard L, Eden TO, Kinsey SE, Lilleyman J, Richards SM, Medical Research Council, National Cancer Research Network Childhood Leukaemia Working Party. Toxicity and efficacy of 6-thioguanine versus 6-mercaptopurine in childhood lymphoblastic leukaemia: A randomised trial. Lancet 2006 Oct 14;368(9544):1339-48.

59. Bunt SK, Yang L, Sinha P, Clements VK, Leips J, Ostrand-Rosenberg S. Reduced inflammation in the tumor microenvironment delays the accumulation of myeloid-derived suppressor cells and limits tumor progression. Cancer Res 2007 Oct 15;67(20):10019-26.

60. Hanson EM, Clements VK, Sinha P, Ilkovitch D, Ostrand-Rosenberg S. Myeloid-derived suppressor cells down-regulate L-selectin expression on CD4+ and CD8+ T cells. J Immunol 2009 Jul 15;183(2):937-44.

61. Sinha P, Okoro C, Foell D, Freeze HH, Ostrand-Rosenberg S, Srikrishna G. Proinflammatory S100 proteins regulate the accumulation of myeloid-derived suppressor cells. J Immunol 2008 Oct 1;181(7):4666-75.

62. Goodsen LH, Barvick L, Stone RG, Ibach M, Palmer J. Inhibition screening data using sarcoma 180 and adenocarcinoma E0771. Cancer Res 1955;Suppl. 2:81-102.

63. Ewens A, Mihich E, Ehrke MJ. Distant metastasis from subcutaneously grown E0771 medullary breast adenocarcinoma. Anticancer Res 2005 Nov-Dec;25(6B):3905-15.

64. Banka CL, Lund CV, Nguyen MT, Pakchoian AJ, Mueller BM, Eliceiri BP. Estrogen induces lung metastasis through a host compartment-specific response. Cancer Res 2006 Apr 1;66(7):3667-72.

65. Meeran SM, Patel SN, Li Y, Shukla S, Tollefsbol TO. Bioactive dietary supplements reactivate ER expression in ER-negative breast cancer cells by active chromatin modifications. PLoS One 2012;7(5):e37748.

66. Zindl CL, Chaplin DD. Immunology. tumor immune evasion. Science 2010 May 7;328(5979):697-8.

67. Kalluri R, Zeisberg M. Fibroblasts in cancer. Nat Rev Cancer 2006 May;6(5):392-401.

68. Pietras K, Ostman A. Hallmarks of cancer: Interactions with the tumor stroma. Exp Cell Res 2010 May 1;316(8):1324-31.

69. Swann JB, Smyth MJ. Immune surveillance of tumors. J Clin Invest 2007 May;117(5):1137-46.

70. Dunn GP, Old LJ, Schreiber RD. The immunobiology of cancer immunosurveillance and immunoediting. Immunity 2004 Aug;21(2):137-48.

71. Croci DO, Zacarias Fluck MF, Rico MJ, Matar P, Rabinovich GA, Scharovsky OG. Dynamic cross-talk between tumor and immune cells in orchestrating the immunosuppressive network at the tumor microenvironment. Cancer Immunol Immunother 2007 Nov;56(11):1687-700.

72. Whiteside TL. Immune suppression in cancer: Effects on immune cells, mechanisms and future therapeutic intervention. Semin Cancer Biol 2006 Feb;16(1):3-15.

73. Penn I. Tumors of the immunocompromised patient. Annu Rev Med 1988;39:63-73.

74. Pardoll D. Does the immune system see tumors as foreign or self? Annu Rev Immunol 2003;21:807-39.

75. Kaplan DH, Shankaran V, Dighe AS, Stockert E, Aguet M, Old LJ, Schreiber RD. Demonstration of an interferon gamma-dependent tumor surveillance system in immunocompetent mice. Proc Natl Acad Sci U S A 1998 Jun 23;95(13):7556-61.

76. Shankaran V, Ikeda H, Bruce AT, White JM, Swanson PE, Old LJ, Schreiber RD. IFNgamma and lymphocytes prevent primary tumour development and shape tumour immunogenicity. Nature 2001 Apr 26;410(6832):1107-11.

77. Street SE, Trapani JA, MacGregor D, Smyth MJ. Suppression of lymphoma and epithelial malignancies effected by interferon gamma. J Exp Med 2002 Jul 1;196(1):129-34.

78. Galon J, Costes A, Sanchez-Cabo F, Kirilovsky A, Mlecnik B, Lagorce-Pages C, Tosolini M, Camus M, Berger A, Wind P, et al. Type, density, and location of immune cells within human colorectal tumors predict clinical outcome. Science 2006 Sep 29;313(5795):1960-4.

79. Pages F, Berger A, Camus M, Sanchez-Cabo F, Costes A, Molidor R, Mlecnik B, Kirilovsky A, Nilsson M, Damotte D, et al. Effector memory T cells, early metastasis, and survival in colorectal cancer. N Engl J Med 2005 Dec 22;353(25):2654-66.

80. Smyth MJ, Godfrey DI, Trapani JA. A fresh look at tumor immunosurveillance and immunotherapy. Nat Immunol 2001 Apr;2(4):293-9.

81. Ryan JC, Seaman WE. Divergent functions of lectin-like receptors on NK cells. Immunol Rev 1997 Feb;155:79-89.

82. Lanier LL. Activating and inhibitory NK cell receptors. Adv Exp Med Biol 1998;452:13-8.

83. Bauer S, Groh V, Wu J, Steinle A, Phillips JH, Lanier LL, Spies T. Activation of NK cells and T cells by NKG2D, a receptor for stress-inducible MICA. Science 1999 Jul 30;285(5428):727-9.

84. Whiteside TL, Herberman RB. The role of natural killer cells in immune surveillance of cancer. Curr Opin Immunol 1995 Oct;7(5):704-10.

85. Albertsson PA, Basse PH, Hokland M, Goldfarb RH, Nagelkerke JF, Nannmark U, Kuppen PJ. NK cells and the tumour microenvironment: Implications for NK-cell function and anti-tumour activity. Trends Immunol 2003 Nov;24(11):603-9.

86. Van Kaer L, Joyce S. Innate immunity: NKT cells in the spotlight. Curr Biol 2005 Jun 7;15(11):R429-31.

87. Gallucci S, Matzinger P. Danger signals: SOS to the immune system. Curr Opin Immunol 2001 Feb;13(1):114-9.

88. Zitvogel L, Casares N, Pequignot MO, Chaput N, Albert ML, Kroemer G. Immune response against dying tumor cells. Adv Immunol 2004;84:131-79.

89. Bennett SR, Carbone FR, Karamalis F, Miller JF, Heath WR. Induction of a CD8+ cytotoxic T lymphocyte response by cross-priming requires cognate CD4+ T cell help. J Exp Med 1997 Jul 7;186(1):65-70.

90. Smyth MJ, Crowe NY, Hayakawa Y, Takeda K, Yagita H, Godfrey DI. NKT cells - conductors of tumor immunity? Curr Opin Immunol 2002 Apr;14(2):165-71.

91. Brigl M, Brenner MB. CD1: Antigen presentation and T cell function. Annu Rev Immunol 2004;22:817-90.

92. Dhodapkar MV, Geller MD, Chang DH, Shimizu K, Fujii S, Dhodapkar KM, Krasovsky J. A reversible defect in natural killer T cell function characterizes the progression of premalignant to malignant multiple myeloma. J Exp Med 2003 Jun 16;197(12):1667-76.

93. Joyce S. CD1d and natural T cells: How their properties jump-start the immune system. Cell Mol Life Sci 2001 Mar;58(3):442-69.

94. Hansen MH, Nielsen H, Ditzel HJ. The tumor-infiltrating B cell response in medullary breast cancer is oligoclonal and directed against the autoantigen actin exposed on the surface of apoptotic cancer cells. Proc Natl Acad Sci U S A 2001 Oct 23;98(22):12659-64.

95. Nzula S, Going JJ, Stott DI. Antigen-driven clonal proliferation, somatic hypermutation, and selection of B lymphocytes infiltrating human ductal breast carcinomas. Cancer Res 2003 Jun 15;63(12):3275-80.

96. Kurnick JT, Ramirez-Montagut T, Boyle LA, Andrews DM, Pandolfi F, Durda PJ, Butera D, Dunn IS, Benson EM, Gobin SJ, et al. A novel autocrine pathway of tumor escape from immune recognition: Melanoma cell lines produce a soluble protein that diminishes expression of the gene encoding the melanocyte lineage melan-A/MART-1 antigen through down-modulation of its promoter. J Immunol 2001 Aug 1;167(3):1204-11.

97. Bai XF, Liu JQ, Joshi PS, Wang L, Yin L, Labanowska J, Heerema N, Zheng P, Liu Y. Different lineages of P1A-expressing cancer cells use divergent modes of immune evasion for T-cell adoptive therapy. Cancer Res 2006 Aug 15;66(16):8241-9.

98. Irmler M, Thome M, Hahne M, Schneider P, Hofmann K, Steiner V, Bodmer JL, Schroter M, Burns K, Mattmann C, et al. Inhibition of death receptor signals by cellular FLIP. Nature 1997 Jul 10;388(6638):190-5.

99. Reed JC. The survivin saga goes in vivo. J Clin Invest 2001 Oct;108(7):965-9.

100. Weller M, Malipiero U, Aguzzi A, Reed JC, Fontana A. Protooncogene bcl-2 gene transfer abrogates Fas/APO-1 antibody-mediated apoptosis of human malignant glioma cells and confers resistance to chemotherapeutic drugs and therapeutic irradiation. J Clin Invest 1995 Jun;95(6):2633-43.

101. Bird CH, Sutton VR, Sun J, Hirst CE, Novak A, Kumar S, Trapani JA, Bird PI. Selective regulation of apoptosis: The cytotoxic lymphocyte serpin proteinase inhibitor 9 protects against granzyme B-mediated apoptosis without perturbing the fas cell death pathway. Mol Cell Biol 1998 Nov;18(11):6387-98.

102. Cheng J, Zhou T, Liu C, Shapiro JP, Brauer MJ, Kiefer MC, Barr PJ, Mountz JD. Protection from fas-mediated apoptosis by a soluble form of the fas molecule. Science 1994 Mar 25;263(5154):1759-62.

103. Munn DH. Indoleamine 2,3-dioxygenase, tumor-induced tolerance and counter-regulation. Curr Opin Immunol 2006 Apr;18(2):220-5.

104. Bellone G, Turletti A, Artusio E, Mareschi K, Carbone A, Tibaudi D, Robecchi A, Emanuelli G, Rodeck U. Tumor-associated transforming growth factor-beta and interleukin-10 contribute to a systemic Th2 immune phenotype in pancreatic carcinoma patients. Am J Pathol 1999 Aug;155(2):537-47.

105. Sinha P, Okoro C, Foell D, Freeze HH, Ostrand-Rosenberg S, Srikrishna G. Proinflammatory S100 proteins regulate the accumulation of myeloid-derived suppressor cells. J Immunol 2008 Oct 1;181(7):4666-75.

106. Becker C, Fantini MC, Schramm C, Lehr HA, Wirtz S, Nikolaev A, Burg J, Strand S, Kiesslich R, Huber S, et al. TGF-beta suppresses tumor progression in colon cancer by inhibition of IL-6 trans-signaling. Immunity 2004 Oct;21(4):491-501.

107. Kim R, Emi M, Tanabe K, Arihiro K. Tumor-driven evolution of immunosuppressive networks during malignant progression. Cancer Res 2006 Jun 1;66(11):5527-36.

108. Steinman RM, Hawiger D, Nussenzweig MC. Tolerogenic dendritic cells. Annu Rev Immunol 2003;21:685-711.

109. Simpson KD, Templeton DJ, Cross JV. Macrophage migration inhibitory factor promotes tumor growth and metastasis by inducing myeloid-derived suppressor cells in the tumor microenvironment. J Immunol 2012 Nov 2.

110. Suzuki E, Kapoor V, Jassar AS, Kaiser LR, Albelda SM. Gemcitabine selectively eliminates splenic gr-1+/CD11b+ myeloid suppressor cells in tumor-bearing animals and enhances antitumor immune activity. Clin Cancer Res 2005 Sep 15;11(18):6713-21.

111. Ostrand-Rosenberg S. Myeloid-derived suppressor cells: More mechanisms for inhibiting antitumor immunity. Cancer Immunol Immunother 2010 Oct;59(10):1593-600.

112. Fujii S, Shimizu K, Hemmi H, Fukui M, Bonito AJ, Chen G, Franck RW, Tsuji M, Steinman RM. Glycolipid alpha-C-galactosylceramide is a distinct inducer of dendritic cell function during innate and adaptive immune responses of mice. Proc Natl Acad Sci U S A 2006 Jul 25;103(30):11252-7.

113. Schneiders FL, de Bruin RC, Santegoets SJ, Bonneville M, Scotet E, Scheper RJ, Verheul HM, de Gruijl TD, van der Vliet HJ. Activated iNKT cells promote Vgamma9Vdelta2-T cell anti-tumor effector functions through the production of TNF-alpha. Clin Immunol 2012 Feb;142(2):194-200.

114. Motohashi S, Okamoto Y, Yoshino I, Nakayama T. Anti-tumor immune responses induced by iNKT cell-based immunotherapy for lung cancer and head and neck cancer. Clin Immunol 2011 Aug;140(2):167-76.

115. Richter J, Neparidze N, Zhang L, Nair S, Monesmith T, Sundaram R, Miesowicz F, Dhodapkar KM, Dhodapkar MV. Clinical regressions and broad immune activation following combination therapy targeting human NKT cells in myeloma. Blood 2012 Oct 24.

116. Ambrosino E, Terabe M, Halder RC, Peng J, Takaku S, Miyake S, Yamamura T, Kumar V, Berzofsky JA. Cross-regulation between type I and type II NKT cells in regulating tumor immunity: A new immunoregulatory axis. J Immunol 2007 Oct 15;179(8):5126-36.

117. Halder RC, Aguilera C, Maricic I, Kumar V. Type II NKT cell-mediated anergy induction in type I NKT cells prevents inflammatory liver disease. J Clin Invest 2007 Aug;117(8):2302-12.

118. Terabe M, Swann J, Ambrosino E, Sinha P, Takaku S, Hayakawa Y, Godfrey DI, Ostrand-Rosenberg S, Smyth MJ, Berzofsky JA. A nonclassical non-Valpha14Jalpha18 CD1d-restricted (type II) NKT cell is sufficient for down-regulation of tumor immunosurveillance. J Exp Med 2005 Dec 19;202(12):1627-33.

119. Roncarolo MG, Bacchetta R, Bordignon C, Narula S, Levings MK. Type 1 T regulatory cells. Immunol Rev 2001 Aug;182:68-79.

120. Zou W. Regulatory T cells, tumour immunity and immunotherapy. Nat Rev Immunol 2006 Apr;6(4):295-307.

121. Schmidt A, Oberle N, Krammer PH. Molecular mechanisms of treg-mediated T cell suppression. Front Immunol 2012;3:51.

122. Facciabene A, Motz GT, Coukos G. T-regulatory cells: Key players in tumor immune escape and angiogenesis. Cancer Res 2012 May 1;72(9):2162-71.

123. Facciabene A, Peng X, Hagemann IS, Balint K, Barchetti A, Wang LP, Gimotty PA, Gilks CB, Lal P, Zhang L, et al. Tumour hypoxia promotes tolerance and angiogenesis via CCL28 and T(reg) cells. Nature 2011 Jul 13;475(7355):226-30.

124. Fallarino F, Grohmann U, Hwang KW, Orabona C, Vacca C, Bianchi R, Belladonna ML, Fioretti MC, Alegre ML, Puccetti P. Modulation of tryptophan catabolism by regulatory T cells. Nat Immunol 2003 Dec;4(12):1206-12.

125. Grossman WJ, Verbsky JW, Barchet W, Colonna M, Atkinson JP, Ley TJ. Human T regulatory cells can use the perforin pathway to cause autologous target cell death. Immunity 2004 Oct;21(4):589-601.

126. Grossman WJ, Verbsky JW, Tollefsen BL, Kemper C, Atkinson JP, Ley TJ. Differential expression of granzymes A and B in human cytotoxic lymphocyte subsets and T regulatory cells. Blood 2004 Nov 1;104(9):2840-8.

127. Onizuka S, Tawara I, Shimizu J, Sakaguchi S, Fujita T, Nakayama E. Tumor rejection by in vivo administration of anti-CD25 (interleukin-2 receptor alpha) monoclonal antibody. Cancer Res 1999 Jul 1;59(13):3128-33.

128. Shimizu J, Yamazaki S, Sakaguchi S. Induction of tumor immunity by removing CD25+CD4+ T cells: A common basis between tumor immunity and autoimmunity. J Immunol 1999 Nov 15;163(10):5211-8.

129. Solinas G, Germano G, Mantovani A, Allavena P. Tumor-associated macrophages (TAM) as major players of the cancer-related inflammation. J Leukoc Biol 2009 Nov;86(5):1065-73.

130. Allavena P, Mantovani A. Immunology in the clinic review series; focus on cancer: Tumour-associated macrophages: Undisputed stars of the inflammatory tumour microenvironment. Clin Exp Immunol 2012 Feb;167(2):195-205.

131. Bottazzi B, Polentarutti N, Acero R, Balsari A, Boraschi D, Ghezzi P, Salmona M, Mantovani A. Regulation of the macrophage content of neoplasms by chemoattractants. Science 1983 Apr 8;220(4593):210-2.

132. Kacinski BM. CSF-1 and its receptor in ovarian, endometrial and breast cancer. Ann Med 1995 Feb;27(1):79-85.

133. Gordon S, Martinez FO. Alternative activation of macrophages: Mechanism and functions. Immunity 2010 May 28;32(5):593-604.

134. Mantovani A, Savino B, Locati M, Zammataro L, Allavena P, Bonecchi R. The chemokine system in cancer biology and therapy. Cytokine Growth Factor Rev 2010 Feb;21(1):27-39.

135. Almand B, Clark JI, Nikitina E, van Beynen J, English NR, Knight SC, Carbone DP, Gabrilovich DI. Increased production of immature myeloid cells in cancer patients: A mechanism of immunosuppression in cancer. J Immunol 2001 Jan 1;166(1):678-89.

136. Ostrand-Rosenberg S, Sinha P, Beury DW, Clements VK. Cross-talk between myeloid-derived suppressor cells (MDSC), macrophages, and dendritic cells enhances tumor-induced immune suppression. Semin Cancer Biol 2012 Feb 1.

137. Elkabets M, Ribeiro VS, Dinarello CA, Ostrand-Rosenberg S, Di Santo JP, Apte RN, Vosshenrich CA. IL-1beta regulates a novel myeloid-derived suppressor cell subset that impairs NK cell development and function. Eur J Immunol 2010 Dec;40(12):3347-57.

138. Montero AJ, Diaz-Montero CM, Kyriakopoulos CE, Bronte V, Mandruzzato S. Myeloid-derived suppressor cells in cancer patients: A clinical perspective. J Immunother 2012 Feb-Mar;35(2):107-15.

139. Youn JI, Collazo M, Shalova IN, Biswas SK, Gabrilovich DI. Characterization of the nature of granulocytic myeloid-derived suppressor cells in tumor-bearing mice. J Leukoc Biol 2012 Jan;91(1):167-81.

140. Mandruzzato S, Solito S, Falisi E, Francescato S, Chiarion-Sileni V, Mocellin S, Zanon A, Rossi CR, Nitti D, Bronte V, et al. IL4Ralpha+ myeloid-derived suppressor cell expansion in cancer patients. J Immunol 2009 May 15;182(10):6562-8.

141. Youn JI, Nagaraj S, Collazo M, Gabrilovich DI. Subsets of myeloid-derived suppressor cells in tumor-bearing mice. J Immunol 2008 Oct 15;181(8):5791-802.

142. Movahedi K, Guilliams M, Van den Bossche J, Van den Bergh R, Gysemans C, Beschin A, De Baetselier P, Van Ginderachter JA. Identification of discrete tumor-induced myeloid-derived suppressor cell subpopulations with distinct T cell-suppressive activity. Blood 2008 Apr 15;111(8):4233-44.

143. Yang L, Huang J, Ren X, Gorska AE, Chytil A, Aakre M, Carbone DP, Matrisian LM, Richmond A, Lin PC, et al. Abrogation of TGF beta signaling in mammary carcinomas recruits gr-1+CD11b+ myeloid cells that promote metastasis. Cancer Cell 2008 Jan;13(1):23-35.

144. Kujawski M, Kortylewski M, Lee H, Herrmann A, Kay H, Yu H. Stat3 mediates myeloid cell-dependent tumor angiogenesis in mice. J Clin Invest 2008 Oct;118(10):3367-77.

145. Cheng P, Corzo CA, Luetteke N, Yu B, Nagaraj S, Bui MM, Ortiz M, Nacken W, Sorg C, Vogl T, et al. Inhibition of dendritic cell differentiation and accumulation of myeloid-derived suppressor cells in cancer is regulated by S100A9 protein. J Exp Med 2008 Sep 29;205(10):2235-49.

146. Sinha P, Clements VK, Bunt SK, Albelda SM, Ostrand-Rosenberg S. Cross-talk between myeloid-derived suppressor cells and macrophages subverts tumor immunity toward a type 2 response. J Immunol 2007 Jul 15;179(2):977-83.

147. Mundy-Bosse BL, Lesinski GB, Jaime-Ramirez AC, Benninger K, Khan M, Kuppusamy P, Guenterberg K, Kondadasula SV, Chaudhury AR, La Perle KM, et al. Myeloid-derived suppressor cell inhibition of the IFN response in tumor-bearing mice. Cancer Res 2011 Aug 1;71(15):5101-10.

148. Corzo CA, Cotter MJ, Cheng P, Cheng F, Kusmartsev S, Sotomayor E, Padhya T, McCaffrey TV, McCaffrey JC, Gabrilovich DI. Mechanism regulating reactive oxygen species in tumor-induced myeloid-derived suppressor cells. J Immunol 2009 May 1;182(9):5693-701.

149. Lu T, Gabrilovich DI. Molecular pathways: Tumor-infiltrating myeloid cells and reactive oxygen species in regulation of tumor microenvironment. Clin Cancer Res 2012 Sep 15;18(18):4877-82.

150. Srivastava MK, Sinha P, Clements VK, Rodriguez P, Ostrand-Rosenberg S. Myeloid-derived suppressor cells inhibit T-cell activation by depleting cystine and cysteine. Cancer Res 2010 Jan 1;70(1):68-77.

151. Naito Y, Saito K, Shiiba K, Ohuchi A, Saigenji K, Nagura H, Ohtani H. CD8+ T cells infiltrated within cancer cell nests as a prognostic factor in human colorectal cancer. Cancer Res 1998 Aug 15;58(16):3491-4.

152. Murdoch C, Muthana M, Coffelt SB, Lewis CE. The role of myeloid cells in the promotion of tumour angiogenesis. Nat Rev Cancer 2008 Aug;8(8):618-31.

153. Yang L, DeBusk LM, Fukuda K, Fingleton B, Green-Jarvis B, Shyr Y, Matrisian LM, Carbone DP, Lin PC. Expansion of myeloid immune suppressor Gr+CD11b+ cells in tumor-bearing host directly promotes tumor angiogenesis. Cancer Cell 2004 Oct;6(4):409-21.

154. Ko JS, Zea AH, Rini BI, Ireland JL, Elson P, Cohen P, Golshayan A, Rayman PA, Wood L, Garcia J, et al. Sunitinib mediates reversal of myeloid-derived suppressor cell accumulation in renal cell carcinoma patients. Clin Cancer Res 2009 Mar 15;15(6):2148-57.

155. Ko JS, Rayman P, Ireland J, Swaidani S, Li G, Bunting KD, Rini B, Finke JH, Cohen PA. Direct and differential suppression of myeloid-derived suppressor cell subsets by sunitinib is compartmentally constrained. Cancer Res 2010 May 1;70(9):3526-36.

156. Shojaei F, Wu X, Malik AK, Zhong C, Baldwin ME, Schanz S, Fuh G, Gerber HP, Ferrara N. Tumor refractoriness to anti-VEGF treatment is mediated by CD11b+Gr1+ myeloid cells. Nat Biotechnol 2007 Aug;25(8):911-20.

157. Hoechst B, Ormandy LA, Ballmaier M, Lehner F, Kruger C, Manns MP, Greten TF, Korangy F. A new population of myeloid-derived suppressor cells in hepatocellular carcinoma patients induces CD4(+)CD25(+)Foxp3(+) T cells. Gastroenterology 2008 Jul;135(1):234-43.

158. Tu S, Bhagat G, Cui G, Takaishi S, Kurt-Jones EA, Rickman B, Betz KS, Penz-Oesterreicher M, Bjorkdahl O, Fox JG, et al. Overexpression of interleukin-1beta induces gastric inflammation and cancer and mobilizes myeloid-derived suppressor cells in mice. Cancer Cell 2008 Nov 4;14(5):408-19.

159. Dolcetti L, Marigo I, Mantelli B, Peranzoni E, Zanovello P, Bronte V. Myeloid-derived suppressor cell role in tumor-related inflammation. Cancer Lett 2008 Aug 28;267(2):216-25.

160. Ranjan D, Chen C, Johnston TD, Jeon H, Nagabhushan M. Curcumin inhibits mitogen stimulated lymphocyte proliferation, NFkappaB activation, and IL-2 signaling. J Surg Res 2004 Oct;121(2):171-7.

161. Tu SP, Jin H, Shi JD, Zhu LM, Suo Y, Lu G, Liu A, Wang TC, Yang CS. Curcumin induces the differentiation of myeloid-derived suppressor cells and inhibits their interaction with cancer cells and related tumor growth. Cancer Prev Res (Phila) 2012 Feb;5(2):205-15.

162. Vincent J, Mignot G, Chalmin F, Ladoire S, Bruchard M, Chevriaux A, Martin F, Apetoh L, Rebe C, Ghiringhelli F. 5-fluorouracil selectively kills tumor-associated myeloid-derived suppressor cells resulting in enhanced T cell-dependent antitumor immunity. Cancer Res 2010 Apr 15;70(8):3052-61.

163. Ghiringhelli F, Menard C, Puig PE, Ladoire S, Roux S, Martin F, Solary E, Le Cesne A, Zitvogel L, Chauffert B. Metronomic cyclophosphamide regimen selectively depletes CD4+CD25+ regulatory T cells and restores T and NK effector functions in end stage cancer patients. Cancer Immunol Immunother 2007 May;56(5):641-8.

164. Kusmartsev S, Cheng F, Yu B, Nefedova Y, Sotomayor E, Lush R, Gabrilovich D. All-trans-retinoic acid eliminates immature myeloid cells from tumor-bearing mice and improves the effect of vaccination. Cancer Res 2003 Aug 1;63(15):4441-9.

165. Nefedova Y, Fishman M, Sherman S, Wang X, Beg AA, Gabrilovich DI. Mechanism of all-trans retinoic acid effect on tumor-associated myeloid-derived suppressor cells. Cancer Res 2007 Nov 15;67(22):11021-8.

166. De Santo C, Salio M, Masri SH, Lee LY, Dong T, Speak AO, Porubsky S, Booth S, Veerapen N, Besra GS, et al. Invariant NKT cells reduce the immunosuppressive activity of influenza A virus-induced myeloid-derived suppressor cells in mice and humans. J Clin Invest 2008 Dec;118(12):4036-48.

167. Nowak AK, Robinson BW, Lake RA. Gemcitabine exerts a selective effect on the humoral immune response: Implications for combination chemo-immunotherapy. Cancer Res 2002 Apr 15;62(8):2353-8.

168. Berzins SP, Smyth MJ, Baxter AG. Presumed guilty: Natural killer T cell defects and human disease. Nat Rev Immunol 2011 Feb;11(2):131-42.

169. Imai K, Kanno M, Kimoto H, Shigemoto K, Yamamoto S, Taniguchi M. Sequence and expression of transcripts of the T-cell antigen receptor alpha-chain gene in a functional, antigen-specific suppressor-T-cell hybridoma. Proc Natl Acad Sci U S A 1986 Nov;83(22):8708-12.

170. Lantz O, Bendelac A. An invariant T cell receptor alpha chain is used by a unique subset of major histocompatibility complex class I-specific CD4+ and CD4-8- T cells in mice and humans. J Exp Med 1994 Sep 1;180(3):1097-106.

171. Tupin E, Kinjo Y, Kronenberg M. The unique role of natural killer T cells in the response to microorganisms. Nat Rev Microbiol 2007 Jun;5(6):405-17.

172. Bai L, Constantinides MG, Thomas SY, Reboulet R, Meng F, Koentgen F, Teyton L, Savage PB, Bendelac A. Distinct APCs explain the cytokine bias of alpha-galactosylceramide variants in vivo. J Immunol 2012 Mar 5.

173. Taniguchi M, Harada M, Kojo S, Nakayama T, Wakao H. The regulatory role of Valpha14 NKT cells in innate and acquired immune response. Annu Rev Immunol 2003;21:483-513.

174. Kawano T, Nakayama T, Kamada N, Kaneko Y, Harada M, Ogura N, Akutsu Y, Motohashi S, Iizasa T, Endo H, et al. Antitumor cytotoxicity mediated by ligand-activated human V alpha24 NKT cells. Cancer Res 1999 Oct 15;59(20):5102-5.

175. Kunii N, Horiguchi S, Motohashi S, Yamamoto H, Ueno N, Yamamoto S, Sakurai D, Taniguchi M, Nakayama T, Okamoto Y. Combination therapy of in vitro-expanded natural killer T cells and alpha-galactosylceramide-pulsed antigen-presenting cells in patients with recurrent head and neck carcinoma. Cancer Sci 2009 Jun;100(6):1092-8.

176. Swann JB, Uldrich AP, van Dommelen S, Sharkey J, Murray WK, Godfrey DI, Smyth MJ. Type I natural killer T cells suppress tumors caused by p53 loss in mice. Blood 2009 Jun 18;113(25):6382-5.

177. Patel O, Pellicci DG, Uldrich AP, Sullivan LC, Bhati M, McKnight M, Richardson SK, Howell AR, Mallevaey T, Zhang J, et al. Vbeta2 natural killer T cell antigen receptor-mediated recognition of CD1d-glycolipid antigen. Proc Natl Acad Sci U S A 2011 Nov 22;108(47):19007-12.

178. Girardi E, Maricic I, Wang J, Mac TT, Iyer P, Kumar V, Zajonc DM. Type II natural killer T cells use features of both innate-like and conventional T cells to recognize sulfatide self antigens. Nat Immunol 2012 Sep;13(9):851-6.

179. Gao B, Radaeva S, Park O. Liver natural killer and natural killer T cells: Immunobiology and emerging roles in liver diseases. J Leukoc Biol 2009 Sep;86(3):513-28.

180. Matsuda JL, Naidenko OV, Gapin L, Nakayama T, Taniguchi M, Wang CR, Koezuka Y, Kronenberg M. Tracking the response of natural killer T cells to a glycolipid antigen using CD1d tetramers. J Exp Med 2000 Sep 4;192(5):741-54.

181. Brennan PJ, Tatituri RV, Brigl M, Kim EY, Tuli A, Sanderson JP, Gadola SD, Hsu FF, Besra GS, Brenner MB. Invariant natural killer T cells recognize lipid self antigen induced by microbial danger signals. Nat Immunol 2011 Oct 30;12(12):1202-11.

182. Fujii S, Shimizu K, Kronenberg M, Steinman RM. Prolonged IFN-gamma-producing NKT response induced with alpha-galactosylceramide-loaded DCs. Nat Immunol 2002 Sep;3(9):867-74.

183. Cerundolo V, Silk JD, Masri SH, Salio M. Harnessing invariant NKT cells in vaccination strategies. Nat Rev Immunol 2009 Jan;9(1):28-38.

184. Xiao W, Li L, Zhou R, Xiao R, Wang Y, Ji X, Wu M, Wang L, Huang W, Zheng X, et al. EBV-induced human CD8(+) NKT cells synergise CD4(+) NKT cells suppressing EBV-associated tumours upon induction of Th1-bias. Cell Mol Immunol 2009 Oct;6(5):367-79.

185. Milpied P, Massot B, Renand A, Diem S, Herbelin A, Leite-de-Moraes M, Rubio MT, Hermine O. IL-17-producing invariant NKT cells in lymphoid organs are recent thymic emigrants identified by neuropilin-1 expression. Blood 2011 Sep 15;118(11):2993-3002.

186. Parekh VV, Wilson MT, Olivares-Villagomez D, Singh AK, Wu L, Wang CR, Joyce S, Van Kaer L. Glycolipid antigen induces long-term natural killer T cell anergy in mice. J Clin Invest 2005 Sep;115(9):2572-83.

187. Sullivan BA, Kronenberg M. Activation or anergy: NKT cells are stunned by alpha-galactosylceramide. J Clin Invest 2005 Sep;115(9):2328-9.

188. Chang WS, Kim JY, Kim YJ, Kim YS, Lee JM, Azuma M, Yagita H, Kang CY. Cutting edge: Programmed death-1/programmed death ligand 1 interaction regulates the induction and maintenance of invariant NKT cell anergy. J Immunol 2008 Nov 15;181(10):6707-10.

189. Parekh VV, Lalani S, Kim S, Halder R, Azuma M, Yagita H, Kumar V, Wu L, Kaer LV. PD-1/PD-L blockade prevents anergy induction and enhances the anti-tumor activities of glycolipid-activated invariant NKT cells. J Immunol 2009 Mar 1;182(5):2816-26.

190. Wingender G, Hiss M, Engel I, Peukert K, Ley K, Haller H, Kronenberg M, von Vietinghoff S. Neutrophilic granulocytes modulate invariant NKT cell function in mice and humans. J Immunol 2012 Mar 2.

191. Metelitsa LS, Naidenko OV, Kant A, Wu HW, Loza MJ, Perussia B, Kronenberg M, Seeger RC. Human NKT cells mediate antitumor cytotoxicity directly by recognizing target cell CD1d with bound ligand or indirectly by producing IL-2 to activate NK cells. J Immunol 2001 Sep 15;167(6):3114-22.

192. Reschner A, Hubert P, Delvenne P, Boniver J, Jacobs N. Innate lymphocyte and dendritic cell cross-talk: A key factor in the regulation of the immune response. Clin Exp Immunol 2008 May;152(2):219-26.

193. Kikuchi A, Nieda M, Schmidt C, Koezuka Y, Ishihara S, Ishikawa Y, Tadokoro K, Durrant S, Boyd A, Juji T, et al. In vitro anti-tumour activity of alpha-galactosylceramide-stimulated human invariant Valpha24+NKT cells against melanoma. Br J Cancer 2001 Sep 1;85(5):741-6.

194. Ishikawa A, Motohashi S, Ishikawa E, Fuchida H, Higashino K, Otsuji M, Iizasa T, Nakayama T, Taniguchi M, Fujisawa T. A phase I study of alpha-galactosylceramide (KRN7000)-pulsed dendritic cells in patients with advanced and recurrent non-small cell lung cancer. Clin Cancer Res 2005 Mar 1;11(5):1910-7.

195. Motohashi S, Nagato K, Kunii N, Yamamoto H, Yamasaki K, Okita K, Hanaoka H, Shimizu N, Suzuki M, Yoshino I, et al. A phase I-II study of alpha-galactosylceramide-pulsed IL-2/GM-CSF-cultured peripheral blood mononuclear cells in patients with advanced and recurrent non-small cell lung cancer. J Immunol 2009 Feb 15;182(4):2492-501.

196. Uchida T, Horiguchi S, Tanaka Y, Yamamoto H, Kunii N, Motohashi S, Taniguchi M, Nakayama T, Okamoto Y. Phase I study of alpha-galactosylceramide-pulsed antigen presenting cells administration to the nasal submucosa in unresectable or recurrent head and neck cancer. Cancer Immunol Immunother 2008 Mar;57(3):337-45.

197. Smyth MJ, Thia KY, Street SE, Cretney E, Trapani JA, Taniguchi M, Kawano T, Pelikan SB, Crowe NY, Godfrey DI. Differential tumor surveillance by natural killer (NK) and NKT cells. J Exp Med 2000 Feb 21;191(4):661-8.

198. Nishikawa H, Kato T, Tanida K, Hiasa A, Tawara I, Ikeda H, Ikarashi Y, Wakasugi H, Kronenberg M, Nakayama T, et al. CD4+ CD25+ T cells responding to serologically defined autoantigens suppress antitumor immune responses. Proc Natl Acad Sci U S A 2003 Sep 16;100(19):10902-6.

199. Crowe NY, Coquet JM, Berzins SP, Kyparissoudis K, Keating R, Pellicci DG, Hayakawa Y, Godfrey DI, Smyth MJ. Differential antitumor immunity mediated by NKT cell subsets in vivo. J Exp Med 2005 Nov 7;202(9):1279-88.

200. Kitamura H, Iwakabe K, Yahata T, Nishimura S, Ohta A, Ohmi Y, Sato M, Takeda K, Okumura K, Van Kaer L, et al. The natural killer T (NKT) cell ligand alpha-galactosylceramide demonstrates its immunopotentiating effect by inducing interleukin (IL)-12 production by dendritic cells and IL-12 receptor expression on NKT cells. J Exp Med 1999 Apr 5;189(7):1121-8.

201. Banchet-Cadeddu A, Henon E, Dauchez M, Renault JH, Monneaux F, Haudrechy A. The stimulating adventure of KRN 7000. Org Biomol Chem 2011 May 7;9(9):3080-104.

202. Veerapen N, Brigl M, Garg S, Cerundolo V, Cox LR, Brenner MB, Besra GS. Synthesis and biological activity of alpha-galactosyl ceramide KRN7000 and galactosyl (alpha1-->2) galactosyl ceramide. Bioorg Med Chem Lett 2009 Aug 1;19(15):4288-91.

203. Wu D, Xing GW, Poles MA, Horowitz A, Kinjo Y, Sullivan B, Bodmer-Narkevitch V, Plettenburg O, Kronenberg M, Tsuji M, et al. Bacterial glycolipids and analogs as antigens for CD1d-restricted NKT cells. Proc Natl Acad Sci U S A 2005 Feb 1;102(5):1351-6.

204. Blauvelt ML, Khalili M, Jaung W, Paulsen J, Anderson AC, Brian Wilson S, Howell AR. Alpha-S-GalCer: Synthesis and evaluation for iNKT cell stimulation. Bioorg Med Chem Lett 2008 Dec 15;18(24):6374-6.

205. Patel O, Cameron G, Pellicci DG, Liu Z, Byun HS, Beddoe T, McCluskey J, Franck RW, Castano AR, Harrak Y, et al. NKT TCR recognition of CD1d-alpha-C-galactosylceramide. J Immunol 2011 Nov 1;187(9):4705-13.

206. Sullivan BA, Nagarajan NA, Wingender G, Wang J, Scott I, Tsuji M, Franck RW, Porcelli SA, Zajonc DM, Kronenberg M. Mechanisms for glycolipid antigen-driven cytokine polarization by Valpha14i NKT cells. J Immunol 2010 Jan 1;184(1):141-53.

207. Molling JW, Kolgen W, van der Vliet HJ, Boomsma MF, Kruizenga H, Smorenburg CH, Molenkamp BG, Langendijk JA, Leemans CR, von Blomberg BM, et al. Peripheral blood IFN-gamma-secreting Valpha24+Vbeta11+ NKT cell numbers are decreased in cancer patients independent of tumor type or tumor load. Int J Cancer 2005 Aug 10;116(1):87-93.

208. Najera Chuc AE, Cervantes LA, Retiguin FP, Ojeda JV, Maldonado ER. Low number of invariant NKT cells is associated with poor survival in acute myeloid leukemia. J Cancer Res Clin Oncol 2012 Aug;138(8):1427-32.

209. Yanagisawa K, Seino K, Ishikawa Y, Nozue M, Todoroki T, Fukao K. Impaired proliferative response of V alpha 24 NKT cells from cancer patients against alpha-galactosylceramide. J Immunol 2002 Jun 15;168(12):6494-9.

210. Tachibana T, Onodera H, Tsuruyama T, Mori A, Nagayama S, Hiai H, Imamura M. Increased intratumor Valpha24-positive natural killer T cells: A prognostic factor for primary colorectal carcinomas. Clin Cancer Res 2005 Oct 15;11(20):7322-7.

211. Metelitsa LS, Wu HW, Wang H, Yang Y, Warsi Z, Asgharzadeh S, Groshen S, Wilson SB, Seeger RC. Natural killer T cells infiltrate neuroblastomas expressing the chemokine CCL2. J Exp Med 2004 May 3;199(9):1213-21.

212. Song L, Asgharzadeh S, Salo J, Engell K, Wu HW, Sposto R, Ara T, Silverman AM, DeClerck YA, Seeger RC, et al. Valpha24-invariant NKT cells mediate antitumor activity via killing of tumor-associated macrophages. J Clin Invest 2009 Jun;119(6):1524-36.

213. Hayakawa Y, Rovero S, Forni G, Smyth MJ. Alpha-galactosylceramide (KRN7000) suppression of chemical- and oncogene-dependent carcinogenesis. Proc Natl Acad Sci U S A 2003 Aug 5;100(16):9464-9.

214. Teng MW, Westwood JA, Darcy PK, Sharkey J, Tsuji M, Franck RW, Porcelli SA, Besra GS, Takeda K, Yagita H, et al. Combined natural killer T-cell based immunotherapy eradicates established tumors in mice. Cancer Res 2007 Aug 1;67(15):7495-504.

215. Yamasaki K, Horiguchi S, Kurosaki M, Kunii N, Nagato K, Hanaoka H, Shimizu N, Ueno N, Yamamoto S, Taniguchi M, et al. Induction of NKT cell-specific immune responses in cancer tissues after NKT cell-targeted adoptive immunotherapy. Clin Immunol 2011 Mar;138(3):255-65.

216. Veldt BJ, van der Vliet HJ, von Blomberg BM, van Vlierberghe H, Gerken G, Nishi N, Hayashi K, Scheper RJ, de Knegt RJ, van den Eertwegh AJ, et al. Randomized placebo controlled phase I/II trial of alpha-galactosylceramide for the treatment of chronic hepatitis C. J Hepatol 2007 Sep;47(3):356-65.

217. Cullen R, Germanov E, Shimaoka T, Johnston B. Enhanced tumor metastasis in response to blockade of the chemokine receptor CXCR6 is overcome by NKT cell activation. J Immunol 2009 Nov 1;183(9):5807-15.

218. Hayakawa Y, Takeda K, Yagita H, Smyth MJ, Van Kaer L, Okumura K, Saiki I. IFN-gamma-mediated inhibition of tumor angiogenesis by natural killer T-cell ligand, alpha-galactosylceramide. Blood 2002 Sep 1;100(5):1728-33.

219. Redmond KM, Wilson TR, Johnston PG, Longley DB. Resistance mechanisms to cancer chemotherapy. Front Biosci 2008 May 1;13:5138-54.

220. Silva AS, Kam Y, Khin ZP, Minton SE, Gillies RJ, Gatenby RA. Evolutionary approaches to prolong progression-free survival in breast cancer. Cancer Res 2012 Oct 12.

221. Cui J, Shin T, Kawano T, Sato H, Kondo E, Toura I, Kaneko Y, Koseki H, Kanno M, Taniguchi M. Requirement for Valpha14 NKT cells in IL-12-mediated rejection of tumors. Science 1997 Nov 28;278(5343):1623-6.

222. MacMillan HF, Lee T, Issekutz AC. Intravenous immunoglobulin G-mediated inhibition of T-cell proliferation reflects an endogenous mechanism by which IgG modulates T-cell activation. Clin Immunol 2009 Aug;132(2):222-33.

223. Matsumoto H, Kawamura T, Kobayashi T, Kanda Y, Kawamura H, Abo T. Coincidence of autoantibody production with the activation of natural killer T cells in alpha-galactosylceramide-mediated hepatic injury. Immunology 2011 May;133(1):21-8.

224. Ito H, Koide N, Hassan F, Islam S, Tumurkhuu G, Mori I, Yoshida T, Kakumu S, Moriwaki H, Yokochi T. Lethal endotoxic shock using alpha-galactosylceramide sensitization as a new experimental model of septic shock. Lab Invest 2006 Mar;86(3):254-61.

225. Biburger M, Tiegs G. Alpha-galactosylceramide-induced liver injury in mice is mediated by TNF-alpha but independent of kupffer cells. J Immunol 2005 Aug 1;175(3):1540-50.

226. Fujii H, Seki S, Kobayashi S, Kitada T, Kawakita N, Adachi K, Tsutsui H, Nakanishi K, Fujiwara H, Ikarashi Y, et al. A murine model of NKT cell-mediated liver injury induced by alpha-galactosylceramide/d-galactosamine. Virchows Arch 2005 Jun;446(6):663-73.

227. Bontkes HJ, Moreno M, Hangalapura B, Lindenberg JJ, de Groot J, Lougheed S, van der Vliet HJ, van den Eertwegh AJ, de Gruijl TD, von Blomberg BM, et al. Attenuation of invariant natural killer T-cell anergy induction through intradermal delivery of alpha-galactosylceramide. Clin Immunol 2010 Sep;136(3):364-74.

228. Nicol AJ, Tazbirkova A, Nieda M. Comparison of clinical and immunological effects of intravenous and intradermal administration of alpha-galactosylceramide (KRN7000)-pulsed dendritic cells. Clin Cancer Res 2011 Aug 1;17(15):5140-51.

229. Kronenberg M. Toward an understanding of NKT cell biology: Progress and paradoxes. Annu Rev Immunol 2005;23:877-900.

230. Tahir SM, Cheng O, Shaulov A, Koezuka Y, Bubley GJ, Wilson SB, Balk SP, Exley MA. Loss of IFN-gamma production by invariant NK T cells in advanced cancer. J Immunol 2001 Oct 1;167(7):4046-50.

231. Demaria S, Kawashima N, Yang AM, Devitt ML, Babb JS, Allison JP, Formenti SC. Immune-mediated inhibition of metastases after treatment with local radiation and CTLA-4 blockade in a mouse model of breast cancer. Clin Cancer Res 2005 Jan 15;11(2 Pt 1):728-34.

232. Steinbauer M, Guba M, Cernaianu G, Kohl G, Cetto M, Kunz-Schughart LA, Geissler EK, Falk W, Jauch KW. GFP-transfected tumor cells are useful in examining early metastasis in vivo, but immune reaction precludes long-term tumor development studies in immunocompetent mice. Clin Exp Metastasis 2003;20(2):135-41.

233. Gambotto A, Dworacki G, Cicinnati V, Kenniston T, Steitz J, Tuting T, Robbins PD, DeLeo AB. Immunogenicity of enhanced green fluorescent protein (EGFP) in BALB/c mice: Identification of an H2-kd-restricted CTL epitope. Gene Ther 2000 Dec;7(23):2036-40.

234. Chang DH, Osman K, Connolly J, Kukreja A, Krasovsky J, Pack M, Hutchinson A, Geller M, Liu N, Annable R, et al. Sustained expansion of NKT cells and antigen-specific T cells after injection of alpha-galactosyl-ceramide loaded mature dendritic cells in cancer patients. J Exp Med 2005 May 2;201(9):1503-17.

235. Schmieg J, Yang G, Franck RW, Tsuji M. Superior protection against malaria and melanoma metastases by a C-glycoside analogue of the natural killer T cell ligand alpha-galactosylceramide. J Exp Med 2003 Dec 1;198(11):1631-41.

236. Oki S, Chiba A, Yamamura T, Miyake S. The clinical implication and molecular mechanism of preferential IL-4 production by modified glycolipid-stimulated NKT cells. J Clin Invest 2004 Jun;113(11):1631-40.

237. Wu TN, Lin KH, Chang YJ, Huang JR, Cheng JY, Yu AL, Wong CH. Avidity of CD1d-ligand-receptor ternary complex contributes to T-helper 1 (Th1) polarization and anticancer efficacy. Proc Natl Acad Sci U S A 2011 Oct 18;108(42):17275-80.

238. Reiner SL, Locksley RM. The regulation of immunity to leishmania major. Annu Rev Immunol 1995;13:151-77.

239. Mozaffari F, Lindemalm C, Choudhury A, Granstam-Bjorneklett H, Helander I, Lekander M, Mikaelsson E, Nilsson B, Ojutkangas ML, Osterborg A, et al. NK-cell and T-cell functions in patients with breast cancer: Effects of surgery and adjuvant chemo- and radiotherapy. Br J Cancer 2007 Jul 2;97(1):105-11.

240. Giaccone G, Punt CJ, Ando Y, Ruijter R, Nishi N, Peters M, von Blomberg BM, Scheper RJ, van der Vliet HJ, van den Eertwegh AJ, et al. A phase I study of the natural killer T-cell ligand alpha-galactosylceramide (KRN7000) in patients with solid tumors. Clin Cancer Res 2002 Dec;8(12):3702-9.

241. Kojo S, Elly C, Harada Y, Langdon WY, Kronenberg M, Liu YC. Mechanisms of NKT cell anergy induction involve cbl-b-promoted monoubiquitination of CARMA1. Proc Natl Acad Sci U S A 2009 Oct 20;106(42):17847-51.

242. van der Vliet HJ, Molling JW, Nishi N, Masterson AJ, Kolgen W, Porcelli SA, van den Eertwegh AJ, von Blomberg BM, Pinedo HM, Giaccone G, et al. Polarization of Valpha24+ Vbeta11+ natural killer T cells of healthy volunteers and cancer patients using alpha-galactosylceramide-loaded and environmentally instructed dendritic cells. Cancer Res 2003 Jul 15;63(14):4101-6.

243. Toura I, Kawano T, Akutsu Y, Nakayama T, Ochiai T, Taniguchi M. Cutting edge: Inhibition of experimental tumor metastasis by dendritic cells pulsed with alpha-galactosylceramide. J Immunol 1999 Sep 1;163(5):2387-91.

244. Uldrich AP, Crowe NY, Kyparissoudis K, Pellicci DG, Zhan Y, Lew AM, Bouillet P, Strasser A, Smyth MJ, Godfrey DI. NKT cell stimulation with glycolipid antigen in vivo: Costimulation-dependent expansion, bim-dependent contraction, and hyporesponsiveness to further antigenic challenge. J Immunol 2005 Sep 1;175(5):3092-101.

245. Hammami I, Chen J, Murschel F, Bronte V, De Crescenzo G, Jolicoeur M. Immunosuppressive activity enhances central carbon metabolism and bioenergetics in myeloid-derived suppressor cells in vitro models. BMC Cell Biol 2012 Jul 4;13:18,2121-13-18.

246. Solito S, Falisi E, Diaz-Montero CM, Doni A, Pinton L, Rosato A, Francescato S, Basso G, Zanovello P, Onicescu G, et al. A human promyelocytic-like population is responsible for the immune suppression mediated by myeloid-derived suppressor cells. Blood 2011 Aug 25;118(8):2254-65.

247. Ueha S, Shand FH, Matsushima K. Myeloid cell population dynamics in healthy and tumor-bearing mice. Int Immunopharmacol 2011 Jul;11(7):783-8.

248. Ilkovitch D, Carrio R, Lopez DM. uPA and uPA-receptor are involved in cancer-associated myeloid-derived suppressor cell accumulation. Anticancer Res 2012 Oct;32(10):4263-70.

249. Obermajer N, Muthuswamy R, Lesnock J, Edwards RP, Kalinski P. Positive feedback between PGE2 and COX2 redirects the differentiation of human dendritic cells toward stable myeloid-derived suppressor cells. Blood 2011 Nov 17;118(20):5498-505.

250. Umansky V, Sevko A. Overcoming immunosuppression in the melanoma microenvironment induced by chronic inflammation. Cancer Immunol Immunother 2012 Feb;61(2):275-82.

251. Miller BE, Aslakson CJ, Miller FR. Efficient recovery of clonogenic stem cells from solid tumors and occult metastatic deposits. Invasion Metastasis 1990;10(2):101-12.

252. Skelton D, Satake N, Kohn DB. The enhanced green fluorescent protein (eGFP) is minimally immunogenic in C57BL/6 mice. Gene Ther 2001 Dec;8(23):1813-4.

253. Han WG, Unger WW, Wauben MH. Identification of the immunodominant CTL epitope of EGFP in C57BL/6 mice. Gene Ther 2008 May;15(9):700-1.

254. Mattarollo SR, West AC, Steegh K, Duret H, Paget C, Martin B, Matthews GM, Shortt J, Chesi M, Bergsagel PL, et al. NKT cell adjuvant-based tumor vaccine for treatment of myc oncogene-driven mouse B-cell lymphoma. Blood 2012 Oct 11;120(15):3019-29.

255. Nagato K, Motohashi S, Ishibashi F, Okita K, Yamasaki K, Moriya Y, Hoshino H, Yoshida S, Hanaoka H, Fujii S, et al. Accumulation of activated invariant natural killer T cells in the tumor microenvironment after alpha-galactosylceramide-pulsed antigen presenting cells. J Clin Immunol 2012 Oct;32(5):1071-81.

256. Thapa P, Zhang G, Xia C, Gelbard A, Overwijk WW, Liu C, Hwu P, Chang DZ, Courtney A, Sastry JK, et al. Nanoparticle formulated alpha-galactosylceramide activates NKT cells without inducing anergy. Vaccine 2009 May 26;27(25-26):3484-8.

257. Farrand KJ, Dickgreber N, Stoitzner P, Ronchese F, Petersen TR, Hermans IF. Langerin+ CD8alpha+ dendritic cells are critical for cross-priming and IL-12 production in response to systemic antigens. J Immunol 2009 Dec 15;183(12):7732-42.

258. Germanov E, Veinotte L, Cullen R, Chamberlain E, Butcher EC, Johnston B. Critical role for the chemokine receptor CXCR6 in homeostasis and activation of CD1d-restricted NKT cells. J Immunol 2008 Jul 1;181(1):81-91.

259. Shimaoka T, Seino K, Kume N, Minami M, Nishime C, Suematsu M, Kita T, Taniguchi M, Matsushima K, Yonehara S. Critical role for CXC chemokine ligand 16 (SR-PSOX) in Th1 response mediated by NKT cells. J Immunol 2007 Dec 15;179(12):8172-9.

260. Kobayashi K, Tanaka Y, Horiguchi S, Yamamoto S, Toshinori N, Sugimoto A, Okamoto Y. The effect of radiotherapy on NKT cells in patients with advanced head and neck cancer. Cancer Immunol Immunother 2010 Oct;59(10):1503-9.

261. Rico MJ, Rozados VR, Mainetti LE, Zacarias Fluck MF, Matar P, Scharovsky OG. Regulatory T cells but not NKT I cells are modulated by a single low-dose cyclophosphamide in a B cell lymphoma tumor-model. Exp Oncol 2012;34(1):38-42.

262. Gu B, Sun P, Yuan Y, Moraes RC, Li A, Teng A, Agrawal A, Rheaume C, Bilanchone V, Veltmaat JM, et al. Pygo2 expands mammary progenitor cells by facilitating histone H3 K4 methylation. J Cell Biol 2009 Jun 1;185(5):811-26.

263. Olkhanud PB, Damdinsuren B, Bodogai M, Gress RE, Sen R, Wejksza K, Malchinkhuu E, Wersto RP, Biragyn A. Tumor-evoked regulatory B cells promote breast cancer metastasis by converting resting CD4(+) T cells to T-regulatory cells. Cancer Res 2011 May 15;71(10):3505-15.

264. Olkhanud PB, Baatar D, Bodogai M, Hakim F, Gress R, Anderson RL, Deng J, Xu M, Briest S, Biragyn A. Breast cancer lung metastasis requires expression of chemokine receptor CCR4 and regulatory T cells. Cancer Res 2009 Jul 15;69(14):5996-6004.

265. Chen L, Huang TG, Meseck M, Mandeli J, Fallon J, Woo SL. Rejection of metastatic 4T1 breast cancer by attenuation of treg cells in combination with immune stimulation. Mol Ther 2007 Dec;15(12):2194-202.

266. Cho HJ, Jung JI, Lim do Y, Kwon GT, Her S, Park JH, Park JH. Bone marrow-derived, alternatively activated macrophages enhance solid tumor growth and lung metastasis of mammary carcinoma cells in a Balb/C mouse orthotopic model. Breast Cancer Res 2012 May 22;14(3):R81.